UNIVERSITY OF CALIFORNIA, SAN DIEGO

Understanding the Mechanism and Improving the Design of a Myocardial Matrix Hydrogel for Post-Infarct Repair

A dissertation submitted in partial satisfaction of the requirements for the degree Doctor of Philosophy

in

Bioengineering

by

Jean Wang Wassenaar

Committee in charge

Professor Karen L. Christman, Chair
Professor Anthony N. DeMaria
Professor Andrew D. McCulloch
Professor Mark Mercola
Professor Shyni Varghese

2016

The Dissertation of Jean Wang Wassenaar is approved, and it is acceptable in quality and form for publication on microfilm and electronically:

Chair

University of California, San Diego

2016

Dedication

To my father, who taught me how exciting research can be when I was seven, when he took me to the lab with him in the evenings to finish experiments.

To my mother, who was the perfect role model and whose hard work and aspirations is the reason I get to pursue my dreams.

To my husband, who has patiently accompanied me through six years of this journey already and supported me every step of the way.

Epigraph

Imagine a circle that contains all of human knowledge.

By the time you finish elementary school, you know a little.

By the time you finish high school, you know a bit more.

With a bachelor's degree, you gain a specialty.

A master's degree deepens that specialty.

Reading research papers takes you to the edge of human knowledge.

Once you're at the boundary, you focus.

You push at the boundary for a few years.

Until one day, the boundary gives way.

And, that dent you've made is a called a PhD.

Of course, the world looks different to you now.

So don't forget the bigger picture.

Keep pushing.

The Illustrated Guide to the Ph.D.

by Matt Might

Table of Contents

List of Figures and Tables

Acknowledgements

I would like to thank the many people who made this dissertation possible. First of all, to my advisor, Dr. Karen Christman, who has given me the freedom and support to study whatever topics have struck my interest. I appreciate all her encouragement and advice in the last four years, which have helped me to develop into an independent scientist and researcher. Just as important to my growth were my thesis committee and other faculty members at UCSD and elsewhere, without their expertise I would have been lost in the data. But without Rebecca Braden and Colin Luo, the data may have never come into existence and so I am forever grateful to their endless hours of surgeries that were integral to my studies. I chose to join the Christman Lab for my PhD not solely because of my interest in the research, but also because of the wonderful people that I to work with everyday. I am in debt to Dr. Jennifer Singelyn and Dr. Sonya Sonnenberg, whose previous work in the lab I completely relied on for my own thesis (I've lost count how many times I've typed "Singelyn et al" in referencing those papers). Thank you to the current lab members, especially Dr. Roberto Gaetani, Dr. Mary Nguyen, Jessica Ungerleider, and Sophia Suarez, for the endless discussions on my projects and more importantly, for keeping me sane in the last two years. I also wanted to thank the wonderful undergraduate students I've worked with, Natalie Lomayesva and Julian Garcia, not only for their help with my projects but also teaching me how to become a mentor. Thank you to my friends – from medical school, bioengineering, MSTP, and San Diego – who have been my community and support network for the last six years. And lastly, I wouldn't be here without my family and especially my husband, who has been my biggest cheerleader this entire journey.

Chapter 1, in part, is a reprint of the material as it is published in: Jean J. Wang and Karen L. Christman. "Hydrogels for Cardiac Repair" in Cardiac Regeneration and Repair Volume II: Biomaterials and Tissue Engineering (R.-K. Li and R.D. Weisel, ed), Woodhead Publishing (2014). The dissertation author was the primary author of this manuscript.

Chapter 2, in part, is a reprint of the material as it is published in: Jean W. Wassenaar, Robert G. Gaetani, Julian J. Garcia, Rebecca L. Braden, Colin G. Luo, Diane Huang, Anthony N. DeMaria, Jeffrey H. Omens and Karen L. Christman. “Evidence for the Mechanisms Underlying the Functional Benefits of a Myocardial Matrix Hydrogel for Post-MI treatment”. (2016) *J Am Coll Cardiol*, 67(9):1074-86. The dissertation author was the primary author of this manuscript.

Chapter 4, in part, is a reprint of the material as it is published in: Jean W. Wassenaar, Robert G. Gaetani, Julian J. Garcia, Rebecca L. Braden, Colin G. Luo, Diane Huang, Anthony N. DeMaria, Jeffrey H. Omens and Karen L. Christman. “Evidence for the Mechanisms Underlying the Functional Benefits of a Myocardial Matrix Hydrogel for Post-MI treatment”. (2016) *J Am Coll Cardiol*, 67(9):1074-86; and also in part, a reprint of material as it is published in: Jean W. Wassenaar, Rebecca L. Braden, Colin G. Luo, and Karen L. Christman. “Modulating *in vivo* degradation rate of injectable extracellular matrix hydrogels”. (2016) *J Mater Chem B*, 4: 2794-802. The dissertation author was the primary author of both manuscripts.

Vita

Education

2008	Bachelor of Science in Biomedical Engineering at Johns Hopkins University
2009-2011	Medical Student at University of California, San Diego
2011-2016	Graduate Student in Bioengineering at University of California, San Diego
2016	Doctor in Philosophy in Bioengineering at University of California, San Diego

Publications

Wassenaar, J.W., Braden, R.L., Osborn, K.G. and Christman, K.L. (2016) "Modulating *in vivo* degradation rate of injectable extracellular matrix hydrogels". *J Mater Chem B*, 4:2794-802.

Wassenaar, J.W., Gaetani, R.G., Garcia, J., Braden, R.L., Luo, C., Huang, D., DeMaria, A.N., Omens, J.H. and Christman, K.L. (2016). "Evidence for the mechanisms underlying the functional benefits of a myocardial matrix hydrogel for post-MI treatment". *J Am Coll Cardiol*, 67(9):1074-86.

Wassenaar, J.W., Boss, G.R., and Christman, K.L. (2015) "Decellularized skeletal muscle as an in vitro model for studying drug-extracellular matrix interactions". *Biomaterials*, 64:108-14.

Merna, N, Fung, K.N., **Wang, J.J.**, King, C.R., Hansen, K.C., Christman, K.L. and George, S.C. (2015) "Differential β3 integrin expression regulates the response of human lung and cardiac fibroblasts to extracellular matrix and its components". *Tissue Eng*, 21:2195-205.

Wang, J.J. and Christman, K.L. (2014) "Chapter 2. Hydrogels for cardiac repair". In Cardiac Regeneration and Repair, edited by R.-K. Li and R.D. Weisel, 17-48. Woodhead Publishing.

Seif-Naraghi, S.B., Singelyn, J.M., Salvatore, M.A., Osborn, K.G., **Wang, J.J.**, Sampat, U., Kwan, O.L., Strachan, G.M., Wong, J., Schup-Magoffin, P.J., Braden, R.L., Bartels, K., DeQuach, J.A., Preul, M., Kinsey, A.M., DeMaria, A.N., Dib, N. and Christman, K.L. (2013) "Safety and efficacy of an injectable extracellular matrix hydrogel for treating myocardial infarction". *Sci Transl Med*, 5(173): p173ra25.

Singelyn, J.M., Sundaramurthy, P., Johnson, T.D., Schup-Magoffin, P.J., Hu, D.P., Faulk, D.M., **Wang, J.**, Mayle, K.M., Bartels, K., Salvatore, M., Kinsey, A.M., DeMaria, A.N., Dib, N. and Christman, K.L. (2012) "Catheter-deliverable hydrogel derived from decellularized ventricular extracellular matrix increases endogenous cardiomyocytes and preserves cardiac function post-myocardial infarction". *J Am Coll Cardiol*, 59(8):751-63

Patents

Boss, G., Chan, A., Brenner, M., Brennar-Mahon, S., Bebarta, V.S., Jiang, J, Christman, K and **Wang, J.** (2014) “Methods and compositions for treatment of cyanide and hydrogen sulfide toxicity”. Patent number WO2014100834A1.

Fields of Study

Major Field: Bioengineering

Studies in Cell Engineering and Glycobiology

Professor Kevin Yarema

Studies in Magenetic Resonance Spectroscopic Imaging

Professor Dieter Meyerhoff

Studies in Cardiac Tissue Engineering

Professor Karen Christman

Abstract of the Dissertation

Understanding the Mechanism and Improving the Design of a Myocardial Matrix Hydrogel for Post-Infarct Repair

by

Jean Wang Wassenaar

Doctor of Philosophy in Bioengineering

University of California, San Diego, 2016

Professor Karen L. Christman, Chair

With improved management of patients with acute myocardial infarctions (MI), the prevalence in heart failure (HF) post-MI is expected to rise. Currently, the only successful treatments for HF are total heart transplantation and left ventricular (LV) assist devices, but their uses are limited by the availability of donor hearts and invasiveness of the procedure. In the last decade, advancements have been made towards developing injectable hydrogels for the purpose

of cardiac repair. Injections of hydrogels alone have been shown to attenuate the decline in cardiac function and LV remodeling typically seen after MI in both large and small animals models. One of these hydrogels was previously developed by our lab and derived from decellularized porcine ventricular myocardium. The goal of this thesis was study to the mechanisms by which injections of the myocardial matrix hydrogel improve cardiac repair post-MI and improve upon its cardioreparative effects. To better understand how this myocardial matrix is able to induce the beneficial effects observed post-MI, a whole transcriptome microarray was performed on infarct tissue collected from matrix or saline injected infarcts. We showed through pathway analysis that the effects of the injection were dividable into several tissue level phenotypes. To better understand these *in vivo* phenomena, we wanted to recapitulate the observations by cell culture *in vitro* with the myocardial matrix. Several cell behaviors relevant to the infarct milieu were studied, including cardiac progenitor cell migration, cardiomyocyte apoptosis, cardiac fibroblast metallomatrix proteinase (MMP) production, and macrophage polarization. We demonstrated that the form of the matrix that is presented to the cells have a dramatic effect on the cellular response, whether through the 3D hydrogel or as soluble peptides released during degradation. In addition, different fractions of the degradation products also have different bioactivity. Results from these *in vitro* experiments suggested that the bioactivity of the myocardial matrix and its degradation products seemed to be essential to its cardioreparative effects post-MI; thus, we investigated whether this could be enhanced by prolonging the degradation rate of the hydrogel. Through these studies, we provided the first steps towards elucidating the mechanism of actions of the myocardial matrix, by defining the tissue level changes that it induces in infarcted myocardium and identifying the bioactivity in both the hydrogel form and degradation products.

Chapter 1: Hydrogels for Cardiac Repair

1.1. Introduction

Progression towards heart failure (HF) after myocardial infarction (MI) begins with cardiomyocyte loss from ischemic injury [1] followed by influx of inflammatory cells such as monocytes and neutrophils [2]. Release and activation of matrix metalloproeases (MMPs) from the inflammatory infiltrate further exacerbates the decline in heart function by digesting the extracellular matrix (ECM), followed by deposition of fibrillar crosslinked collagen. Loss of myocyte cell mass and subsequence replacement fibrosis causes left ventricular (LV) wall thinning and dilatation [1]. Biomaterials and tissue engineering based approaches have been explored over the past decade to prevent and treat post-MI HF by attempting to replace the ECM and/or cells that are lost post-MI [3,4]. Cardiac patches, which involve placement of a biomaterial scaffold, either alone or with cells or therapeutics on the epicardial surface, have shown success in animal models [5,6]. Injectable hydrogels, which are the focus of this chapter, have also been widely explored over the past decade because of their potential to be delivered minimally invasively. As a wall-bulking agent, hydrogels could shift some of the abnormal stresses of the myocardium, potentially stabilizing the infarct and reducing its expansion. Furthermore, injected hydrogels can act as a scaffold that serves the function of the degraded ECM, supporting surviving cardiomyocytes while providing a niche for endogenous cell recruitment and potentially exogenously delivered cells. This chapter will begin with a discussion of hydrogel chemistry and properties relevant to cardiac repair and then focus on those hydrogels that have been injected alone or used as a delivery vehicle for cells and therapeutics for cardiac repair post-MI.

1.2. Hydrogel Properties

Hydrogels are water-swollen networks of crosslinked polymer chains. Due to their highly hydrated nature, hydrogels exhibit many tissue-like characteristics, making them a favorable class of materials for use in tissue engineering applications. For cardiac repair, hydrogels must have the additional property of being able to gel *in situ* once injected into the myocardium. The

transition for the liquid, solubilized phase of the material to the semi-solid hydrogel state is termed the sol-gel transition. For a material to undergo sol-gel transition, the soluble state must have low viscosity to allow for passage through the injection needle and gel by crosslinking mechanisms that occurs selectively after injection [7]. Alternatively, a shear-thinning hydrogel could also be used, whereby some physically crosslinked hydrogel can undergo viscous flow under shear stress (needle injection) and then self-heal to recover the gel state [8], although this approach has yet to be explored for injection into the myocardium.

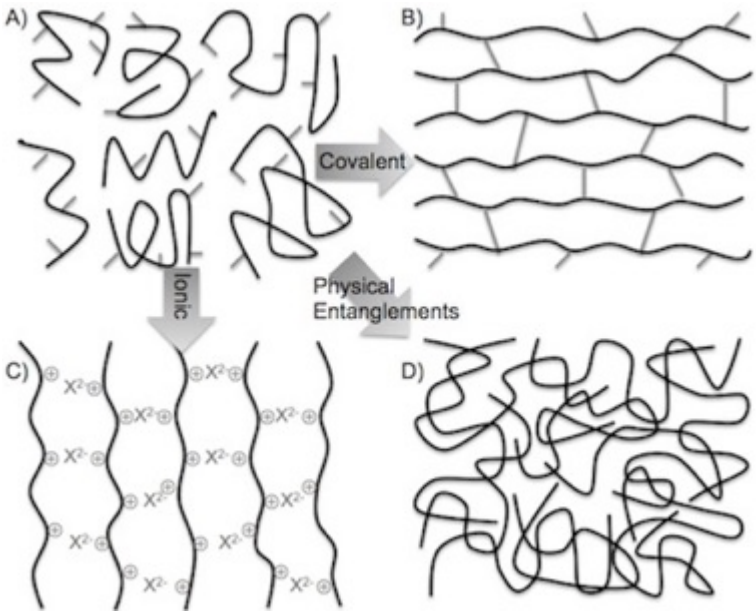

Figure 1.1 Hydrogel crosslinking mechanisms. Polymers in solution (A) with side groups (in grey) capable of forming covalent bonds (B) or ionic interactions (C); alternatively, gelation can occur by physical entanglements (D) of the polymer strands.

Hydrogel gelation occurs through crosslinking of the polymer chains by a variety of mechanisms such as covalent bonds, ionic interactions, and physical entanglements (Figure 1.1). Covalent crosslinking results from chemical bonds that form between two polymer strands that result in a permanent link. Covalently crosslinking is often achieved by the use of a small molecule crosslinker, which allows for more control of the crosslinking density [9]. However,

toxicity of the crosslinking agent needs to be assessed, since un-reacted crosslinkers and crosslinked degradation products can sometimes cause adverse effects. For example, glutaraldehyde (GA), a commonly used crosslinker for naturally derived hydrogels, can potentially elicit cytotoxic and immunogenic responses [10]. In comparison, enzymatic crosslinking, such as fibrin polymerization by thrombin, may be favorable since its degradation products are likely to be naturally occurring in the body. Unlike the covalently crosslinked hydrogels, ionic crosslinking is reversible; it occurs when a poly-cationic or poly-anionic polymer associates with a multivalent ion of the opposite charge. As the multivalent ions that bind the polymer chains together diffuse away, the crosslinks are broken and the hydrogel dissolutes, sometimes leading to uncontrolled degradation of the hydrogel. An example of this is alginate, an anionic polysaccharide derived from seaweed that is commonly used, which forms a gel once mixed with divalent cations such as calcium or magnesium [11]. Hydrogels that are sensitive to a specific stimulus, such as temperature or pH, are termed “smart hydrogels” and particularly useful. For cardiac repair, they allow for targeted gelation once injected into the infarcted region. The most extensively studied of which is poly(N-isopropylacrylamide) (PNIPAAm), a thermally responsive synthetic hydrogel that transitions from sol-to-gel reversibly at the physiological temperature range [12]. Its amphiphilic nature is what gives it this interesting property. At below body temperature, the hydrogel is soluble due to entropic effects allowing hydrophilic and hydrophobic moieties to neighbor. Once the temperature is raised, PNIPAAm passes its lower critical (LCST) solution temperature such that enthalpy favors the orderly formation of hydrogen bonds between the hydrophilic domains, forming the temporary crosslinks of the hydrogel [13]. Many naturally derived hydrogels are also temperature sensitive; examples include gelatin, collagen, Matrigel, and decellularized ECM hydrogels, whose peptides self-assemble at physiologic temperature and pH to form gels through entanglements of the peptide chains.

Crosslinking of the polymer chains not only forms the hydrogel, but also controls many aspects of the hydrogel properties. Increased crosslinking density is associated with increased

mechanical strength, gelation time, and prolonged degradation. Thus, the degree of crosslinking of a hydrogel can be manipulated to achieve the properties desired for cardiac repair. For example, ECM protein based hydrogels created from collagen, gelatin, or decellularized matrices generally have weaker mechanical properties; crosslinking is a popular method for enhancing the strength of these hydrogels [14-16]. At the same time, crosslinking can also affect the degradation rate of the hydrogel. While not all hydrogels used for cardiac repair are degradable, tissue reparative effects may be better if controlled degradation can be achieved such that the scaffold degrades as regenerative occurs [9]. Degradation of hydrogels typically occurs by hydrolysis, enzymatic action, or dissolution, all of which can be variable depending on the *in vivo* milieu at the infarct site.

1.3. Injectable Hydrogels Alone for Cardiac Repair

1.3.1. Naturally Derived Materials

Naturally derived hydrogels are composed of biologic macromolecules including proteins, polysaccharides, and/or polynucleotides. Many of these materials are extracted from mammalian sources including proteins such as collagen, gelatin, and elastin, and glycoproteins like fibrinogen [17]. In addition, hydrogels can be derived from non-mammalian sources as well, including polysaccharides from plants (cellulose), seaweed (alginate), and crustaceans (chitosan), or made in bacteria (hyaluronic acid (HA)). More recently, natural materials are being developed and utilized by decellularization of tissues or organs such that the complex mixture of ECM components can be harnessed [18,19]. Compared to synthetic polymers, naturally derived materials have the advantage of greater biocompatibility, being biodegradable with nontoxic degradation products, and most possess inherent motifs for cellular interactions.

Using a naturally derived hydrogel, Christman *et al.* [20] were the first to demonstrate that injection of a biomaterial alone is sufficient to attenuate the decline of cardiac function in a rat MI

model. Specifically, injection of fibrin glue into ischemic LV one-week post MI preserved fractional shortening and infarct wall thickness evaluated at five weeks post-injection [20]. A follow-up histological study revealed that fibrin alone was able to reduce infarct size and stimulate arteriole formation within the infarct zone [21]. Fibrin glue is formed by enzymatic polymerization of fibrinogen, a plasma glycoprotein involved in the clotting cascade. In addition to the advantages of a naturally derived material, fibrin is also capable of serving as a reservoir for several growth factors [22], and its degradation products have shown to be angiogenic [23], chemotactic and mitogenic [24,25]

Since these initial studies, many naturally derived hydrogels have been injected into cardiac tissue to promote post-MI repair; examples include gelatin, collagen, Matrigel, small intestine matrix, myocardial matrix, pericardial matrix, hyaluronic acid (HA), alginate and chitosan [4]. While most of these materials have shown varying degrees of success in small animal models of MI (rat models as the majority), few have progressed to large animal models necessary for clinical translation. Thus, focus of this section will be paid to those natural hydrogels that show improved cardiac repair after infarction in large animals. Several reviews have been written that cover the numerous small animal studies that have been performed to date [4,26-28].

After demonstrating that injection of an alginate solution into infarcted rat myocardium prevents infarct expansion and LV remodeling in a preliminary study [29], Leor *et al.* [30] progressed to developing alginate into a catheter-deliverable therapy for post-MI repair in a swine model. They postulated that a hydrogel designed as an injectable cardiac repair therapy should: 1) gel at infarct site only; 2) have rapid, controllable gelation to prevent detrimental effects on myocardial function and remote organs; 3) impart tissue-bulking properties to support damaged myocardium 4) be biodegradable; 5) nonimmunogenic; and 6) nonthrombogenic. As a ionically crosslinked hydrogel, the alginate solution is homogenized with calcium gluconate, then injected into the coronary arteries three to four days after MI. Since the vessels of ischemic myocardium are damaged and permeable, the low viscosity solution is able to penetrate the infarct zone and

undergo phase transition *in situ* (Figure 1.2). As a biomaterial, alginate has the notable attribute of having low thrombogenicity [31,32], a property that is necessary for intracoronary delivery. From a safety perspective, the authors demonstrated that injections of up to 4 mL of alginate solution did not cause intravascular microthrombi downstream [30]. Furthermore, post-mortem histology showed, when injected into coronaries of healthy hearts, that alginate did not infiltrate the myocardium or remote tissue. Animals were followed until 30- and 60-days after MI. Comparisons of LV morphometrics at two months to three days (pre-injection time point) post-MI showed that change in LV diastolic and systolic areas were significantly reduced with both 2 mL and 4 mL alginate injections and the 2 mL implants were able to preserve anterior wall thickness and increase scar thickness. Functionally, although changes in fractional shortening did not show a difference between alginate-injected and saline-injected hearts, there was a significant difference in the E/A ratio, which is indicative of diastolic dysfunction [33]. At two months, the alginate was completely degraded with the infarct containing increased myofibroblasts compared to saline-treated hearts. Results from this preclinical work lead to a Phase I clinical trial to study the safety and feasibility of intracoronary alginate infusions in acute MI patients (ClinicalTrials.gov identifier NCT00557531). Currently, this technology is being evaluated in a Phase II trial to prevent ventricular remodeling and congestive heart failure in patients who have had a ST elevation MI with successful percutaneous stent placement (NCT01226563).

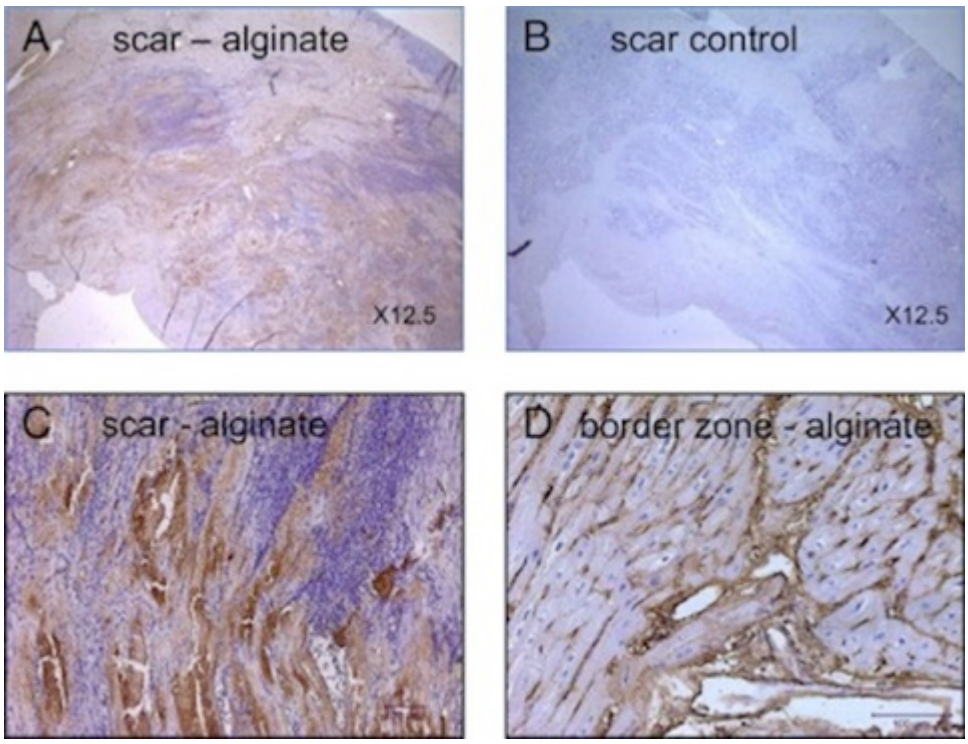

Figure 1.2 Coronary-infused alginate forms an hydrogel in infarcted myocardium. Biotinylated alginate is visible as brown staining two hours after injection in the myocardium (A) but not in the saline injected controls (B). Higher power views reveal delivery of alginate to the infarct area (C) with some hydrogel infiltration into the ECM but without affecting viable cardiomyocytes in the border zone (D).

The low thrombogenicity of alginate is largely attributed to reduced protein adsorption from its hydrophilic character [9,32], which, while desired for intracoronary delivery, may be disadvantageous for tissue repair since this limits its ability for cellular interaction. In fact, mammalian cells do not have receptors that recognize alginate [11]. To improve the cell-scaffold interaction, Yu *et al.* [34] conjugated the cell adhesion ligand arginine-glycine-asparagine (RGD) to alginate and injected it into a rat chronic infarct model. 5-weeks post injection, both modified and unmodified alginate showed similar effects on cardiac function and morphology compared to control phosphate buffer saline (PBS) injections – increased fractional shortening and stable LV internal dimensions – but no differences between treatment groups. However, RGD-modified alginate did show increased arteriole density within the infarct compared to unmodified group.

The disparity between histological and functional results could be due to the model chosen for the study – additional arteriole formation from the injection of a peptide-modified hydrogel at 5-weeks post-infarct could be too late to confer further benefit to cardiac function. Tsur-Gang *et al.* [35] also took a similar approach to modify alginate by covalently attaching various peptides that were cell adhesive (RGD, YIGSR) or nonspecific (RGE). Using a rat total occlusion infarct model, alginate solutions were injected 7 days after MI. Consistent with previous studies, alginate injected groups showed improved LV contractility and reduced dilatation; however, peptide-modified groups resembled saline-treated animals. The 3 treatment groups also did not show any difference in extent of myofibroblast infiltration or angiogenesis, despite promising results *in vitro*. The difference in results between these 2 similar studies [34,35] could be due to a variety of reasons – the rodent infarct model chosen for the study, the injection time point, peptide density, and chemistry used to attach peptides to alginate since this could greatly affect material properties of the hydrogel.

An alternative approach to enhance cell interaction of alginate is by co-polymerization with a biomaterial that facilitates cell adhesion. Mukherjee *et al.* [36] chose this method by combining fibrin sealant with gelatin-graft alginate. This fibrin-alginate composite was injected seven days after infarct was induced in swine using a double-barrel syringe such that crosslinking occurs as the components are mixed as injection occurs. At 28 days after MI (21 days post-infarction), fibrin-alginate injections were shown to prevent infarct expansion, as measured by sonometric markers placed on the epicardium, compared to saline injected controls. The reduction in infarct expansion could potentially be due to the decrease in soluble collagen content within the infarct of hydrogel injected hearts. The authors reported that while fibrillar and total collagen content were increased within the infarct in both groups, as expected with a post-MI fibrotic response, the lower soluble collagen in material injected heart suggests that this collagen is less vulnerable to degradation. Histology of the infarct area revealed remnants of the fibrin-alginate hydrogel at 3 weeks post-injection and presence of foreign body giant cells (FBGCs) in

this group. Macrophages/FBGCs have been known to affect ECM remodeling and fibrosis through secretion of specific MMPs and tissue inhibitors of metalloproteases [37]. This result signifies that biomaterial injections could have an effect on the local matrix remodeling, perhaps by modulating paracrine signals. Unfortunately, beneficial effects in cardiac function and LV dimensions were not seen, potentially because the end point of the study was too early to detect differences.

Of the many studies investigating injectable hydrogels for cardiac repair, relatively few have examined how material properties affect the outcomes on post MI repair and/or regeneration. Ifkovits *et al.* [38] attempted to study one aspect of injected hydrogels – material stiffness – through an ovine MI model. HA was chosen because the mechanical properties of the hydrogel could be modified easily without altering other properties (e.g. time of gelation, tissue distribution after injection, degradation rate). By changing the number of reactive methacrylate groups, two hydrogels were synthesized with different compressive moduli, 7.7 kPa (MeHA low) and 43 kPa (MeHA high); for comparison, the modulus of cardiac tissue is 5.8 kPa [38]. Injections were made 30 minutes after ligation of the coronary arteries and the animals were sacrificed at eight weeks post infarct, upon which histological analysis revealed that hydrogels were still present. While both hydrogels were able to increase infarct thickness compared to control infarcts that received no injection, only the HA hydrogel with higher stiffness was able to reduce infarct expansion significantly (Figure 1.3). With LV volumes a similar pattern emerged; however, this was not significant. There was also no difference in ejection fraction or cardiac output. Histological evaluation showed limited cellular response to the HA hydrogel, without the increased macrophage and myofibroblast infiltration that is typically seen with injected hydrogels.

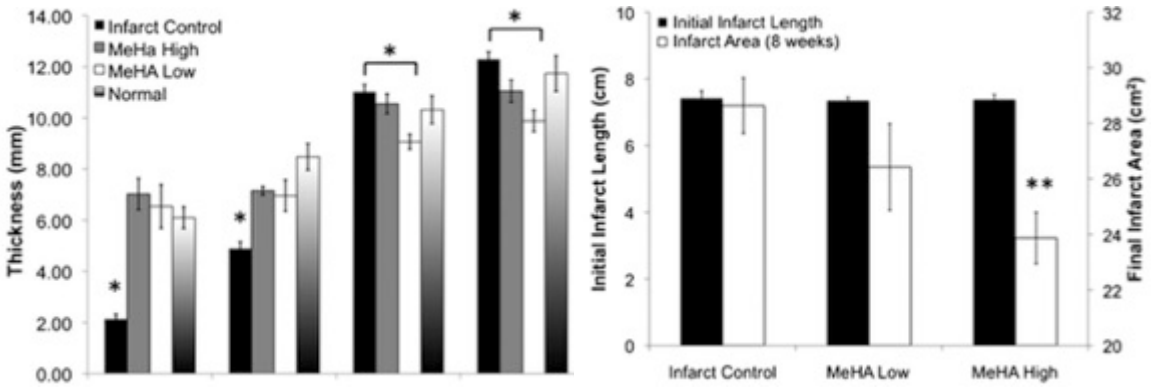

Figure 1.3 Hyaluronon hydrogels (HA) with different mechanical properties have different effects on infarct remodeling. Injection of HA hydrogels with higher compressive moduli (MeHA high) was able to better increase infarct thickness (left) and limit infarct expansion (right) compared to weaker hydrogels (MeHA low) [reprinted with permission].

Building upon the HA system with tunable mechanical properties developed by Ifkovits *et al.* [38], Tous *et al.* [39] further modified the hydrogels such that the degradation kinetics could be altered while maintaining similar initial mechanics. Using this approach, they created four HA hydrogels, two of which were non-degradable with different compressive moduli similar to the previous study (~7 kPa and ~40 kPa) and two hydrogel that were degradable over three weeks (low HeMA-HA) and ten weeks (high HeMA-HA) with initial mechanics that matched the non-degradable hydrogels respectively. Injections of these hydrogels were made immediately after MI in an ovine model and by the last time point (eight weeks), the low HeMA-HA was completely degraded and only the high HeMA-HA was present minimally in the apex. Histologically, the degradable hydrogels elicited a stronger inflammatory response, perhaps due to release of degradation products. Similar to the previous study, both non-degradable hydrogels were able to increase infarct thickness; however, only the slowly degraded high HeMA-HA was able to increase thickness and only the apical infarct, possibly corresponding to the presence of the hydrogel. In terms of LV geometry, only the stiffer non-degradable hydrogel was able to significantly reduce change in end systolic volume. But this difference in LV remodeling by the

hydrogels with different mechanical and degradation properties was not reflected in functional parameters, where ejection fraction was the same for all hydrogels compared to infarct controls.

Of the naturally derived hydrogels discussed so far, none have specifically been designed as a cardiac-specific material for tissue regeneration and repair. Furthermore, polysaccharide hydrogels such as alginate, HA, and chitosan do not possess the inherent factors for cellular interactions. Singelyn *et al.* [40] sought to address this by developing a hydrogel derived by decellularized porcine ventricular tissue. In a rat ischemia-reperfusion model, injection of the myocardial matrix hydrogel attenuated the decline in ejection fraction and reduced end systolic and end diastolic volume expansion [41]. To demonstrate proof-of-concept for clinical translation, the same study also demonstrated that the myocardial matrix hydrogel is deliverable minimally invasively by a trans-endocardial catheter. A subsequent study analyzed the myocardial matrix hydrogel's effect on cardiac function and regeneration in a porcine MI model. When comparing changes from pre-MI to pre-euthanasia (three months), analysis of functional parameters showed that injection of the myocardial matrix hydrogel reduced LV volumes, decreased infarct expansion, and improved both global and regional cardiac function [42]. Histologically, hydrogel injections significantly reduced collagen content within the infarct and increased cardiac muscle at the endocardium compared to controls. It was established that the hydrogel was hemocompatible when analyzed by standard blood tests; specifically, standard concentrations of the myocardial matrix mixed with human platelet-enriched plasma did not cause platelet activation and even a 4-fold higher concentration only resulted in minimal platelet activation that was not deemed as clinically significant. To assess the biocompatibility of a xenogeneic hydrogel for clinical translation, the porcine derived myocardial matrix was injected into the healthy rat myocardium. At 28 days, the hydrogel was completely degraded; later time points revealed no observable signs of chronic inflammation with presence of spindle cells, indicating a reparative remodeling process. Lastly, direct injection of the hydrogel into LV lumen of healthy rats did not cause embolizations or remote ischemic damage.

1.3.2. Synthetic Materials

Compared to the naturally derived hydrogels mentioned above, synthetic hydrogels have the advantage of being easily tailorable for a wide range of properties with little batch-to-batch variability. Furthermore, use of synthetic materials can avoid the potential issue of immunogenicity and transmission of xenogenic pathogens, such as viruses and prion proteins [43]. However, synthetic materials do have inherent disadvantages. Polymers such as polyethylene glycol (PEG) and PNIPAAm are generally considered to have poor biodegradability [44]. For those synthetic biomaterials that are degradable, their degradation products can sometimes be toxic or cause undesirable responses. Examples of this can even include commonly used hydrogels for tissue engineering such as polyglycolic acid (PGA) and polylactic acid (PLA), whose acidic degradation products released from hydrolytic cleavage of the hydrogel chains are known to cause adverse tissue reactions [45]. Lastly, unless modified, synthetic hydrogels lack the motifs that permit cell adhesion and interaction.

Zhang *et al.* [46] sought to address these issues by pioneering the development of a class of spontaneously self-assembling oligopeptides. The peptide nanofibers (NFs) are generally self-complementary amphiphilic sequences that have repeating units of positively and negatively charged residues separated by hydrophobic residues [43]. Since this synthetic polymer is composed of natural building blocks, the resultant material is biodegradable with degradation products that can be used in normal bodily functions. Furthermore, several sequences (EAK16 and RAD16) were shown to be able to promote cell adhesion in an integrin-independent fashion [47]. In addition, some integrin isoforms may recognize RAD sequence due to its similarity to RGD [48]. While the peptides are soluble at low pH and osmolarity, they transition to a 3-dimensional scaffold at physiologic conditions [49] and support attachment, growth, and differentiation of mammalian cell lines [50,51]. In particular, Davis *et al.* [52] showed that intramyocardial injections of peptide NFs into healthy rat hearts promoted recruitment of

endogenous endothelial and smooth muscle cells. Lin *et al.* [53] investigated the use of these peptide NFs for cardiac repair in a MI model in mini pigs. Injections of the peptide NFs were made immediately after permanent occlusion of the coronary artery. At 28 days after MI, animals were sacrificed while the majority of injected NFs still persisted. In terms of LV remodeling, NF injections were able to increase thickness of the intraventricular septum and improve LV diastolic and systolic volume. Functionally, while diastolic function (as measured by –dP/dt) improved, ejection fraction and +dP/dt did not.

So far, the peptide NFs are the only synthetic hydrogel that have demonstrated to have beneficial effects towards cardiac repair post MI in large animal models. Other synthetic materials that have been injected in small animal models include PEG based hydrogels [54-57] and PNIPAAm based hydrogels [58-61]. PEG has been one of the most widely used synthetic hydrogels for tissue engineering due to its biocompatibility. Because of its high degree of hydrophilicity, it is often favored in applications such as surface modification of biomaterials where protein adsorption is undesirable [9]. However, in cardiac repair, lack of protein adsorption and subsequent cellular interaction may be not be advantageous for promoting regeneration by infiltrating cells. As a thermally sensitive smart hydrogel, PNIPAAm allows for rapid gelation post injection as temperature of the material is raised above its LCST in the myocardium. In the hydrogel state, PNIPAAm is considered hydrophobic such that protein adsorption and cell attachment is possible. However, both PEG and PNIPAAm are not inherently bioactive and are non-degradable, thus most approaches that use these synthetic polymers have taken advantage of the ease by which they can be modified with other polymers and biomolecules to improve upon these properties [62].

1.3.3. Mechanisms of Action of Injected Hydrogels

While many injected hydrogels have been shown to preserve cardiac function and prevent LV remodeling in animal models of MI, the exact mechanism of this benefit remains

unknown. Wall *et al.* [63] were the first to suggest that improvements seen with intramyocardial injections of cells and/or materials are due to passive structural support of the injectant to the damaged myocardium. Using a finite element model, injections of various volumes and stiffnesses were stimulated in an ovine LV with an anteroapical infarct. Calculated local stress responses show that small changes in wall volume (0.5% to 5%) can reduce fiber stress at the border zone that are typically elevated after myocardium damage. Stiffer materials were able to bear more of the load and thus further reduce stresses in the remote and border zone. Similarly, as mentioned above, Ifkovits *et al.* [38] showed that injection of a HA hydrogel with stiffness higher than that of myocardium was better able to preserve infarct expansion compared to a weaker gel, but it did not significantly affect cardiac function. End diastolic and end systolic pressure volume relationships, ejection fraction and stroke volume all demonstrated improvement with injections of a non-contractile material [63]. Results from this theoretical analysis suggests that improved LV function and morphology by a hydrogel injection could be due to offloading of stresses and increase of wall thickness by the material. However, whether this prevents the deleterious LV remodeling in the long term remains to be seen, since the finite element model is only capable of simulating short-term effects immediately after hydrogel injection.

In vivo, the mechanical effects that hydrogel injections play on cardiac remodeling is much more difficult to elucidate, since many of the hydrogels used so far may have biological activity as well. Rane *et al.* [56] sought to distinguish effects of hydrogel injection as purely mechanical reinforcement, as speculated by Wall *et al.* [63], by using PEG because it is bioinert, non-degradable, and can be injected to form a gel *in situ*. Injections of a PEG hydrogel with stiffness similar to commonly injected polymers (0.5 kPa) were made 9 days after a rat total occlusion MI model. While the PEG hydrogel was able to significantly increase wall thickness, there was still a significant increase in LV end diastolic volume and end systolic volume (Figure 1.4), and decrease in ejection fraction at seven weeks post-MI. Histologically, the PEG hydrogel elicited very little cellular response except for a thin layer of encapsulation, as expected for a non-

degradable biomaterial. Results from this study indicates that passive wall thickening alone is insufficient towards prevents negative LV remodeling or improve cardiac function. This implication is similarly reflected by Dobner *et al.* (2009), where injection of a non-degradable PEG-vinyl sulfone hydrogel immediately post-MI showed some benefits in reducing end diastolic diameter at two and four weeks post-MI but not at 13 weeks). Furthermore, wall thinning was only prevented in four weeks and not 13 weeks, indicating that prolonged wall bulking is insufficient in the attenuation of negative LV remodeling. Perhaps this is reflective of the computational outcome from Wall *et al.* (2006), which only demonstrated the short-term mechanical effects of an injected hydrogel, and not the long-term implications.

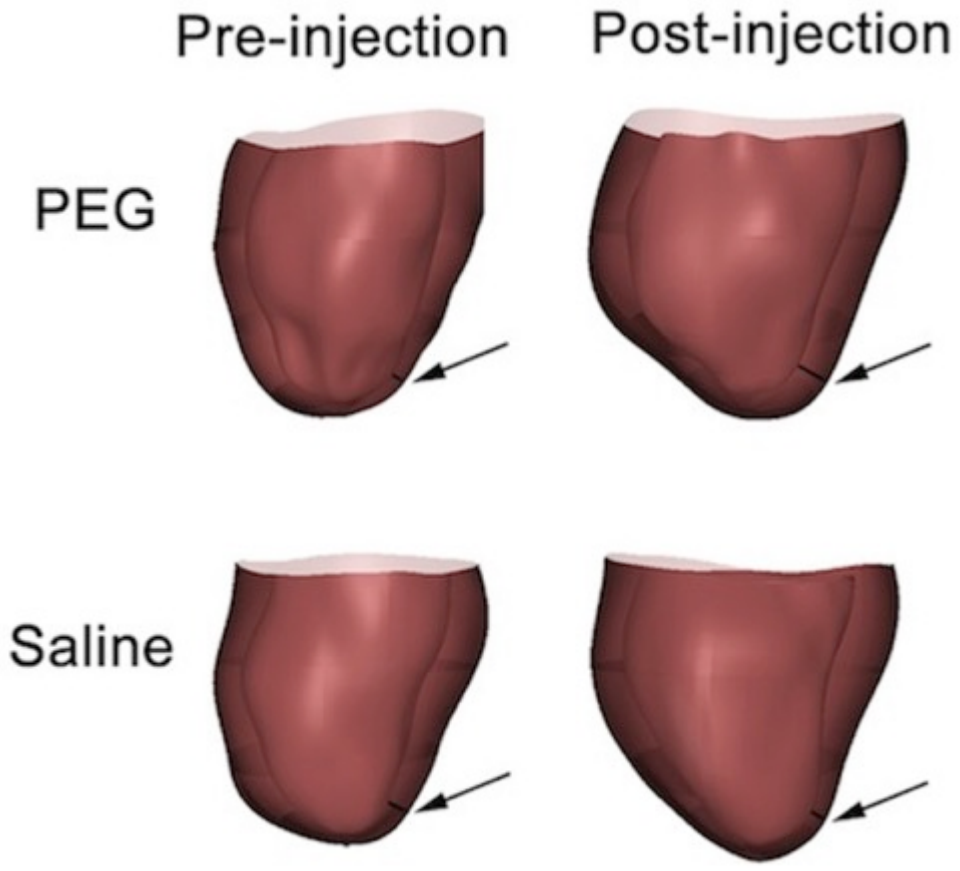

Figure 1.4 Finite element representations of the left ventricle before and after injection of a non-degradable bio-inert PEG hydrogel or saline. Wall thickening (arrow) of the infarct is detected after PEG injections, however LV lumen dilatation occurred in both groups [reprinted with permission].

Beyond mechanical reinforcement, an alternative mechanism of the benefit of injected hydrogels towards post-MI cardiac repair could be the bioactivity of materials. Evidence for the bioactivity of naturally derived polymers is abundant. Collagen, fibrin, and Matrigel injections into infarcted area have been shown to induce myofibroblast migration [64]. In addition, large numbers of non-contractile cells are also seen; it's been hypothesized that infiltration of these cells could benefit infarct remodeling by modulating the inflammatory response and produce beneficial paracrine effects [4]. For example, fibronectin fragments, a degradation product of ECM, can recruit pro-remodeling macrophages and stimulate them to release cytokines to protect hypoxic myocytes from apoptosis [65]. As mentioned previously, presence of integrin binding sites on protein hydrogels could also provide cell attachment moieties, which are essential for cell function and survival. Many previously injected materials also exhibit signs of increased neovascularization, possibly diminishing LV remodeling by reperfusion of the damaged myocardium. Angiogenic factors within naturally derived hydrogels include fragment E in fibrin [23], hepI and hepIII fragments on collagen IV [66].

Inherent in the difference in reported findings for injected hydrogels for cardiac repair is the selection of injection and evaluation time points. Injection time points occur from immediately post MI induction until 2 months after initial infarct. The timing of the injection has consequences on the eventual therapeutic benefit of the hydrogel. Landa *et al.* (2008) explored that difference between alginate injections in an acute MI model (7 days post-infarct) and a chronic MI model (2 months post-infarct) in rats. Using a similar calcium-crosslinked alginate solution that Leor *et al.* (2004; 2009) utilized, they examined how changes in injection timing affect cardiac remodeling and function at 2 months after treatment, when majority of the alginate hydrogel has been degraded. For the acute MI model, at 8 weeks improved LV morphology, as assessed by anterior wall diastolic and systolic thickness, LV end diastolic and end systolic dimensions, and LV end diastolic and end systolic area (Landa *et al.*, 2008). However, functional improvements in fractional shortening and fractional area change were not detected. In the chronic MI model, while

differences in LV morphology and function were not detected in direct comparisons between alginate treated animals and saline-injected controls. However, significant differences were detected once comparisons were made as a percentage change from baseline values within each group in anterior wall thickness, LV end systolic dimensions, and fractional area change. Results of this study indicates that while hydrogel injection in a chronic infarct MI model can have some beneficial effects in thickening the infarct and potentially affecting LV remodeling to a certain degree, injections made in a recent infarct can have a much greater impact on cardiac repair and regeneration.

In terms of timing of studies, selection of the study termination time point could also affect results. The studies described here have varied from 2 weeks to 3 months post injection. Terminating the study too early could risk only reporting of short-term beneficial effects, as suggested by Wall *et al.* [63], while the long-term outcome remains unknown. This could be particularly important in cases of degradable hydrogels since their effect on LV morphology and function could be in part attributed to wall bulking and offloading of stresses in the infarct region. Thus, analysis and conclusions drawn prior to complete degradation of the hydrogel could overlook the long-term therapeutic effects of injectable hydrogels.

To determine the ideal study termination point, it is necessary to evaluate the degradation rate of the hydrogel *in vivo*. So far, for the different types of degradable hydrogels that have been injected intramyocardially for post-MI repair, only Tous *et al.* [39] have modulated the degradation rate of their HA system. The effect that changes in hydrogel degradation could have a dual effect on cardiac repair: 1) mechanical effects of hydrogel presence towards wall bulking and stress reduction; and 2) prolonged release of bioactive peptides that may extend the recruitment of pro-regenerative cell types and neovasculature. In Tous *et al.* [39]'s study, hydrogels with faster degradation rates were not able to increase infarct thickness and degradable hydrogels had no effect on LV volumes compared to more stable hydrogels. In a study from Yu *et al.* (2009a), the question of material residence time was partially addressed. Alginate and fibrin were injected in

rats 5 weeks after an ischemia-reperfusion MI model. While both hydrogels initially improved LV geometry and function at 2 days post-injection as compared to saline controls, only the alginate treated groups showed significant persistent improvement at 5 weeks. Yu *et al.* [67] observed that at 5 weeks, presence of alginate could still be identified by histology while fibrin was completely reabsorbed, leading them to propose that long-term benefits on cardiac function could be affected by persistence of the injected hydrogel. However, this study was performed on two different materials, each with its unique bioactive properties; therefore, it is uncertain whether the difference in beneficial effects is due to material residence time or intrinsic bioactivity of the two hydrogels.

The biologic effect of different naturally derived hydrogels was investigated by Huang *et al.* [64]. Collagen, Matrigel, and fibrin were chosen because they were three commercially available biomaterials that are able to transition from liquid to hydrogel after intramyocardial injection. Injections were made 1-week after an ischemia-reperfusion MI model in the rat. At 5 weeks post-injection, all 3 hydrogel were able to increase angiogenesis when compared to PBS injected controls. However, only collagen was able to significantly enhance myofibroblast influx, indicating some difference in the biologic response elicited by the various injected hydrogels. Implications on cardiac function and LV remodeling were not investigated in this study and thus, differences in bioactivity could not be correlated to functional outcomes. Unfortunately, few studies so far have directly compared different hydrogels against each other, making it difficult to determine of advantages of use of one over another. Since the procedure, timing, and evaluation criteria chosen by each group of investigators also differ, this further complicates the elucidation of the mechanism by which injectable hydrogels promote cardiac repair post-infarction.

1.4. Hydrogels as a Platform for Co-Delivery

1.4.1. Cells

Cellular cardiomyoplasty has been widely explored as a potential therapeutic strategy for cardiac repair and regeneration [68-70]. The approach involves transplantation of cells suspended in a liquid such as saline or cell culture medium into infarcted tissue or border zone by intramyocardial injections. Unfortunately, current clinical trials using bone marrow derived cells show mixed results in improvement of LV ejection fraction after transplantation partially due to poor cell engraftment and survival after delivery [71]. It has been shown that while transplanted cells remain viable shortly after implantation, by one week only ~1% of cells remain by TUNEL analysis [72]. Most of the cell death seen within the first few days of transplantation is likely caused by the combination of ischemia, inflammation, and anoikis, or apoptosis induced by disruption of cell-matrix interactions [73,74]. Christman *et al.* [21] were the first to demonstrate that injection of cells along with a hydrogel can improve cell transplant survival in a rat MI model. This study used neonatal rat skeletal myoblasts with a fibrin injection and showed that compared to conventional liquid delivery, fibrin improved myoblast survival by more than two-fold. Injection of myoblasts with fibrin increased fractional shortening and infarct thickness [20], but this was not statistically different than injection of fibrin alone. Since then, the use of fibrin as a delivery vehicle to enhance success of cellular cardiomyoplasty has been demonstrated with bone marrow cells [75], marrow-derived cardiac stem cells [76], and adipose-derived stem cells [77,78].

Other naturally derived hydrogels that have been used to deliver cell therapy include chitosan [79,80], Matrigel [81], and RGD-modified alginate [82]. As mentioned previously, alginate lacks the intrinsic motifs for cell adhesion, thus to prevent anoikis of transplanted cells, modifications to alginate must be made to provide cell-matrix interactions. Yu *et al.* [82] used a RGD-modified alginate to encapsulate human mesenchymal stem cells (hMSCs). Microbeads generated from this solution and injected in an ischemia reperfusion model in nude rats showed persistence of hMSCs in microcapsules at seven days and two weeks, while hMSCs injected with medium were only detectable at one day. To address the various causes of poor cell survival (ischemic conditions, anoikis, and release of inflammatory factors), Laflamme *et al.* [81]

developed a multi-pronged approach, which they termed a prosurvival cocktail (PSC) and included Matrigel to prevent anoikis, cyclosporine A for immune-suppression, a caspase inhibitor, anti-mitochondrial-apoptotic peptide Bcl-XL, insulin-like growth factor, and a compound that mimics ischemic conditioning. Use of PSC improved human ESC (hESC)-derived cardiomyocyte transplantation survival and increased graft size by seven-fold from one to four weeks post-injection.

Of the synthetic hydrogels, PEG based [83,84], PNIPAAm based hydrogels [60,85], peptide NFs [86], and hydroxypropyl methylcellulose [87] have been injected along with cells in small animal MI models for cardiac repair. As mentioned previously, PEG and PNIPAAm lack inherent bioactivity and are non-degradable, however, they are easily modifiable with biomolecules to improve these characteristics. Kraehenbuehl *et al.* [83] modified PEG-vinyl sulfone hydrogels with MMP cleavable peptides and integrin binding ligands to produce a cell adhesive and degradable hydrogel. Similarly, Wall *et al.* [60] also sought to modify the thermoresponsive synthetic hydrogel PNIPAAm with the addition of MMP degradable peptide crosslinkers and RGD-containing peptide sequences. Injections were made with mouse bone marrow-derived mesenchymal stem cells (MSCs) into a murine total occlusion model immediately post infarct. At six-weeks, MSCs were detectable in 38% of hearts when injected with the hydrogel, but were unidentifiable when injected alone. Interestingly, use of Matrigel resulted in 25% of hearts with detectable cells, indicating that synthetic hydrogels, with biomimetic modifications, could support cell-matrix interactions and diminish anoikis equally or better compared to naturally derived hydrogels. In the study by Mathieu *et al.* [87], it's interesting to note that injection of the silanized hydoxyproypl methylcellulose (siHPMC) alone did not improve echocardiograph measurements at eight-weeks, possibly due to its lack of intrinsic bioactivity. However, injection of MSCs with siHPMC did significantly improve LV end systolic diameter, fractional shortening, and ejection fraction.

1.4.2. Therapeutics

Delivery of various therapeutic molecules, too, can be enhanced through use of a hydrogel vehicle; this can include growth factors, cytokines, small molecules, and gene plasmids to enhance the regeneration and repair of infarcted myocardium. However, the high diffusion rate combined with short active half-live of these molecules makes it difficult for them to be used as MI therapies. Meanwhile, co-delivery with a hydrogel can prolong and target the release of these therapeutic molecules, avoiding the detrimental side effects that can occur with extended systemic exposure.

1.4.2.1 Growth factor delivery

Perhaps the most widely used growth factor to be delivered with an injectable hydrogel for cardiac repair post-MI has been basic fibroblast growth factor (bFGF or FGF-2). As a potent angiogenic agent, administration of bFGF in various animal models of MI has already shown to stimulate cardiac angiogenesis [88-90]. The most common delivery method for bFGF to infarcted myocardium has been through gelatin encapsulation [91-95] where bFGF is released as the hydrogel is degraded. The ability to modify the iso-electric point of gelatin during the fabrication process to generate either a negatively charged acidic hydrogel or a positively charged basic hydrogel makes it particularly useful for drug delivery [96]. Sakakibara *et al.* [92] demonstrated that gelatin microspheres extended bFGF presence *in vivo* from 3 to 15 days and was associated with increased vessel density. Shao *et al.* [95] noted that while capillary density was not further enhanced by the prolonged release of bFGF in microspheres compared to bFGF injection alone, arteriole density in the bFGF-gelatin group was significantly higher than either bFGF or gelatin alone. Yamamoto *et al.* [91] and Iwakura *et al.* [93] further demonstrated that this newly developed vasculature is perfused and capable of increasing myocardial blood flow to the infarcted region. Functionally, Iwakura *et al.* [93], Shao *et al.* [95], and Liu *et al.* [94] reported improved ejection fraction in the bFGF-gelatin group while Yamamoto *et al.* [91] was not able to

correlate the neovascularization to a functional benefit. Other than gelatin microspheres, delivery of bFGF to infarcted myocardium has also been accomplished with chitosan [97], fibrin [98], and PNIPAAm-based hydrogels [59].

Another commonly used angiogenic growth factor is vascular endothelial growth factor (VEGF). To prolong the release of VEGF in infarcted myocardium, Wu *et al.* [57] conjugated VEGF to a PEG-based hydrogel with ester groups that allowed for hydrolytic degradation such that VEGF is released over the same time frame as hydrogel dissolution. In a rat MI model, this tethered approach was able to increase blood vessel density compared to hydrogel alone, hydrogel mixed with VEGF (but not covalently linked), and PBS controls. Furthermore, this trend is reflected in functional measurements, LV morphology, and scar geometry. VEGF has also been delivered by intramyocardial injection with synthetic peptide NFs, through non-covalent interaction with the oligopeptides in a mini pig MI model [99]. Although a weaker interaction, this approach was still sufficient in prolonging VEGF retention up to 14 days and resulted in increased arteriole and artery density. The combined therapy was also able to improve LV fractional shortening compared to other treatment groups. Interesting, capillary density increased with both VEGF alone and NF alone; furthermore, VEGF induced angiogenesis similarly as the VEGF with NF group, suggesting that arteriogenesis and not angiogenesis to be more important in cardiac repair.

Peptide nanofibers have also been used to deliver platelet-derived growth factor (PDGF), which are retained by weak molecular interactions with the amphiphilic peptides [100]. Similar to VEGF, PDGF could be retained past 14 days *in vivo*. Furthermore, the authors ascertained that the delivered PDGF led to activation of the PDGF signaling pathways in cardiomyocytes that resulted in reduced cardiomyocyte apoptosis after infarction. A subsequent longer-term study showed that even at 4 months, an increase in blood flow and vascular density compared to NF-only and non-injected controls was maintained [101]. Furthermore, improvements in cardiac function and LV geometry over NF-only and non-injected controls were also maintained.

In order to deliver growth factors more specifically and controlled, Davis *et al.* [102] modified the synthetic, self-assembling peptides with biotin, such that the therapeutic molecule of interest could be attached by streptavidin binding. Insulin-like growth factor 1 (IGF-1) was chosen for intramyocardial delivery because it promotes survival of cardiomyocytes. Post injection, IGF tethered on peptide NFs was still detectable at 84 days, compared to unmodified IGF, which was un-measurable after day three. Activity of the biotinylated IGF-1 was maintained *in vivo*, leading to Akt activation and decreased activation of caspase-3. Furthermore, tethered IGF-1 promoted survival of co-delivered cardiomyocytes. Fractional shortening and LV dilatation was improved when IGF-1 tethered onto peptide NFs was co-injected with cardiomyocytes; interestingly, this effect is reversed when Akt double-negative cardiomyocytes were injected, suggesting a very IGF-1 specific effect.

Besides growth factors, other protein biologics have also been delivered to infarcted myocardium by hydrogel injection. Segers *et al.* [103] designed a variant of stromal cell derived factor 1 (SDF-1) that is immune to MMP-2 and exopeptidase cleavage while still capable of chemotactic activity. Use of a PEG-based hydrogel also allowed for the sustained local release of erythropoietin, which has cardio-protective effects but can cause polycythemia and subsequent thrombo-embolic consequences if systemically administered [104].

1.4.2.2. Multi-Compound Delivery

Use of hydrogels as a delivery vehicle also presents a unique advantage to allow for co-delivery of two or more growth factors and the ability to control their release. Hao *et al.* [105] developed an alginate hydrogel that would allow sequenced release of VEGF then PDGF. Difference in release patterns was likely due to different affinity that the growth factors have for alginate. The timing of this release was chosen such that VEGF induced endothelial cell migration and angiogenesis is followed by PDGF induced smooth muscle cell recruitment and growth. This is reflected histologically as the dual growth factor delivery had similar capillary density compared

to VEGF alone but was able to induce higher arteriogenesis compared to either growth factor alone.

Also seeking to enhance the development of more mature vessel formation in the infarct, Kim *et al.* [106] delivered an alternative duo of growth factors, PDGF and bFGF, using self assembling peptide NFs. Like previously mentioned studies using peptide NFs for growth factor delivery [99], the interaction is hypothesized to be a non-covalent adsorption of growth factors on the nanofibers. Interestingly, release of PDGF from the peptide NFs resembled an exponential burst release profile, compared to bFGF, which exhibited a linear dose-dependent release. This disparity could reflect a difference in binding affinity the growth factors have for the amphiphilic oligopeptides. Dual growth factor delivery in the peptide NF system was able to dramatically improve infarct geometry, increase vessel density, and decrease cardiomyocyte apoptosis.

Ruvinov *et al.* [107] also sequentially delivered IGF-1 and hepatocyte growth factor (HGF) in an alginate hydrogel. As mentioned previously, IGF-1 is known to be cardioprotective, and HGF has been shown to be pro-angiogenic and anti-fibrotic; thus, dual delivery may lead to synergistic effects in cardiac repair. To accomplish the successive delivery, alginate was modified with sulfates to mimic the sulfated glycosaminoglycans (GAGs) of the ECM that naturally have affinity for endogenous growth factors. Once again, release kinetics depended on the equilibrium-binding constant and the amount of growth factor loaded. Injection of this dual-growth factor hydrogel resulted in a less fibrosis, increased vessel density, decreased apoptosis, increased proliferative cells, and evidence of cardiac regeneration.

To make a hydrogel system for growth factor delivery with release kinetics that are responsive to the myocardium regeneration process, Salimath *et al.* [108] developed a PEG-based hydrogel with MMP-cleavable sites. As a result, growth factor release from the hydrogel can be accelerated with cellular infiltration and remodeling of the scaffold. This was demonstrated *in vitro* when release of VEGF and HGF escalated with increasing concentrations of collagenase. Injection of this growth factor loaded hydrogel immediately after infarction in a rat ischemia

reperfusion model significantly increased vessel density, decreased fibrosis, promoted progenitor cell recruitment, and improved cardiac function.

1.4.2.3. Gene Delivery

An alternative to delivery of growth factors and other protein-based therapeutics is through a plasmid coding the gene of interest. Once transfected into a cell, the plasmid can provide a much more sustained depot for release of the growth factor. Like growth factors, the diminished success of plasmid delivery due to its high diffusivity can be improved by co-delivery with a hydrogel, termed a gene-activated matrix. Instead of VEGF delivery, Kwon *et al.* [109] delivered VEGF plasmids in a rat MI model by amphiphilic synthetic block co-polymer composed of PEG and polypropyl glycol (PPG). Injection of this plasmid-loaded hydrogel one-week post-infarct lead to increased VEGF expression in the myocardium, reduced fibrosis, and increased angiogenesis. Concerned that prolonged VEGF expression in the myocardium can lead to detrimental effects, such as angioma formation, Christman *et al.* [110] decided to use pleiotrophin (PTN) as an alternative angiogenic agent. The PTN plasmid was injected with fibrin glue one-week post-infarct in the rat and showed that PTN with fibrin glue significantly increased arteriole density compared to either alone. Furthermore, microbead perfusion demonstrated that these newly formed vasculatures were functional.

1.5. Delivery Strategies of Hydrogels

Similar to the cell delivery routes outlined by Stamm *et al.* [111] in Figure 1.5, hydrogel delivery to the myocardium can be accomplished by trans-epicardial direct injection, intracoronary infusion, and trans-endocardial catheter injection. However, the delivery of hydrogels to the infarcted myocardium offers unique challenges compared to the more commonly investigated cellular cardiomyoplasty. These materials must be able to be maintained in a liquid state outside the body prior to the injection procedure (which can be over an hour long), yet quickly transition to

a hydrogel state once injected. The vast majority of the hydrogels mentioned in this chapter have been injected by direct intramyocardial (or trans-epicardial) injection. For clinical translation, this would require a surgical based administration, which is not ideal for a patient that just suffered an acute MI. In order for these injectable hydrogel therapies to be delivered immediately to approximately one-week post infarct in patients (like most of studies mentioned above), a minimally invasive method is preferred. So far, only two hydrogels have been shown to be deliverable via catheter delivery in a large animal MI model, intracoronary infused calcium crosslinked alginate [30] and trans-endocardial injected myocardial matrix [41,42]. Use of the intracoronary infusion method has the advantage of using standard catheter lab technology such that additional training is unnecessary. Additionally it does not directly puncture the myocardium [28]. However, this approach requires a material with a unique set of properties, namely one that is highly nonthrombogenic, capable of crossing damaged vasculature, and can gel selectively in the infarct site. Given these criteria, it is likely that this approach is only applicable to acute MI. Furthermore, control of the volume of hydrogel that is delivered to the infarct site is difficult since material is lost in the systemic circulation. The trans-endocardial approach taken by Singelyn *et al.* [41] may prove to be a tenable approach for more hydrogel systems. This procedure would require the hydrogel to remain liquid for prolonged periods during preparation and the catheter procedure, have the suitable viscosity and gelation kinetics for multiple catheter injections, and gel quickly once in the myocardium. Although hemocompatibility of the hydrogel is less of an issue compared to intracoronary infusion, nonthrombogenicity is still preferred since leakage into the bloodstream is known to occur with trans-endocardial catheter delivery of cells [112]. Currently, use of a trans-endocardial catheter is not routine, thus specialized training using the catheter will be needed for the application of this technology, as well as any imaging modality required for targeted injection. Another limiting factor towards the translation of several hydrogels mentioned in this chapter is the use of a double-barrel delivery system. Fibrin, HA, and several synthetic hydrogels all require this delivery set up such that different soluble components can be

added together immediately prior to injection since gelation is triggered once mixing occurs. Unfortunately, current catheter technologies are not compatible with this type of delivery system; however, new crosslinking chemistries, such as oxime crosslinking may open up this possibility [113]. As new hydrogel systems are being developed for cardiac repair, it is important to consider the clinical translatability of the material, namely the ability for minimally invasive catheter delivery.

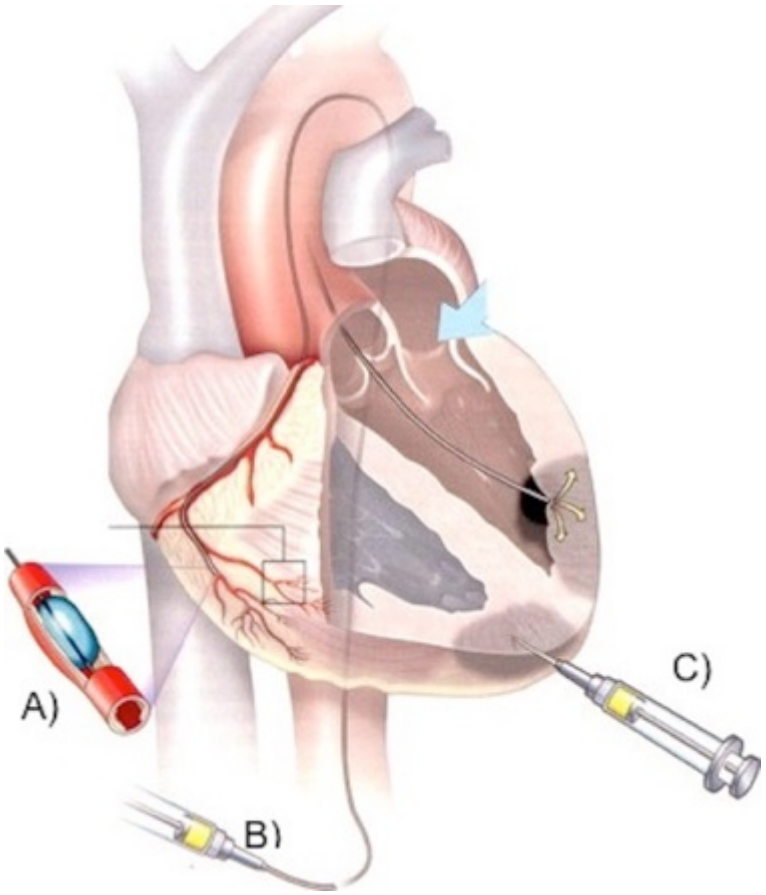

Figure 1.5 Methods for hydrogel delivery into the myocardium. A) Intracoronary infusion by an inflated percutaneous transluminal coronary angioplasty (PTCA) balloon; B) Trans-endocardial delivery via a catheter; C) Trans-epicardial delivery by direct injection [reprinted with permission].

1.6. Scope of the Dissertation

Currently, the only biomaterial alone therapy for MI that has advanced beyond pre-clinical development is the intracoronary infused calcium-crosslinked alginate hydrogel. Recent results from a first-in-man study indicate that the therapy is well-tolerated and shows promise in slowing

progression to HF [114]. As discussed in the previous section, a potential factor in limiting the translation of hydrogels for post-infarct cardiac repair is the ability for the material to be delivered through a minimally invasive approach. Currently, the only other hydrogel that has this potential is the myocardial matrix derived from decellularized porcine ventricular ECM developed previously in our lab. To facilitate its transition to clinical studies, it is important that we improve our understanding of the mechanisms of action of the myocardial matrix. In addition, a better comprehension of the underlying biological changes that drive the functional effects allows us to improve the design of the matrix, further enhancing its therapeutic benefit.

The first chapter investigates the underlying tissue level changes that are induced by injection of the myocardial matrix into the infarcted myocardium. We provide both transcriptional and histological evidence that the myocardial matrix either directly or indirectly induces 1) modulation of the infarct inflammatory response, 2) reduction in cardiomyocyte apoptosis, 3) enhancement of vessel development, 4) inhibition of LV hypertrophy 5) alteration of the myocardial metabolism, and 6) recruitment of cardiac progenitor cells.

The second chapter demonstrates that different components of the degradation products of the myocardial matrix elicit different cell behaviors. We hypothesized that degradation of ECM-derived hydrogels *in vivo* is as a two step process where initially peptides that do not participate in self-assembly diffuse out from the hydrogel followed by active proteolysis of the remaining portion by endogenous proteases. We describe a procedure that mimics this process *in vitro* and show evidence that the two fractions of the degradation products have different bioactivity. In addition, the forms of the myocardial matrix to which cells are exposed to, whether through a 3D hydrogel or as soluble peptides, also affect cell behavior.

The third chapter examines whether prolonging the degradation of the myocardial matrix would enhance its cardioreparative effects post-MI. We experimented with several crosslinkers as well as use of an MMP inhibitor to modify the degradation rate and show that while crosslinkers are able to easily alter the material properties of ECM-derived hydrogels *in vitro*, no crosslinkers

currently exist for injectable collagen-based materials *in vivo*. We demonstrate that use of doxycycline as an MMP inhibitor allows for degradation rate to be modulated without affecting other material properties and is an effective agent *in vivo* to slow down degradation. However, prolonged degradation of the myocardial matrix through the addition of doxycycline did not significantly affect the effects post-MI.

The last chapter summarizes the results of this dissertation and includes further discussion on its implications for the translation of the myocardial matrix to the clinic. Lastly, it suggests further work that needs to be done for the success of injectable hydrogels as therapies for post-infarct repair.

Chapter 1, in part, is a reprint of the material as it is published in: Jean J. Wang and Karen L. Christman. “Hydrogels for Cardiac Repair” in Cardiac Regeneration and Repair Volume II: Biomaterials and Tissue Engineering (R.-K. Li and R.D. Weisel, ed), Woodhead Publishing (2014). The dissertation author was the primary author of this manuscript.

Chapter 2: Transcriptional and Histological Evidence for the Therapeutic Effects of the Myocardial Matrix on Post-Infarct Repair

2.1. Introduction

As discussed previously in Chapter 1, progression from acute MI to chronic HF begins with an initial ischemic injury, resulting in progressive myocyte loss through both necrotic and apoptotic mechanisms [1], and migration of inflammatory cells into the injured myocardium [2]. Release and activation of matrix metalloproteinases (MMP) from the inflammatory infiltrate further exacerbates the decline in heart function by digesting the extracellular matrix (ECM) proteins, followed by subsequent deposition of fibrillar cross-linked collagen. Loss of myocyte cell mass and replacement fibrosis causes left ventricular (LV) wall thinning and dilation [1], beginning the downward spiral of negative LV remodeling. This loss of cardiomyocytes was once thought to be a one-directional process, since the heart has long been considered as terminally differentiated. However, in the last decade, discovery of the existence of multipotent cardiac stem cells (CSCs) that reside in the heart and capability of existing cardiomyocytes to proliferate have shifted the paradigm to the heart as an organ capable of self-regeneration, albeit minimal [115]. Unfortunately, these processes result in a slow rate of myocyte turnover that is insufficient to compensate for the billions of cardiomyocytes lost after MI [116]. In addition to loss of myocytes, function of surviving cardiomyocytes is also altered. The heart has a high energy demand, and recent studies have shown that dysregulation in cardiac metabolism post MI contributes notably towards cardiac dysfunction in HF [117-119].

Currently, the only successful treatments for end-stage HF are total heart transplantation and LV assist devices, but their uses are limited by the availability of donor hearts and the invasiveness of the procedure. Unfortunately, the 5-year survival rate for HF patients is only 50% [120], necessitating the development of therapies to prevent progression of HF following MI. We had previously developed an injectable myocardial matrix hydrogel, derived from decellularized porcine ventricular ECM, that has shown to prevent negative LV remodeling and the decline in cardiac function typically seen after MI when injected into both rat [41] and pig [42] models. To better understand the underlying mechanisms by which injections of the myocardial matrix improves post-MI repair, we performed a whole transcriptome microarray analysis on the gene

expression changes within the infarcted myocardium as a result of the injection. We demonstrate that samples collected from matrix-injected hearts have a distinct transcriptome from saline injected controls by 1-week post injection. We identified the main pathways altered by the myocardial matrix to be involved in the inflammatory response, apoptosis, vessel development, cardiac development, and metabolism. We further confirmed the activation of these pathways through PCR of key genes as well as immunohistological quantification. As discussed in chapter 1, interest in developing non-pharmacological therapies to treat MI has been expanding in the last decade [121]. However, initial clinical trials involving cell transplantation to report widely variable effects on long term heart function, with likely only a moderate effect based on meta-analysis [122]. Improving our understanding of the tissue level changes that ultimately contributes to restoration of cardiac function and halt in LV remodeling post-MI may facilitate the transition of better therapeutics to the clinic.

2.2. Materials and Methods

2.2.1. Myocardial matrix preparation

Porcine ventricular myocardium was decellularized by sodium dodecyl sulfate (SDS) and then partially digested with pepsin as previously described [40-42]. The liquid myocardial matrix was adjusted to pH 7.4 with NaOH and 10x PBS and brought to 6 mg/mL, on ice, then aliquoted and immediately frozen at -80C and lyophilized. Lyophilized partially digested myocardial matrix was rehydrated with sterile water at least 30 minutes prior to injection or hydrogel formation.

2.2.2. Surgical Procedures

All procedures in this study were approved by the Committee on Animal Research at the University of California, San Diego and the Association for the Assessment and Accreditation of Laboratory Animal Care. Adult female Sprague Dawley rats (225 to 250 g) were used in this study. A left thoracotomy allowed access to the heart and MI was induced by 25-minute ischemia-reperfusion of the left coronary artery [41]. One week post-MI, rats were arbitrarily assigned to

receive injections of either 75 uL of saline or myocardial matrix directly into the myocardium by accessing through the diaphragm as previously reported [20,40,41].

2.2.3. Tissue Processing

At three days or one week after injection, rats were euthanized with sodium pentobarbital (200 mg/kg) and their hearts immediately removed. Two groups of animals were used for the one week time point, for RNA isolation and histology, respectively. At the three day time point, hearts were sliced into nine 1 mm coronal slices using a Rat Heart Slice Matrix (Zivic Instruments) such that odd slices could be for histological analysis, while even slices could be used for RNA isolation. All tissue used for histological analysis, were fresh frozen in Tissue Tek OCT freezing medium and cryosectioned into 10 μm sections. Slides were stained with H&E for identification of infarcted tissue. Hearts with infarcts that extended over 30% of the LV were included in the study (n = 6 per group, per time point). For RNA isolation, the infarct wall was isolated by gross dissection then flash frozen at -80C for RNA isolation with the RNEasy Mini Kit with on-column DNAse digestion (Qiagen). RNA concentration and purity (A260/A280, A260/A230) were measured by a NanoDrop spectrophotometer (Thermo Scientific).

2.2.4. RNA Microarray Analysis

All sample labeling and microarray chip processing were performed by the Veterans Medical Research Foundation Microarray & NGS Core in San Diego. RNA integrity was also validated from the ratio of 28s/18s ribosomal RNA using an Agilent 2100 Bioanalyzer. RNA from two infarcts were combined for analysis on one microarray chip to reduce biological variability (n = 3 arrays per group, per time point). cDNA was synthesized from 1 μg of total RNA (pooled 500 ng from each rat) using the Affymetrix GeneChip WT PLUS Reagent Kit. Whole transcriptome microarray analysis was performed using Affymetrix GeneChip Rat Gene 2.0 ST array. The web-based VAMPIRE microarray suite [123] was used for raw data variance modeling and statistical testing. Myocardial matrix treated infarcts were compared to saline injection within each time

point using student t-tests. Differentially expressed genes were selected based on a false discover rate (FDR) of $q < 0.05$ to correct for multiple comparisons. Biological interpretation was performed using Ingenuity Pathway Analysis and Panther Gene Ontology (GO) Classification System. GeneSpring GX (Agilent Technologies) was also used for GO analysis as well as principle component analysis and hierarchical clustering.

2.2.5. Quantitative Polymerization Chain Reaction (qPCR)

The same RNA used microarray analysis was also used for PCR validation of select differentially expressed genes. cDNA was reverse transcribed from 1 µg of total RNA from each rat (unpooled) via SuperScript III Reverse Transcriptase kit (Life Technologies). SYBR Green Real-Time PCR Master Mix (Life Technologies) was used with a final concentration of 1 µM for forward and reverse primers. Primer sequences are in Table 2.1. Samples were run in technical duplicates on a CFX96 Touch Real-Time PCR Detection System (Bio-Rad) with the following thermal cycles: 2 min at 50 °C, 10 min at 95 °C, followed by 40 cycles of 15 s at 95 °C and 1 min at 60 °C. All data was normalized to 18s rRNA.

Table 2.1 PCR Primer Sequences. Forward and reverse primer sequences for all differentially expressed genes whose expression was validated using PCR and the housekeeping gene 18s rRNA.

	Forward Sequence (5'-3')	Reverse Sequence (5'-3')
18s rRNA	GGATCCATTGGAGGGCAAGT	CCCAAGATCCAACTACGAGCTT
ALOX15	GATGGGTGTCTACCGCATCC	CCTCTCCATGCTGTCCAACC
Ang2	GACCAGTGGGCATCGCTAC	CTGGTTGGCTGATGCTACTG
Bcl-2	GATAACGGAGGCTGGGATGC	ATGCACCCAGAGTGATGCAG
Casp3	AATTCAAGGGACGGGTCATG	GCTTGTGCGCGTACAGTTTC
Cat	GGACCAGTACAACTCCCAGAAG	ACTCCATCCAGCGATGATTACT
CD68	CACTTCGGGCCATGCTTCT	AGGACCAGGCCAATGATGAG
ESRRγ	CCAAGAGACTGTGCTTAGTGTG	TCTCACATTCATTCGTGGCC
FGF1	AGGATTCTTCCCGATGGCA	AGCTGAATGTGCTGGTCGC
GATA4	CTGTGCCAACTGCCAGACTA	AGATTCTTGGGCTTCCGTTT
HMOX1	CACGCATATACCCGCTACCT	CCAGAGTGTTCATGCGAGCA
IL1RA	CTCTCCTTCTCATCCTTCTGTTTC	AGCAATGAGCTGGTTGTTCCTC
MEF2d	CCCCTGCTGGAGGACAAGTA	TGCATGGAGCTCTGATTGGA
MMP12	TGCAGCTGTCTTTGATCCAC	TCCAATTGGTAGGCTCCTTG
Myocd	GTGCCTTGTTGGAGTAAGAGTGC	GTCAGTCTATGTCCCGATAATGCC
Nkx2.5	CATTTTATCCGCGAGCCTAC	GTCTGTCTCGGCTTTGTCCA
PGC-1α	CGATGACCCTCCTCACACCA	TTGGCTTGAGCATGTTGCG
PGF	CCATGGACTTTGACCACTGC	TCAAGAGAATCTGGCTTGGCA
PPARα	TCATACTCGCAGGAAAGACTAGCA	GCACAAGGTCTCCATGTCATGT
PPARδ	AGGGGTGCAAGGGCTTCTT	CACTTGTTGCGGTTCTTCTTCTG
SPP1	TCCGATGAGGCTATCAAGGTC	TGCTCCAGGCTGTGTGTT
Tbx5	TCGCTGTGACTTCGTACCAG	TAACTCCAGGTCGTCACTGC
Tbx20	AAGGAGGCAGCAGAGAACAC	GCACAGAGAGGATGAGGAAGG
VCAM1	GCGAAGGAAACTGGAGAAGACA	ACACATTAGGGACCGTGCAG

2.2.6. Immunohistochemistry

Immunohistochemistry (IHC) was performed on three slides throughout the infarct in each heart (n = 6 per group, per time point) using antibodies targeted the following antigens: CD68 (AbD Serotec MCA341R, 1:100), α-cctinin (Sigma A7811; 1:800), cleaved caspase-3 (Cell Signaling 5A1E; 1:50), von Willebrand Factor (vWF, AbCam ab6994; 1:400), alpha smooth muscle actin (α-SMA, Dako; 1:75), c-Kit (Santa Cruz Biotechnology C-19; 1:100), Nkx2.5 (Santa Cruz Biotecnology N-19; 1:100); Tryptase (AbCam Ab2378; 1:100); PGC-1α (AbCam, ab54481; 1:100). For CD68, tissue sections were incubated with horseradish peroxidase (HRP) conjugated

goat-anti-mouse IgG, followed by diaminobenzidine (DAB) for five minutes. All other primary antibodies were visualized by addition of Alexa Fluor 488 or 568 secondary antibodies (Life Technologies). In fluorescent slides, nuclei were visualized with Hoescht 33342 (Life Technologies). Sections were mounted with Fluoromount (Sigma) and imaged with an Ariol Platform with the DM6000 B microscope (Leica Biosystems) to allow complete visualization of the tissue section in a single image. Brightfield slides were scanned using the Aperio Scan ScopeCS2 slide scanner (Leica Biosystems).

Macrophages were quantified at the three day time point as CD68+ cells, using the 'Positive Pixel Count V9' algorithm within ImageScope (Aperio) software to detect DAB staining throughout the entire infarct and borderzone of all three tissue sections. Apoptotic cardiomyocytes were identified at both time points by α-actinin+ cells co-labeled with cleaved caspase-3. Double-positive cells were quantified throughout all three tissue sections within the entire borderzone or remote myocardium. Vessel development at both time points were evaluated by both endothelial cells and arterioles in the infarct scar. Endothelial cells were identified by vWF and assessed by quantifying the percentage of green pixels within five randomly selected regions per slide of 0.2 μm^2 each, within the infarct of each section using ImageJ (NIH). Arteriole density was determined by manually counting from the same five regions using the following criteria: 1) co-staining of vWF and α-SMA, 2) having a visible lumen, and 3) Feret diameter greater than 20 μm, as measured by ImageJ. Size distribution of the vessels were binned by the following: large (greater than 100 μm), medium (between 40 and 100 μm), and small (between 20 and 40 μm). For PGC-1α and Nkx2.5 quantification at the one week time point, co-staining was performed with α-actinin to identify cardiomyocytes. To avoid bias, nuclei of cardiomyocytes adjacent to the infarct were pre-selected by identifying Hoechst expression within α-actinin-positive cells, without visualization of PGC-1α and Nkx2.5 staining. After pre-selection, nuclei that were co-localized with PGC-1α or Nkx2.5 positive staining were counted to determine percentage of cardiomyocytes that express either transcription factors. Based on preliminary study and power analysis, 200 cells were counted per heart. At both three days and one week, progenitor cells,

defined by their expression of the tyrosine-protein kinase kit (c-Kit) but negative for tryptase, were manually counted through the entire section of the heart. Mast cells, defined by either double positive expression of c-kit and tryptase, or single positive expression of tryptase, were also similarly quantified. All histological quantification were performed by a blinded investigator.

2.2.7. Statistical Analysis

For PCR and histological analysis, data are presented as mean ± standard error of the mean (SEM) with n = 6. Saline versus matrix injection was compared using unpaired student t-test. Significance was accepted at $p < 0.05$.

2.3. Results

2.3.1. Myocardial Matrix Injection Alters the Infarct Transcriptome

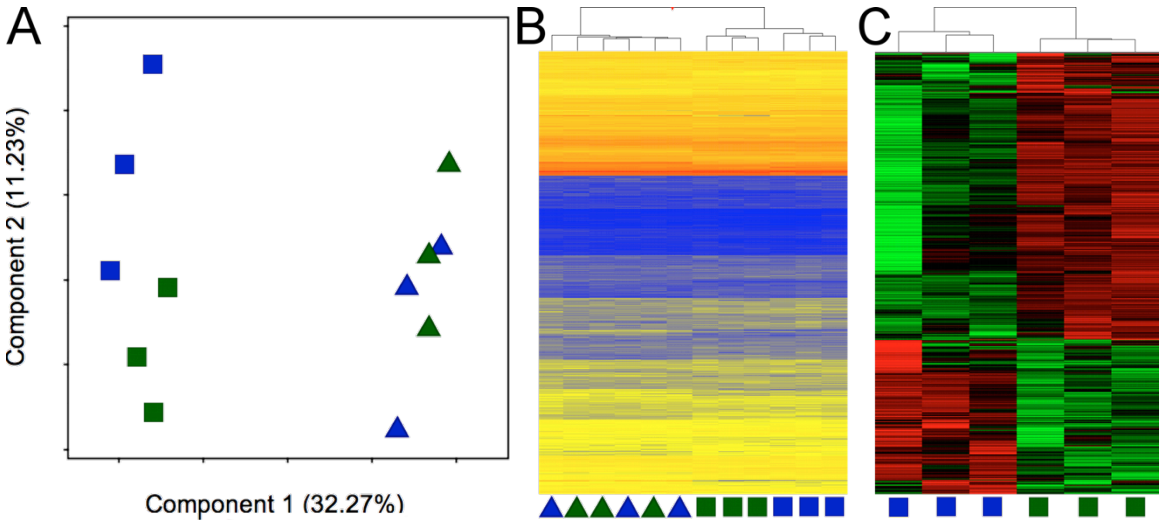

Figure 2.1 Transcriptomes Cluster Separately at 1 Week Post-Injection. Principal component analysis (A) and hierarchical clustering (B) of infarct transcriptomes of all samples indicated that global gene expression after myocardial matrix injection is distinct from control saline injection by 1 weeks. C) Hierarchical clustering of the 2,144 genes differentially expressed at 1 week post-injection. RNA from 2 infarcts were combined for analysis on 1 microarray chip to reduce biological variability (n = 3 arrays per group, per time point). Blue = saline; green = matrix; triangles = 3 days; squares = 1 week.

Principal component analysis (PCA) of all 12 samples demonstrated that 32.04% of the variation in the data could be explained by the first component, which likely represents time

(Figure 2.1A). Within each time point, saline and myocardial matrix injected samples do not cluster separately at three days post-injection. However, by one week post-injection, both PCA (Figure 2.1A) and hierarchical clustering (Figure 2.1B) show separation of transcriptomes from matrix and saline injected infarcts, indicating a shift in global gene expression. Using a FDR cutoff of $q < 0.05$, microarray analysis revealed that, compared to saline injected controls, myocardial matrix injected infarcts had 219 differentially expressed transcriptions at three days (of which 129 are defined, with 98 up-regulated and 31 down-regulated) and 2144 transcripts at one week post injection (of which 1479 are defined, with 963 up-regulated and 516 down-regulated). Using Ingenuity Pathway Analysis, we identified that at three days, the main effects of the myocardial matrix injection are: 1) down-regulation of apoptosis, 2) up-regulation of blood vessel development, and 3) increase in cell movement (Table 2.2). By one week, additional pathways were significantly activated (Table 2.3), including down-regulation of cell death and hypertrophy, and up-regulation of many metabolic processes and gene translation/transcription.

Table 2.2 Pathways with activation z-score of greater than 1 or less than -1 at three days post-injection.

Functions	Diseases or Functions Annotation	p-Value	z-score	# Molecules
	Down-regulated due to matrix injection after three days			
Apoptosis	Apoptosis	8.87E-03	-2.387	10
Cell death	Cell death	7.85E-03	-1.936	12
	Up-regulated due to matrix injection after three days			
Migration	Migration of cells	1.80E-03	1.277	7
Cell movement	Cell movement	4.04E-05	1.467	10
Development	Development of blood vessel	8.27E-03	1.982	4

Table 2.3 Pathways with activation z-score of greater than 1 or less than -1 at one week.

Functions	Diseases or Functions Annotation	p-Value	z-score	# Molecules
	Down-regulated due to matrix injection after one week			
Hypertrophy	Hypertrophy of cells	2.41E-02	-2.176	11
Muscular hypertrophy	Muscular hypertrophy	1.80E-02	-2.001	10
Engulfment	Engulfment of cells	1.06E-02	-1.98	7
Cell death	Cell death of hippocampal neurons	2.03E-03	-1.82	9
Hypertrophy	Hypertrophy of cardiomyocytes	1.06E-02	-1.818	9
Apoptosis	Apoptosis	2.21E-03	-1.793	63
Cell death	Cell death of pheochromocytoma cells	2.76E-03	-1.742	18
Cell death	Cell death	1.19E-04	-1.682	85
Hypertrophy	Hypertrophy	6.66E-03	-1.659	14
Apoptosis	Apoptosis of pheochromocytoma cells	1.03E-02	-1.594	13
Apoptosis	Apoptosis of brain cells	2.09E-02	-1.495	9
Hypertrophy	Hypertrophy of heart	1.39E-03	-1.488	13
Cell death	Cell death of cerebral cortex cells	9.66E-03	-1.445	15
Cell death	Cell death of brain	2.38E-03	-1.398	19
Cell death	Cell death of brain cells	2.76E-03	-1.23	18
Vasoconstriction	Vasoconstriction of blood vessel	2.17E-02	-1.134	7
Cell death	Cell death of muscle cells	6.40E-03	-1.082	18
Cell death	Neuronal cell death	1.03E-02	-1.072	31
	Up-regulated due to matrix injection after one week			
Uptake	Uptake of monosaccharide	2.85E-03	1.005	10
Transport	Transport of carbohydrate	2.42E-02	1.03	8
Oxidation	Oxidation of fatty acid	1.58E-11	1.036	21
Density	Density of mitochondria	3.44E-04	1.067	4
Infiltration	Infiltration of leukocytes	7.65E-03	1.153	7
Oxidation	Oxidation of long chain fatty acid	5.61E-07	1.337	10
Concentration	Concentration of triacylglycerol	2.49E-02	1.387	5
Homeostasis	Cellular homeostasis	9.49E-06	1.403	39
Phosphorylation	Phosphorylation of protein	1.53E-04	1.405	32
Uptake	Uptake of 2-deoxyglucose	1.18E-03	1.455	8
Proliferation	Proliferation of muscle cell lines	5.33E-03	1.489	7
Synthesis	Synthesis of DNA	2.44E-04	1.58	20
Quantity	Quantity of neurons	2.38E-02	1.673	6
Expression	Expression of DNA	3.06E-02	1.746	31
Expression	Expression of RNA	2.80E-02	1.768	41
Transcription	Transcription of DNA	2.58E-02	1.964	30
Infiltration	Infiltration of granulocytes	1.45E-02	1.98	4
Transport	Transport of ion	6.35E-04	2	29
Transport	Transport of cation	8.08E-04	2	22
Transcription	Transcription of RNA	4.25E-02	2.422	35

2.3.2. Inflammatory Response

Injection of the myocardial matrix naturally triggers an inflammatory response, thus it was not a surprise that pathways involved in the immune response including migration and infiltration of various cell types predicted at both the three day and one week time point (Table 2.2 and 2.3). Similarly, a substantial number of genes at both time points – 26.6% at day three and 9.8% at one week – were characterized as part of immune response process (GO:0002376) by GO analysis. To confirm altered expression of these genes, qPCR was performed on key genes using the same RNA isolated for microarray analysis from individual infarcts (unpooled). For comparison, expression of the same genes, as predicted from microarray analysis is listed for reference (Figure 2.2A). Increased expression of CD68 ($p = 0.045$), matrix metalloproteinase 12 (MMP12, $p = 0.043$), and interleukin 1 receptor antagonist (IL1RN, $p = 0.021$) were confirmed at day three (Figure 2.2B), indicative of increased macrophage infiltration as a result of matrix-injection [124,125]. Thus, we sought to quantify this through IHC using a CD68 antibody (Figure 2.2C), but did not find a difference between saline and matrix-injected infarcts at three days (Figure 2.2D). As part of the quantification for cardiac progenitor cells, anti-tryptase staining was also performed to distinguish ckit+ mast cells (Figure 2.2E). Quantification of all tryptase-positive cells showed a trend at three days ($p = 0.052$) and a significant increase at one week ($p = 0.032$) for mast cells (Figure 2.2F).

A

Gene Symbol	Fold Change	p-val
Differentially expressed at three days		
CD68	1.38	7.64E-7
IL1RN	1.65	2.19E-12
MMP12	2.94	2.82E-14

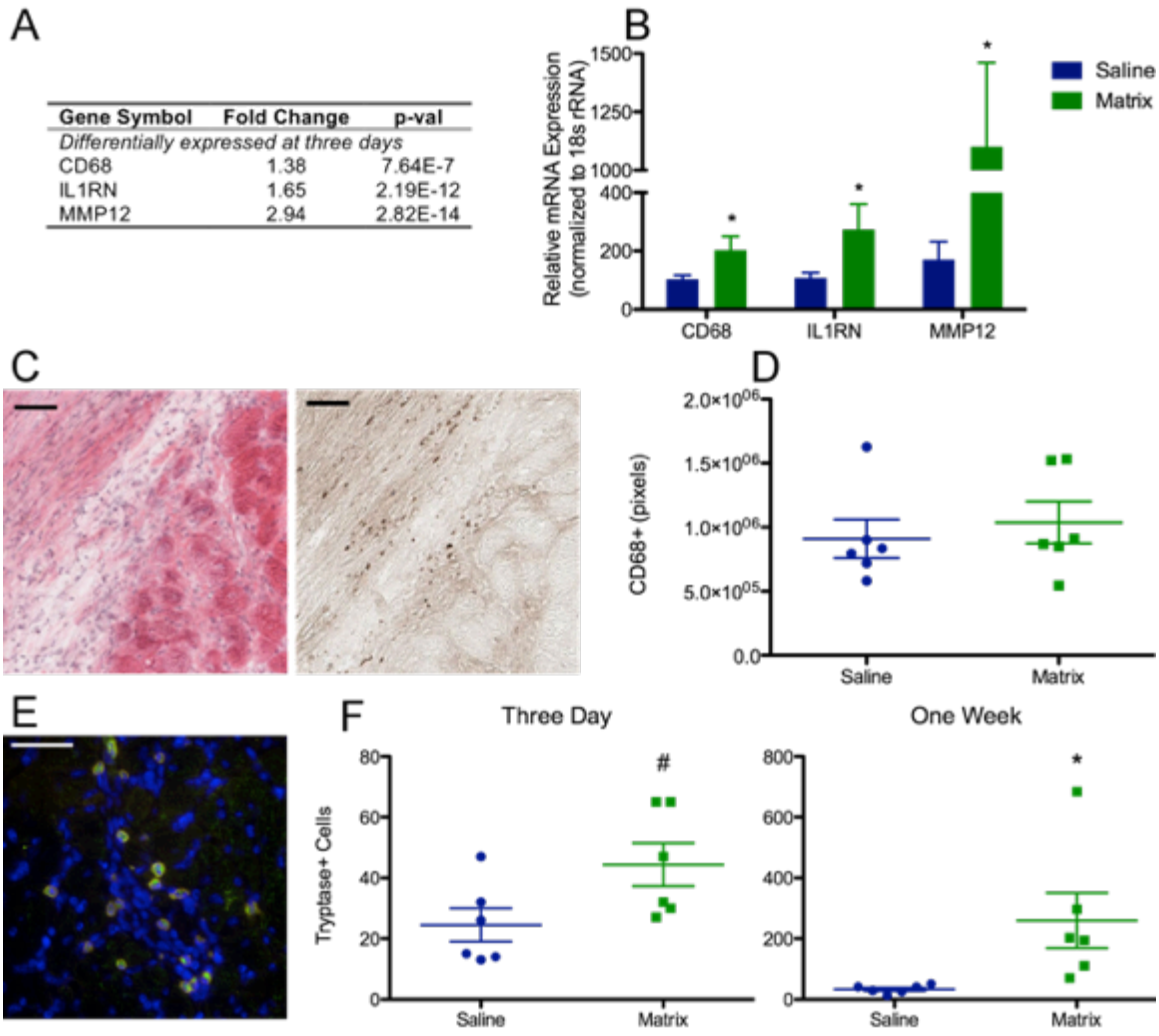

Figure 2.2 Inflammatory response to myocardial matrix injection. A) Differentially expressed genes involved in the inflammatory response from microarray analysis. B) qPCR confirmation of expression of key genes involved in inflammation at three days. C) Example of positive CD68 staining, visualized by DAB (brown) in a myocardial matrix injected infarct day three post-injection (right) along with H&E staining (left) at the corresponding location; scale bar = 50 µm. D) Quantification of CD68 staining in the infarct wall three days post-injection. E) Example of cKit+(green)/tryptase+(red) cells a myocardial matrix injected heart at one week post injection; nuclei are stained blue with Hoescht; scale bar = 50 µm. F) Quantification of trypase-positive mast cells at three days and one week post-injection throughout the entire myocardium. CD68: cluster of differentiation 68, IL1RN: interleukin 1 receptor antagonist, MMP: matrix metalloproteinase 12. (# $p < 0.1$, * $p < 0.05$, ** $p < 0.01$)

2.3.3. Cardiomyocyte Apoptosis

Decreased apoptosis was consistently predicted by Ingenuity at both three days and one week post-injection (Table 2.2 and 2.3). At three days, this is indicated by increased expression of the antioxidative enzyme heme oxygenase 1 (HMOX1), increased expression of the ECM protein osteopontin (SPP1), and decreased expression of lipoxygenase enzyme ALOX15 from the microarray analysis (Figure 2.3A). Expression HMOX1 and SPP1 were confirmed using qPCR ($p = 0.015$ for both, Figure 2.3B). At one week, the microarray data showed increase expression of the anti-apoptosis regulator Bcl-2, increase expression of the antioxidant catalase (Cat), and decreased expression of the apoptosis effector caspase-3 (Casp3, Figure 2.3A). Similarly, qPCR confirmed the significant increased expression of Bcl-2 ($p = 0.006$) and Cat ($p = 0.002$, Figure 2.3B). To determine the effect that myocardial matrix injection may have on cardiomyocytes specifically, we performed anti-cleaved-Casp3 staining with co-labeling of cardiomyocytes using α-actinin (Figure 2.3C). Quantification of the number of Casp3-expressing cardiomyocytes in the infarct wall showed a trend towards decreased apoptotic cardiomyocytes ($p = 0.085$) at three days post-injection within the infarct wall (Figure 2.3D)

A

Gene Symbol	Fold Change	p-value
Differentially expressed at three days		
ALOX15	-1.41	2.61E-7
HMOX1	1.28	9.80E-5
SPP1	2.07	5.36E-24
Differentially expressed at one week		
Bcl-2	1.23	1.35E-3
Casp3	-1.23	1.58E-3
Cat	1.33	1.30E-5

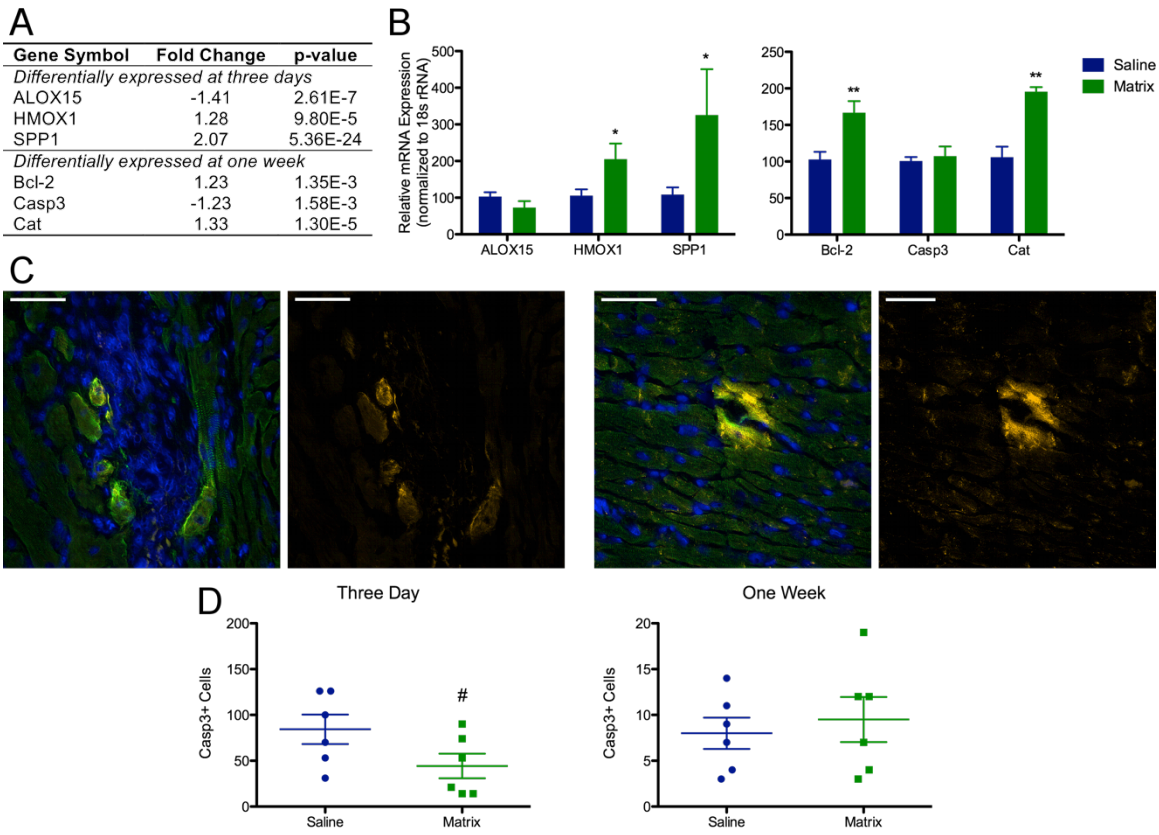

Figure 2.3 Effect that myocardial matrix injection has on apoptosis. A) Differentially expressed genes involved in apoptosis from microarray analysis. B) qPCR confirmation of expression of key genes involved in apoptotic processes at three days and one week post injection. C) Examples of positive cleaved-Casp3-expression in cardiomyocytes; nuclei are stained blue with Hoescht, cardiomyocytes are labeled green (α-actinin), Casp3+ is in red; scale bar = 50 μm. D) Quantification of cleaved-Casp-3 expressing cardiomyocytes within the infarct wall. ALOX15: arachindonate 15-lipoxygenase, Bcl-2: B-cell lymphoma 2, Casp3: caspase-3, Cat: catalase, HMOX1: heme oxygenase-1, SPP1: secreted phosphoprotein 1. (# $p < 0.1$, * $p < 0.05$, ** $p < 0.01$)

2.3.4. Vessel Development

Development of blood vessels was strongly predicted to be activated by Ingenuity at three days post-injection (Table 2.2), as indicated by increase in both the angiogenic placental growth factor (PGF) and endothelial marker vascular cell adhesion molecular 1 (VCAM1, Figure 2.4A). qPCR confirmed increased expression PGF at three days ($p = 0.006$, Figure 2.4B). At one week post-injection, while increased vessels development was not directly predicted, within the gene expression changes that are linked to decreased apoptosis, we noticed that many were growth factors that are associated with angiogenesis and neovascularization; these included decrease in angiopoietin-2 (Ang2) and increase in acidic fibroblast growth factor (FGF1) and vascular endothelial growth factors A and B (VEGFa and VEGFb, Fig. 4A). qPCR confirmed differential expression of Ang2 ($p = 0.012$), VEGFa ($p = 0.034$) and VEGFb ($p = 0.009$), with a trend for FGF1 ($p = 0.053$, Figure 2.4B). To determine whether the increased expression of various growth factors resulted in a change in the infarct vascularization, endothelial and smooth muscle cells within the infarct were labeled with vWF and αSMA (Figure 2.4C). Endothelial cells were quantified by the percentage of green (vWF+) pixels within the infarct and while not significantly different at three days post-injection, by one week, matrix injected groups had significantly higher number of endothelial cells ($p = 0.038$, Figure 2.4D). Quantification of arteriole density showed a similar result, with no difference at three days, but a trend towards increased number of arterioles at one week post-injection in the matrix groups ($p = 0.056$). To further characterize the arterioles, the Feret diameter of the vessels was used to subdivide them into small (< 40 μm), medium (40-100 μm), and large (>100 μm) arterioles. Using this schema, at three days there was a trend for increased number of small arterioles within matrix-injected infarcts ($p = 0.082$) but by one week, the differences has shifted to a significant increase in medium ($p = 0.021$) and a trend for increase in large diameter vessels ($p = 0.065$).

A

Gene Symbol	Fold Change	p-val
Differentially expressed at three days		
PGF	1.29	8.50E-5
VCAM1	1.35	4.61E-6
Differentially expressed at one week		
Ang2	-1.36	6.31E-6
FGF1	1.50	1.85E-9
VEGF-A	1.35	5.36E-6
VEGF-B	1.55	1.12E-10

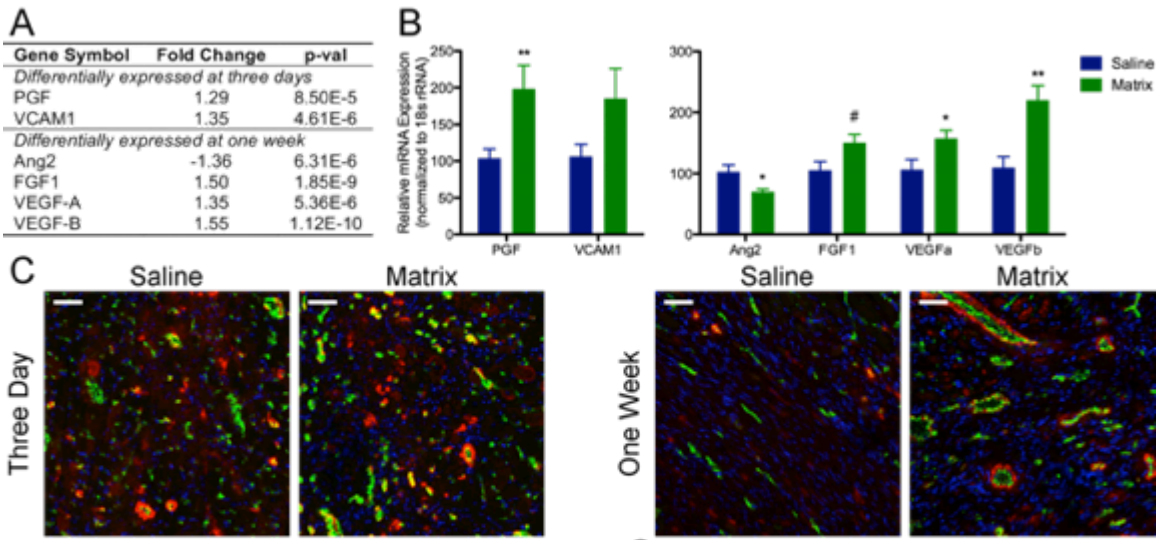

Figure 2.4 Effect that myocardial matrix injection has on blood vessel development. A) Differentially expressed genes involved in vessel development from microarray analysis. B) qPCR confirmation of expression of key genes at three days and one week post injection. C) Representative images from saline or matrix injected infarcts after three days and one week; nuclei are stained blue with Hoescht, endothelial cells are labeled green (von Willebrand Factor), smooth muscle cells are red (α-smooth muscle actin); scale bar = 50 μm.. D) Quantification of endothelial cells migration and arteriole density within the infarct; arteriole quantification is further divided by the Feret Diameter of the vessels. Ang2: angiopoietin 2, FGF1: acidic fibroblast growth factor, PGF: placental growth factor, VCAM1: vascular cell adhesion molecule 1, VEGF: vascular endothelial growth factor. (# $p < 0.1$, * $p < 0.05$, ** $p < 0.01$)

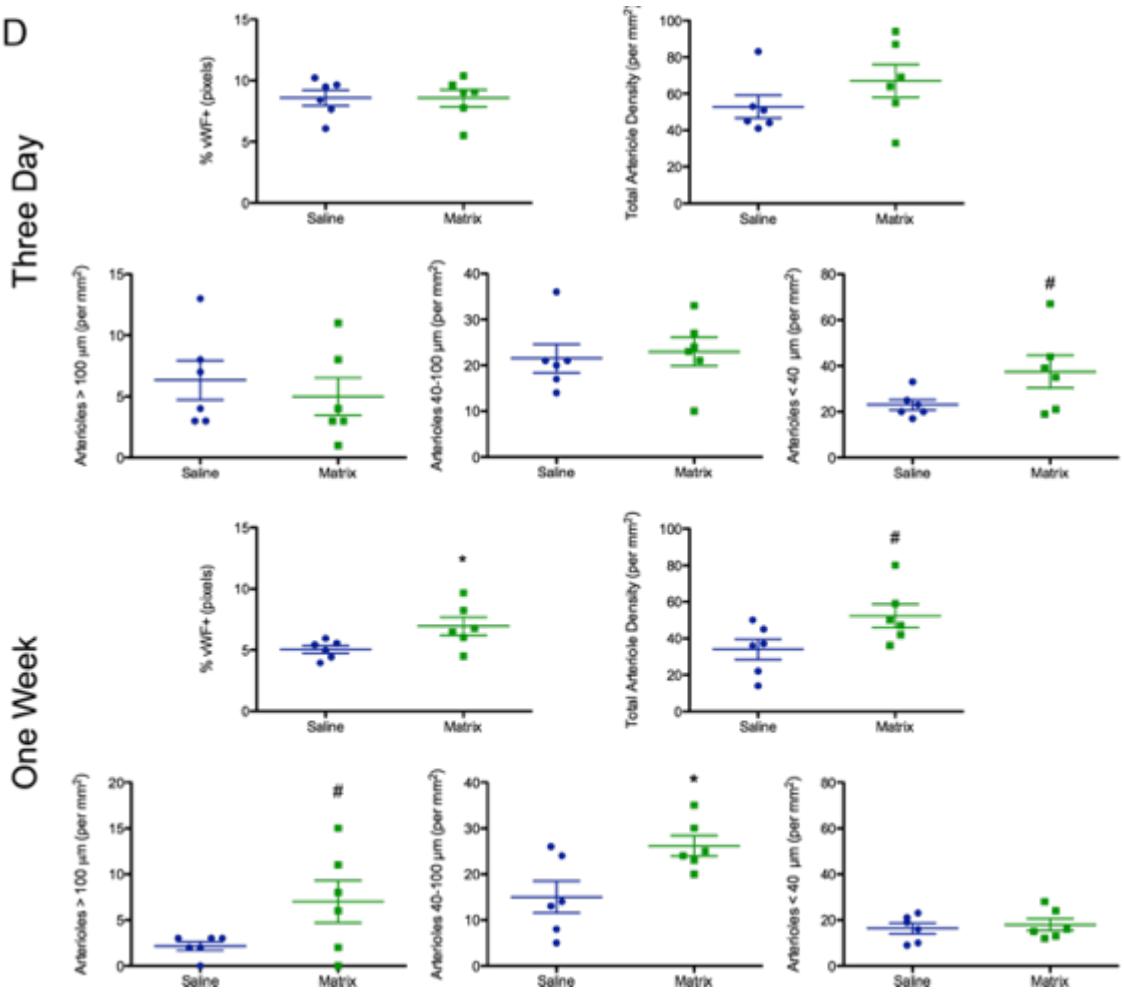

Figure 2.4 Effect that myocardial matrix injection has on blood vessel development. Continued.

2.3.5. Cardiac Metabolism

At one week post-injection, many metabolic pathways where predicted to be activated by Ingenuity Disease & Functions analysis (Table 2.3). Similarly, GO analysis classified as many as 53% of the differentially expressed transcripts to be involved metabolic processes (GO:008152). Within these genes, we identified that several nuclear receptors that regulate metabolism were up-regulated (Figure 2.5A). Notably, this included increased expression of the transcription co-activator PGC-1α and several of the receptors it activates – estrogen related receptor gamma

(ERRγ), peroxisome proliferator-activated receptors alpha (PPARα), and beta/delta (PPARβ/δ) – with quantitative PCR confirming the expression of these genes (p = 0.006, p = 0.001, p = 0.032, p = 0.18, respectively; Figure 2.5B). To determine whether changes in metabolism of cardiomyocytes contributed to this result, IHC was performed to identify expression of PGC-1α specifically within cardiomyocytes, which were identified by α-actinin staining (Figure 2.5C). Quantification of borderzone cardiomyocytes revealed that myocardial matrix injected hearts exhibited higher percentage of PGC-1α expressing myocytes compared to saline injected hearts (p = 0.009, Figure 2.5D).

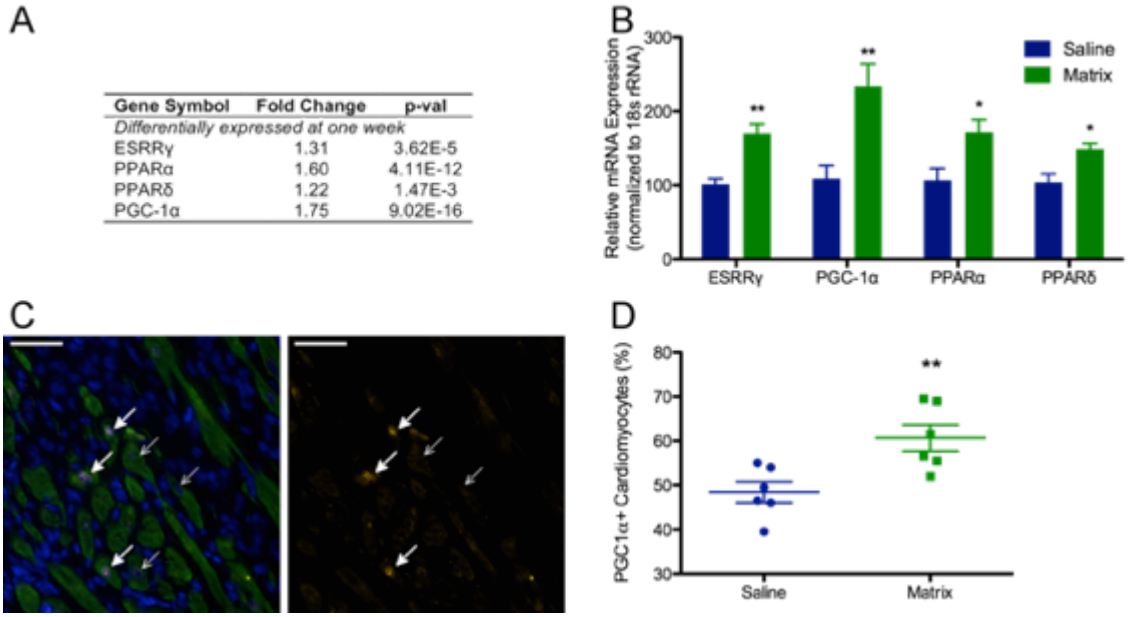

Figure 2.5 Effects that matrix injection has on myocardial metabolism. A) Differentially expressed genes involved in metabolism from microarray analysis. B) qPCR confirmation of expression of key genes involved in metabolic processes at one week post injection. C) Example of PGC-1α expression in cardiomyocytes adjacent to the infarct scar; nuclei are stained blue with Hoescht, cardiomyocytes are labeled green (α-actinin), PGC-1α expression (in red) is limited to the nuclei since it is a transcription factor; thick arrows point to positive PGC-1α stained cardiomyocyte nuclei, thin arrows point to negative nuclei; scale bar = 50 μm. D) Quantification of PGC-1a+ cardiomyocyte nuclei. ERRγ: estrogen-related receptor gamma, PPARα and PPARβ/δ: peroxisome proliferator-activated receptor alpha and beta/delta, PGC-1α: PPAR gamma coactivator 1-alpha. (# $p < 0.1$, * $p < 0.05$, ** $p < 0.01$)

2.3.6. Cardiac Development

Review of the significant GO terms showed several terms associated with development, including cardiovascular system development (GO:0072358 data not shown), due to elevated expression of several cardiac specific transcription factors (Figure 2.6A). qPCR confirmed consistent elevated expression of GATA4 ($p = 0.022$), Nkx2.5 ($p = 0.009$), MEF2d ($p = 0.004$), myocardin (Myocd, $p = 0.004$), Tbx5 ($p = 0.012$), and Tbx20 ($p = 0.043$, Figure 2.6B). IHC was performed using cKit, a commonly used marker for CPCs [126]. Since cKit is also expressed by mast cells [127], tissue sections were co-stained with anti-mast cell tryptase (Figure 2.6C). Quantification of cKit-positive/tryptase-negative cells throughout the myocardium showed that there was a trend at three days ($p = 0.067$) and significant increase at one week ($p = 0.031$) of CPCs in the matrix-injected group (Figure 2.6D).

A

Gene Symbol	Fold Change	p-val
Differentially expressed at one week		
GATA4	1.37	1.82E-6
MEF2d	1.34	7.71E-6
Myocd	1.55	1.01E-10
Nkx2.5	1.44	3.72E-8
Tbx5	1.43	7.32E-8
Tbx20	1.31	4.30E-5

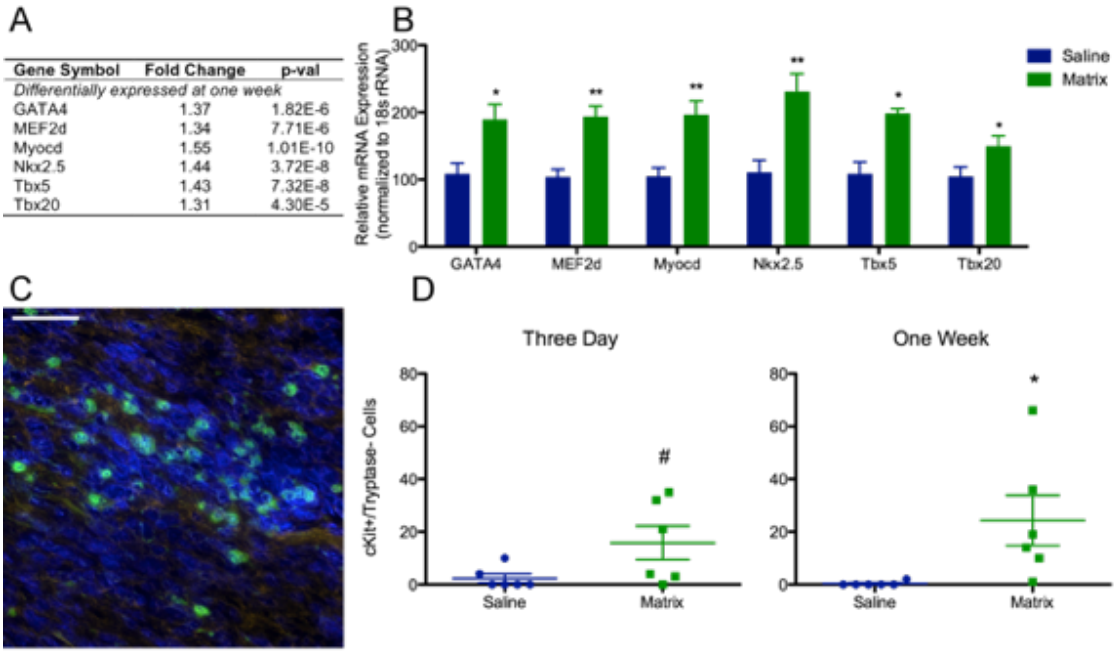

Figure 2.6 Effect that myocardial matrix injection has on cardiac development. A) Differentially expressed genes involved in cardiac development from microarray analysis. B) qPCR confirmation of expression of cardiac transcription factors at one week post injection. C) Example of cKit+(green)/tryptase-(red) cells in the myocardial matrix injected infarct after one week; nuclei are stained blue with Hoescht; scale bar = 50 µm. D) Quantification of cKit+/tryptase- cells at three days and one-week post injection. GATA4: GATA binding protein 4, MEf2d: myocyte enhancer factor 2d, Myocd: myocardin, Nkx2.5: NK2 homeobox 5, Tbx5: T-box 5, Tbx20: T-box 20. (# $p < 0.1$, * $p < 0.05$, ** $p < 0.01$)

2.4. Discussion

Previous small and large animal studies have demonstrated that the myocardial matrix was able to halt the decline in cardiac function and inhibit negative LV remodeling typically seen after MI [41,42]. To better understand the tissue level mechanism of action, we performed an analysis of the infarct gene expression using a whole-transcriptome microarray at both three days and one week post-injection based previous studies indicating cellular infiltration to the injected hydrogel was most pronounced during the first week post-injection [42]. Similar analysis have also been applied to other experimental therapies for MI including cell transplantation [128-130] and injection of cell-derived products [131]. By one week post-injection, the transcriptomes of saline and matrix injected infarcts cluster separately at a global level (for all entities examined), a promising sign of the long-term effect that the myocardial matrix triggers.

Not surprisingly, injection of the myocardial matrix produced an immune response in the infarct as suggested by the increase in cell migration at three days (Table 2.2) and infiltration of various immune cell types at one week (Table 2.3). Gene expression differences within the infarct suggests an increase in macrophage migration in response to the matrix injection with increased transcription of CD68 and MMP12, both predominantly expressed by macrophages [124,125]. However, differences in transcription patterns could also be attributed to changes in immune cell behavior since increase in macrophage infiltration was not demonstrated through anti-CD68 staining. Macrophage phenotype is increasingly recognized as being an important regulator of the immune response and tissue healing, with the characterization of classically-activated M1 and alternatively-activated M2 macrophage that corresponds to the traditional T_H1/ T_H2 paradigm for T-cells [132]. In addition, macrophages polarization in response to decellularized matrices has also been extensively investigated [133-135]. In the heart, it is thought that both types of cells are involved in two distinct phases such that Ly-C^{hi} inflammatory monocytes/classically activated M1 macrophages dominate earlier post-infarct to promote clearance of apoptotic cells and debris, while Ly-C^{low} wound-healing monocytes/alternatively activated M2 macrophages dominate later to induce resolution through angiogenesis and granulation tissue formation [136,137]. Increased

expression of MMP12 and IL1RN both suggest an anti-inflammatory milieu; in particular, MMP12 is known to attenuate the inflammatory response through cleavage and inactivation of CXC- and CC- chemokines [125]. However, collective analysis of all differentially expressed transcripts from the microarray related to the inflammatory response was not conclusive on whether there is a predominance of either M1 or M2 activation. While studies have demonstrated that pro-regenerative M2 macrophages are generally associated with improved outcomes for implanted decellularized matrices through use of IHC [133-135], characterization of macrophages *in vivo* through use of a single antibody is difficult since macrophage phenotype is likely a spectrum and not two distinct populations [138]. The M2 phenotype is particularly heterogeneous, with at least 3 subtypes identified and many markers that are not exclusively expressed by either phenotypes [139]. Lastly, it is likely that both types of monocytes are necessary for post-infarct repair [140] and depletion of either M1 or M2 macrophages inhibits the ability of neonatal hearts to regenerate post-MI [141].

The immune response has been critical in remodeling of decellularized matrices, but current studies have only focused on macrophages [37,133-135], response of other inflammatory cells has received less focus. Since mast cells also express c-Kit, a tyrosine-protein kinase often used to identify progenitor cells in the heart [127], mast cell number in the myocardium was also quantified, with increased numbers found in the matrix-injected group. While mast cells are traditionally associated with an allergic response, current understanding has expanded its involvement to many tissue functions including neovascularization and regulation of the immune response [142]. Rapid mast cell degranulation occurs following ischemia and the released mediators trigger recruitment of other leukocytes as well as prevent cardiomyocyte apoptosis [143]. In later stages, mast cells along with macrophages, orchestrate infarct healing through release of various cytokines and growth factors [143]. Mast cell degranulation products are known to induce proliferation of both fibroblasts and endothelial cells [144]. While one result of this is an association with an adverse fibrotic response post-infarct [145], mast cell products are known to be inherently angiogenic and further increase endothelial secretion of angiogenic, but not

angiostatic chemokines [146]. Furthermore, injection of a low dose of mast cell granules was able to increase capillary density and attenuate LV thinning [147]. In addition, we have previously shown that myocardial matrix injected infarcts were significantly less fibrotic than saline injected controls [42], thus it is unlikely that the increase in mast cells numbers results in increased fibrosis later during infarct progression. This result highlighted the need for studies examining the mast cell response to decellularized matrices. While it is known that mast cell activation may be the first step in the acute inflammatory response to implanted biomaterials [148], its implication on the biocompatibility of decellularized materials, to our knowledge, has not been reported.

After an infarct, cardiomyocyte death peaks 24 hours after the injury and decreases, but continues to be elevated above baseline levels for at least 12 weeks, with the highest percentage occurring in the borderzone in the post-acute period [149]. Thus, delivery of the myocardial matrix at one-week post-infarct can still play an important role in salvaging cardiomyocytes that may be pre-apoptotic. In the histological analysis using anti-cleaved caspase-3, we demonstrate a reduction in cardiomyocyte apoptosis in the infarct wall, corroborating an earlier published result of significantly larger surviving cardiomyocyte islands in the infarct after matrix-injection [41]. Notably, matrix-injected infarcts expressed higher levels of HMOX-1 at three days and catalase at one week, both of which are stress-induced enzymes that reduces reactive oxygen species [150,151]. The fold changes in gene expression are relatively modest (approximately two fold increase of both enzymes by PCR quantification), given the heterogeneous nature of RNA from the infarct wall. However, a three-fold cardiomyocyte-specific increase in catalase activity induced post-infarct was sufficient to decrease hydrogen peroxide levels and improve cardiac function [150].

Macrophages and mast cell recruitment may both contribute to increased vasculature formation. Increase in vessel development, as predicted from the transcriptomic changes, was also reflected in the significant increase in endothelial cells and trend for increased arteriole density at one week post-injection. There were no differences in either metrics between saline and matrix injection after three days and interestingly, the changes over time seem to be due to a

decrease in both endothelial cells and arterioles in the saline-injected controls. Immediately post myocardial infarction, hypoxia-inducible factor 1 (HIF-1) expression triggers transcriptional activation of many angiogenic factors [152], a natural process during wound healing in response to the sudden onset of ischemia. However, decrease in vascular density with time in the infarct scar has been previously reported, with a 63% reduction from one week to four weeks post-MI [153]. This process could be due to vessel regression, a phenomenon well documented in the absence of angiogenic signals [154,155]. Notably, one factor known to induce this process is angiopoietin 2, which was more highly expressed in the saline group compared to matrix. Preservation of the infarct vasculature may be a result of the pro-angiogenic milieu induced by the myocardial matrix injection – whether indirectly, through its effects on other cell types, or directly, from release of bioactive matricryptic peptides from partial proteolysis of the ECM [156]. When arteriole density was broken down by vessel size, it is notable at three days, the difference between matrix and saline injected group was in density of smaller diameter vessels, but at one week, medium and large vessel density were higher in the matrix group. Adaptive arteriogenesis, or remodeling and enlargement of existing vessels, is also mediated by the inflammatory cells and may also contribute to the overall functional improvement seen after myocardial matrix injections [154].

An overall reflection of the above tissue level changes in the infarct wall – altered inflammatory response, improved vascularization, decreased apoptosis – may be the metabolic state of the myocardium. Genes involved metabolic processes made up a majority (53%) of the differentially expressed transcripts using GO analysis. A high-energy demand organ, the healthy heart relies primarily on oxidation of fatty acids for generation of ATP [119]. It has long been known that myocardial ischemia causes a reduction of fatty acid and glucose oxidation due to the anaerobic conditions, a result of which is an increased reliance on glycolysis for energy [157]. PGC-1α, PPARα, PPARβ/δ, and ERRγ are all highly expressed in the heart where PGC-1α activates the transcription of these nuclear receptors to increase fatty acid uptake and oxidation, oxidative phosphorylation, and mitochondrial biogenesis [158,159]. Expression of the targets of

PGC-1α is known to be downregulated in both rodent and human models of heart failure, a response that is likely to be maladpative [160]. Thus, increased transcription of these metabolic regulators in the myocardial matrix-injected infarcts represent a return of myocardial metabolism to a state that is more similar to that of the healthy heart. In addition, metabolic regulation is tightly linked to the inflammatory response [161]. One pathway is through the anti-apoptotic antioxidant HMOX1, which regulates both cardiac mitochondrial biogenesis [162] and anti-inflammatory cytokine expression such as IL-10 and IL1RN [163] through nuclear receptor factors (NRFs), the third family of nuclear factors that are known to be controlled by PGC-1α activation [159]. Conversely, PPARβ/δ activity induces macrophage expression of arginase, a marker of alternative M2 activation [164].

The adult mammalian heart has shown to have a limited ability to regenerate, and many recent efforts have attempted to enhance this ability post-MI for functional restoration [116,126]. Consistent increased expression of many cardiac transcription factors in the myocardial matrix injected group led us to investigate whether there was an increase in cardiac regeneration. GATA4, myocardin, Nkx2.5, Tbx5, and Tbx20 are all expressed throughout various stages of embryonic cardiogenesis [165]. MEF2d, while less prominent compared to MEF2c in heart development, plays an important function in mediating adaption to physiological stresses in the adult heart [166]. Since GATA4, Nkx2.5, and Tbx5 are frequently used to identify various CPC subsets [167], concomitant expression of these cardiac transcription factors could be indicative of increased number of CPCs post-myocardial matrix injection. c-Kit has been a popular marker for identifying CPCs, however, many hematopoietic cells also express c-Kit, including mast cells that reside in the heart [127]. Thus CPCs were identified by their expression of c-kit in the absence of tryptase expression and quantified throughout the myocardium. A significant increase in c-kit+/tryptase- cells were detected in matrix injected groups after one week, suggestive of recruitment or activation of endogenous progenitor cells.

Stimulation of endogenous CPCs to regenerate has been proposed by several studies as a mechanism of action for various transplanted cells, some of which are currently in clinical

trials [168-171]. Loffredo et al. reported that transplantation of bone marrow-derived c-kit+ cells lead to an increase in endogenous cell expression of Nkx2.5 and GATA4 and improvement in ejection fraction, an effect not seen with a similar transplantation of mesenchymal stem cells, leading them to postulate that stimulation of endogenous progenitor activity is a critical mechanism of cell therapy-induced improvement in cardiac function [168]. However, the importance of c-kit+ cells in post-infarct recovery has been a controversial subject and two recent studies have arrived at opposite conclusions. While Ellison et al. demonstrated that c-kit+ CPCs are necessary and sufficient for functional cardiac regeneration [172], van Berlo et al. concluded that endogenous c-kit+ cells produces new cardiomyocytes at a minimal level that is not functionally substantial [173]. In addition, it is also possible that cKit+ endogenous cells contribute to other effects of the myocardial matrix injection. While very few c-kit+ cells became cardiomyocytes post-infarct, van Berlo et al. concluded that a majority of them (77%) differentiated into CD31+ endothelial cells [173]. Similarly, cKit+ cells have also shown to affect myocardial vascularization through secretion of angiogenic cytokines such as VEGF [174], suggesting that they may be the source of several angiogenic growth factors (PGF, VEGFa, VEGFb, FGF1) whose expression was increased in matrix-injected groups.

Alternative sources of the elevated expressions of cardiac transcription include: 1) an increase in cardiomyocyte health, since GATA4, myocardin, Nkx2.5, and Tbx20 are expressed by adult cardiomyocyte and are required for their survival and function [175-178], 2) cardiac hypertrophy, which is associated with elevated GATA4, MEF2d, and Nkx2.5 [166,179,180], and 3) non-myocyte expression such as cardiac fibroblasts, which express high levels of GATA4 and Tbx20 [181]. However, we do not believe these are major contributors of variation between saline and matrix-injected infarcts due to the concomitant increase of six transcription factors for cardiac development. In addition, quantification of long-term cardiac hypertrophy and the fibrotic response, which were both significantly lower in the matrix injected hearts, also do not support these alternative hypothesis.

2.5. Conclusion

We have previously demonstrated that injection of the myocardial matrix into both rat and pigs models of MI attenuates the decline in cardiac function and halts negative LV remodeling [41,42]. In this study, we provide both transcriptional and histological evidence that the myocardial matrix may mediate this through directly or indirectly inducing the following tissue level changes: 1) modulating the inflammatory response, 2) reducing cardiomyocyte apoptosis, 3) enhancing the development of blood vessels, 4) altering myocardial metabolism, and 5) inducing cardiogenesis. These results provide further evidence for the promise of the myocardial matrix as a therapy to prevent the development of HF post-infarction.

Chapter 2, in part, is a reprint of the material as it is published in: Jean W. Wassenaar, Robert G. Gaetani, Julian J. Garcia, Rebecca L. Braden, Colin G. Luo, Diane Huang, Anthony N. DeMaria, Jeffrey H. Omens and Karen L. Christman. “Evidence for the Mechanisms Underlying the Functional Benefits of a Myocardial Matrix Hydrogel for Post-MI treatment”. (2016) *J Am Coll Cardiol*, 67(9):1074-86. The dissertation author was the primary author of this manuscript.

Chapter 3: Effects of the Myocardial Matrix and its Degradation Products on Cardiac Cell Behavior

3.1. Introduction

The use of ECM derived biomaterials as scaffolds for tissue engineering applications has increased dramatically in the past decade [18]. While originally thought of as an inert scaffold that primarily provides structural support to tissue, the ECM is now known to be an important modulator of cell behavior. Since ECM composition can vary widely across tissues, decellularization is a strategy that is increasingly employed since the resulting ECM scaffold retains the native mixture of macromolecules. Further processing of decellularized ECM into a hydrogel form provide an additional advantage since this allows them to be cast in a variety of 3D shapes for cell culture or injected into host tissue for *in situ* tissue engineering. Our lab has previously developed a method for processing tissues by decellularization followed by partial pepsin digestion to create injectable ECM hydrogels [182]. Using this protocol, hydrogels have been successfully derived from a variety of tissues, including heart [40], pericardium [183], skeletal muscle [184], brain [185], and adipose tissue [186]. In addition, other groups have used similar methods of pepsin digestion to produce solubilized ECM from decellularized urinary bladder [187], small intestine submucosa [188], dermis [189], bone [190], and other tissues.

Post-decellularization, the ECM scaffold retains many of its native chemical cues and structural properties. Despite some protein damage from the decellularization process, scaffolds are still able to promote regeneration of injured tissue while their degradation products have shown to be chemoattractant [191], angiogenic [192], and anti-microbial [193]. Furthermore, various growth factors survive tissue processing and are released during scaffold degradation to promote angiogenesis, proliferation, and differentiation [194]. The process of partial pepsin digestion used to form ECM hydrogels can also generate cryptic peptide fragments [156]. For example, fibronectin fragments, a degradation product of ECM, can recruit and stimulate pro-remodeling macrophages to release cytokines to protect hypoxic myocytes from apoptosis [65]. Many previously injected materials also exhibit signs of increased neovascularization [21,40,188].

The myocardial matrix has been previously characterized by our lab [40,41] and the tissue level changes it induced once injected in the heart post-MI was investigated in chapter 2. However, how it interacted with the cells in the infarcted myocardium, whether in the hydrogel form or through its degradation products, is less well understood. To simulate breakdown of the myocardial matrix *in vitro*, we divided the process into two parts. We hypothesize that first, immediately after injection and gelation *in vivo*, there is a burst release of soluble peptides from the myocardial matrix. These peptides do not participate in the self-assembly process of gelation, and are able to diffuse from the hydrogel. *In vitro*, this was simulated by adding PBS or media to the hydrogel and collecting the elution products. In the second phase, inflammatory cells and fibroblasts are recruited to the injection site and begin to secrete various proteases to digest the matrix. This process will be approximated *in vitro* through use of recombinant MMP2 and MMP9, which are upregulated in the post-infarct myocardium and secreted by both the recruited immune cells (neutrophils and macrophages) and the surrounding cells (fibroblasts and myocytes) [195]. Once the two types of degradation products were produced, relevant cell types within the infarct milieu were cultured with the myocardial matrix, whether in contact with the hydrogel form or through exposure of the degradation products. In particular the effects on cardiomyocyte survival, cardiac progenitor recruitment, macrophage phenotype, and cardiac fibroblast ECM production were examined. Identification of the direct effects that the myocardial matrix has on cardiac cell behavior will provide background and preliminary data for further experiments to better understand the molecular basis of the myocardial matrix's mechanism of action.

3.2. Materials and Methods

3.2.1. Preparation of the Myocardial Matrix and Collagen Hydrogels

Porcine ventricular myocardium was decellularized using sodium dodecyl sulfate (SDS) and then pepsin digested as previously described [40-42]. Specifically, 10 mg/mL of myocardial matrix powder was mixed 1 mg/mL pepsin dissolved in 0.1M HCl. After 48 hours of pepsin

digestion, the liquid myocardial matrix was brought to pH 7.4 and 6 mg/mL with NaOH and phosphate buffer saline (PBS). Since the matrix was intended for use in cell culture conditions, care was taken to adjust the final salt concentration to a physiological level of 8 mg/mL NaCl. For experiments involving cell culture on top or encapsulated within the myocardial matrix, collagen I hydrogels were used as controls. Liquid Rat Tail Collagen (Life Technologies) was brought to pH 7.4 per manufacturer's instructions using NaOH, 10x PBS and 1x PBS. Final concentration of collagen was 2.5 mg/mL based on pervious reports determining that at this concentration, collagen hydrogels have similar mechanical properties and fiber architecture as 6 mg/mL ECM derived hydrogels [196]. Gelation of both myocardial matrix and collagen were induced by incubation at 37 °C overnight.

3.2.2. Simulation of Myocardial Matrix Degradation

Degradation of the myocardial matrix is simulated *in vitro* through a two step process depicted by Figure 3.1: 1) diffusion of soluble peptides and 2) digestion of the solid hydrogel by MMPs. After overnight gelation in microcentrifuge tubes, 900 µL of either PBS or media is added to 100 µL myocardial matrix hydrogels. Soluble peptides that do not participate in hydrogel self assembly diffuses into the supernatant which is collected 24 hours later as the "elution" fraction at an 1:10 dilution. Subsequently, 100 µL of active human recombinant MMP2 and MMP9 (Abcam, ab81550 and ab39308) were added to the solid hydrogel portion and incubated at 37 °C. MMP2 and MMP9 were diluted to 5 µg/mL in a MMP activation buffer containing 1 mM 4-aminophenyl mercurial acetate (APMA, Sigma-Aldrich), 0.1 µM ZnCl, and 10 mM $CaCl_2$ dissolved in PBS. After 24 hours of protease digestion, 800 µL of PBS or media was added to each sample to bring the digested peptides to a similar 1:10 dilution as the eluted fraction. Samples were then centrifuged at 5000 g for 5 minutes to pellet the undigested portion, after which the supernatant was removed and represented the "digestion" fraction of the degradation products.

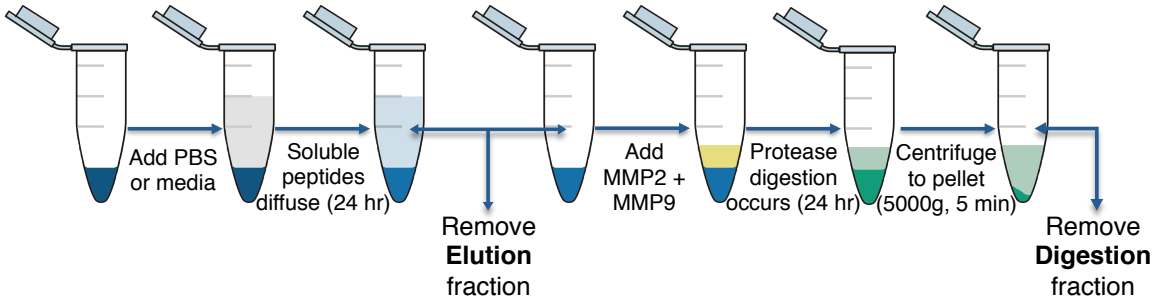

Figure 3.1 Schematic depicting simulation of myocardial matrix hydrogel degradation in vitro. A two step process is used to mimic two different fractions of peptides that cardiac cell may encounter *in vivo* after hydrogel injection. The first are soluble peptides diffusing from the matrix, termed the "elution fraction"; the second are peptides released by MMP digestion to mimic the process *in vivo* as cells migrate to and interact with the injected hydrogel.

For subsequent cell culture experiments, the controls were pepsin or MMP2+9 diluted to the same concentration, for the elution and digestion fraction respectively. Specifically the pepsin solution containing 1 mg/mL pepsin from porcine gastric mucosa (Sigma) was stirred at 48 hours at room temperature in 0.1 M HCl, then brought to pH 7.4 and adjusted to 0.6 mg/mL using NaOH and PBS similar to preparation of the myocardial matrix. This solution is further diluted 1:10 with media to produce a concentration-matched control for the elution fraction. MMP solution was prepared by diluting MMP2 and MMP9, both at 5 µg/mL in 100 µL of MMP activation buffer, with 900 µL of media to match the concentration in the 1:10 dilution digestion fraction.

3.2.3. Characterization of the Degradation Products

Concentration of proteins in the myocardial matrix and the degradation products were quantified with the Pierce BCA Protein Assay Kit (Life Technologies). Liquid myocardial matrix diluted 1:20 fold (to 0.3 mg/mL), elution, and digestion products were frozen then lyophilized (n = 3). To help improve the detection of proteins in the samples, all samples were resuspended in a 5% SDS solution, which was shown to improve collagen detection in colormetric protein assays [197]. Samples were compared against a standard curve, created from bovine serum albumin dissolved in 5% SDS, per manufacturer's procedure for use with a microplate reader. Samples

were incubated at 37 °C for 30 minutes then the corrected absorbance at 562 nm was measured using a BioTek Synergy 4 spectrophotometer (BioTek Instruments). The difference between peptide species with and without MMP digestion was analyzed with SDS Page Gels. After the elution fraction was extracted, solid portion of the hydrogels were either digested with MMP2 and MMP9 as described in section 3.2.2 or incubated with the MMP activation buffer alone. The samples were centrifuged after 24 hours and the supernatant and pellet (component 1 and component 2 respectively) were separated for freezing and lyophilization. Samples were resuspended in 5% SDS and then loaded into NuPAGE 12% Bis-Tris Gels (Life Technologies) according to manufacturer's protocols under reducing conditions using MOPS SDS Running Buffer. Amersham ECL Full-Range Rainbow Molecular Weight Markers (GE Healthcare Life Sciences) was used as the protein ladder. Gel electrophoresis was performed in an Xcell Surelock Minicell (Invitrogen) at constant 200 V for 50 minutes. Protein bands were visualized with Imperial Protein Stain (Thermo Scientific).

3.2.4. Cardiac Progenitor Migration

Human cardiomyocyte progenitor cells (hCMPC) were isolated by sorting for murine Sca-1 antigen [198]. Cells were seeded on 0.1% gelatin and cultured in a growth medium containing EGM-2 (Lonza) and M199 (BioWhittaker) with 10% fetal bovine serum (FBS, Hyclone), 1x penicillin/streptomycin (P/S, Sigma), and 1x MEM non-essential amino acids (BioWhittaker). Cells were switched to serum free media (growth media without FBS) when 75% confluency is reached. After 24 hours serum starvation, cells were trypsinized then fluorescently labeled with 10 μM CFSE Cell Trace (Life Technologies) in PBS for 15 minutes at 37 °C. Cells were washed, resuspended in serum free media and plated onto the upper chamber of FluoroBlok Cell Culture Inserts with 8 μm pores (Corning) placed in 24 well plates. Elution and digestion fractions, along with their respective enzyme-only controls, were added to the wells at both 1:10 and 1:100 dilutions. Serum free media and growth media with 10% FBS were also added, serving as

negative and positive controls. Cell migration across the fluorescently opaque transwell membrane was manually counted at 4 hours and 8 hours after initial seeding onto Fluoroblok inserts from one representative image at 10x taken of the bottom of each insert (n = 3 per condition) using a Carl Zeiss Observer D.1 microscope.

3.2.5. Cardiomyocyte Viability Under Stress

Rat neonatal cardiomyocytes were isolated from 1-day-old Sprague-Dawley rats according to manufacturer's directions using the Neonatal Cardiomyocyte Isolation System (Worthington Biochemical Corporation). The cell suspension collected at the end of the protocol was plated on a tissue culture flask twice for 2 hours each to enrich for cardiomyocytes to improve cardiomyocyte purity, since adherent cardiac fibroblasts are removed from the cell suspension. Optimization of this pre-plating protocol determined that 2 pre-plates at 2 hours each resulted in cardiomyocyte purity of approximately 75-85%. Afterwards, non-attached cells were collected and resuspended in a culture media of 1 g/L glucose DMEM with 10% FBS And 1% P/S. For immunohistochemistry, cells were also plated in 48-well plates coated with 1 mg/mL collagen at 150,000 cells/well (n = 3 wells) and stained with anti-Troponin I (1:100; Abcam ab47003) followed by Alexa Fluor 568 Goat-anti-Rabbit (1:200, Life Technologies). Nuclei were visualized with Hoescht 33342 (Life Technologies). Cardiomyocyte purity was determined by counting with Cell Profiler of four 20x images from each well. For cardiac stress experiments, cells were plated on myocardial matrix or collagen hydrogels formed in 96-well plates at 50,000 cells/well. After overnight culture, media was changed to serum free conditions, with increasing concentrations of hydrogen peroxide (n = 6 per condition). AlamarBlue Cell Viability Reagent (Invitrogen) was added to each well at $1/10^{th}$ the volume of media added. After 4 hours of incubation, 100 µL of media from each well was removed and its fluorescence read by a BioTek Synergy 4 spectrophotometer (excitation = 550 nm, emission = 585 nm). Fluorescence was normalized to readings taken from reference wells under serum-supplemented conditions.

3.2.6. Cardiac Fibroblasts Production of MMPs

Cardiac fibroblasts were collected as the adherent fraction to tissue culture plastic at the end of cardiomyocyte isolation described in section 3.2.5. Fibroblasts were cultured in 1 g/L glucose DMEM with 10% FBS and 1% P/S. Cells were passaged with trypsin once 90% confluency is reached and plated on either collagen or myocardial matrix hydrogels formed in 48-well plates at 120,000 cells/well (n = 6). Fibroblasts were also seeded in 6-well plates at 500,000 cells/well and cultured in serum free media and the degradation products or their respective enzyme only controls at the 1:100 dilution (n = 3). Cells were cultured for 48 hours after which a sample of media from each well was collected. Media were mixed with equal volume of Tris-Glycine SDS Sample Buffer (Life Technologies) and analyzed using Novex Zymogam 10% Gelatin Gels (Life Technologies) per manufacturer instructions. Amersham ECL Full-Range Rainbow Molecular Weight Markers were used as the protein ladder. Gels underwent electrophoresis using the XCell SureLock Mini-Cell for 90 minutes under constant 125 V. Gels were developed using renaturing buffer and developing buffers, then visualized with Imperial Protein Stain. Band intensity was quantified by ImageJ (NIH) Gel Analyzer.

3.2.7. Macrophage Phenotype Characterization

Bone marrow derived macrophages were isolated from adult C57BL/6 mice based on previously published protocols [199,200]. Briefly, bone marrow was isolated from both femurs and tibias and resuspended in macrophage culture media consisting of RPMI-1640 (Sigma) with 30% L-cell media, 20% heat-inactivated FBS, and 1% P/S. L-cell media was collected from L929 mouse fibroblasts cultured in DMEM with 10% heat-inactivated FBS and 1% P/S after 7 days of culture. Bone marrow cells were plated onto petri dishes and cultured for 7 days, during which clonal expansion of macrophages occurs such that the resulting cell population is > 95% F4/80+. Macrophages were collected between day 7 and day 10 of culture by cell scrapers. Macrophages

were encapsulated in 25 µL hydrogels of either myocardial matrix or collagen (n = 24) at a concentration of 300,000 cells/gel. Prior to encapsulation, cells were fluorescently labeled by incubation with Calcein AM (Life Technologies) at 100 nM for 30 minutes. The hydrogel and cell suspension was incubated for 20 minutes at 37 °C to allow gelation before addition of macrophage culture media with 10% AlamarBlue. Viability of encapsulated macrophages was measured by AlamarBlue fluorescence, as described in in section 3.2.5 after 6 hours of culture, after which media was refreshed. Encapsulated cells were cultured for 48 hours and their survival within the hydrogels verified by observation of Calcein fluorescence. RNA from encapsulated macrophages was isolated using the RNeasy Mini Kit (Qiagen) by combining eight 25 µL gels in a single isolation. Macrophages were also plated at 1 million cells/well in 6-well plates and exposed to the myocardial matrix degradation products and enzyme-only controls at the 1:10 dilution. Phenotypic changes were compared to macrophages polarized by the following cytokine inductions: interleukin-4 (IL-4; 20 ng/mL) for 48 hours for M2 or lipopolysaccharide (LPS; 100 ng/mL) and interferon gamma (IFNγ; 20 ng/mL) for 24 hours. For the LPS challenge experiments, 100 ng/mL of LPS was added to plated macrophages after 48-hour exposure to matrix degradation products and enzyme controls for 2 hours. RNA from all plated macrophages was isolated by Trizol extraction (Invitrogen) and treated with DNAse I using the RNAse-Free DNAse Set (Qiagen). RNA quality and concentration from both encapsulation and plated experiments were measured by a NanoDrop 2000c Spectrophotometer (Thermic Scientific). cDNA conversation was performed using 1 µg of total RNA and random hexamer primers with the SuperScript III Reverse Transcriptase kit (Invitrogen). qPCR was performed using the theSYBR Green Real-Time PCR Master Mix (Life Technologies) with a final concentration of 1 µM forward and reverse primers. Primer sequences are in Table 3.1. Samples were run on a CFX96 Touch Real-Time PCR Detection System (Bio-Rad) with the following thermal cycles: 2 min at 50 °C, 10 min at 95 °C, followed by 40 cycles of 15 s at 95 °C and 1 min at 60 °C. Each experiment had an experimental triplicates and technical duplicates. Macrophage polarization for the M1 phenotype

was measured by expression of inducible nitric oxide synthase (iNOS) and tumor necrosis factor alpha (TNFα); M2 phenotype was assessed by expression of arginase-1 (Arg-1) and chitinase 3-like-3 (Ym-1). All data was normalized to GAPDH.

Table 3.1 PCR Primer Sequences. Forward and reverse primer sequences for macrophage phenotype genes and the housekeeping gene GAPDH.

	Forward Sequence (5'-3')	**Reverse Sequence (5'-3')**
GAPDH	CATCAAGAAGGTGGTGAAGC	GTTGTCATACCAGGAAATGAGC
iNOS	CAGCTGGGCTGTACAAACCTT	CATTGGAAGTGAAGCGTTTCG
TNFα	GACCCTCACACTCAGATCATCT	CCACTTGGTGGTTTGCTACGA
Arg-1	GAACACGGCAGTGGCTTTAAC	TGCTTAGTTCTGTCTGCTTTGC
Ym-1	AGAGCAAGAAACAAGCATGG	CTGTACCAGCTGGGAAGAAA

3.2.8. Statistical Analysis

For experiments involving the degradation products and enzyme controls, one-way ANOVAs were performed followed by either Tukey's or Dunnett's post-hoc testing. Comparisons between collagen and myocardial matrix hydrogels were made using student t-test. Significance was accepted at $p < 0.05$. Data and error bars are reported as mean ± standard error of mean.

3.3. Results

3.3.1. Characterization of the Myocardial Matrix Degradation Products

Using the BCA Protein Assay, 3.21 ± 0.24 mg/mL of protein was detected in a hydrogel made from 6 mg/mL of powder myocardial matrix (Table 3.2). Of this, 1.24 ± 0.10 mg/mL was quantified in the eluted fraction, suggesting that a significant portion (39%) of the protein did not participate in hydrogel self-assembly and are able to diffuse out rapidly. While digestion of the remaining hydrogel with MMP2 and MMP9 did not cause complete dissolution, further release of another 0.46 ± 0.10 mg/mL of protein (14%) was quantified by the BCA assay.

Table 3.2 Protein content of the myocardial matrix hydrogel and its degradation products. Protein concentration was measured by the BCA assay.

	Hydrogel	Elution	Digestion
Protein (mg/mL)	3.21 ± 0.24	1.24 ± 0.10	0.46 ± 0.10
% protein	--	38.6 ± 4.2%	14.2 ± 3.3%

To confirm that the recombinant MMPs were active and able to cleave the solid hydrogel portion of the myocardial matrix, the digestion fraction and the remaining pellet of samples collected with and without MMP2+9 addition were run in SDS Page gels (Figure 3.2). Changes in band intensity along with appearance of new bands provide further evidence that the MMPs were able to digest the hydrogel *in vitro*.

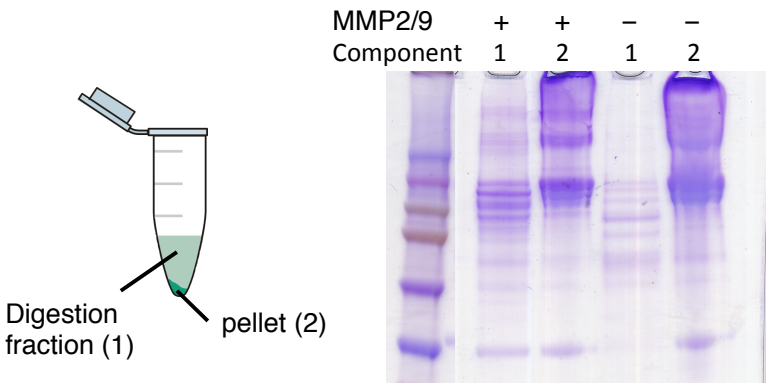

Figure 3.2 MMP2 and MMP9 digestion further degrades the myocardial matrix hydrogel. After elution products were collected by removal of the supernatant, remaining solid hydrogels were digested with MMP2 and MMP9. Control hydrogels were treated with only MMP activation buffer. After 24 hours incubation, samples were centrifuged to pellet the undigested portion (component 2). Both the digested fraction (component 1) and pellet (2) were run on SDS Page hydrogels. Changes in band patterns from samples treated with and without MMP indicate that MMPs were active and cleaved components of the hydrogel.

3.3.2. hCMPCs Migrate Towards Myocardial Matrix Degradation Products

Since it was previously observed that myocardial matrix injected infarcts exhibited increased expression of several cardiac transcription factors as well as increased number of cKit+

cardiac progenitors (chapter 2), the ability of the degradation products to recruit progenitor cells was evaluated. Migration of hCMPC towards the myocardial matrix degradation products were assessed using the transwell insert cell culture system. Serum starved, fluorescently labeled hCMPC were seeded on the top of the opaque membrane and allowed to migrate towards the degradation products and their enzyme controls at both 1:10 (Figure 3.3A) and 1:100 (Figure 3.3B) dilutions. Serum free media and serum supplemented media (10% FBS) served as negative and positive controls, respectively. Migration of cells across the membrane increased with time and concentration of the degradation products. Pepsin and MMP did not induce migration compared to serum free conditions at either concentration. By 8 hours after initial cell seeding, both fractions had significantly higher rate of cell migration compared to their respective enzyme only controls, as well as serum free condition. However, the elution fraction elicited a higher degree of cell migration compared to the digestion fraction. This is especially evident in the 1:100 dilution condition, where at 4 hours, only the elution fraction had significantly higher cell numbers compared to its enzyme-only control pepsin.

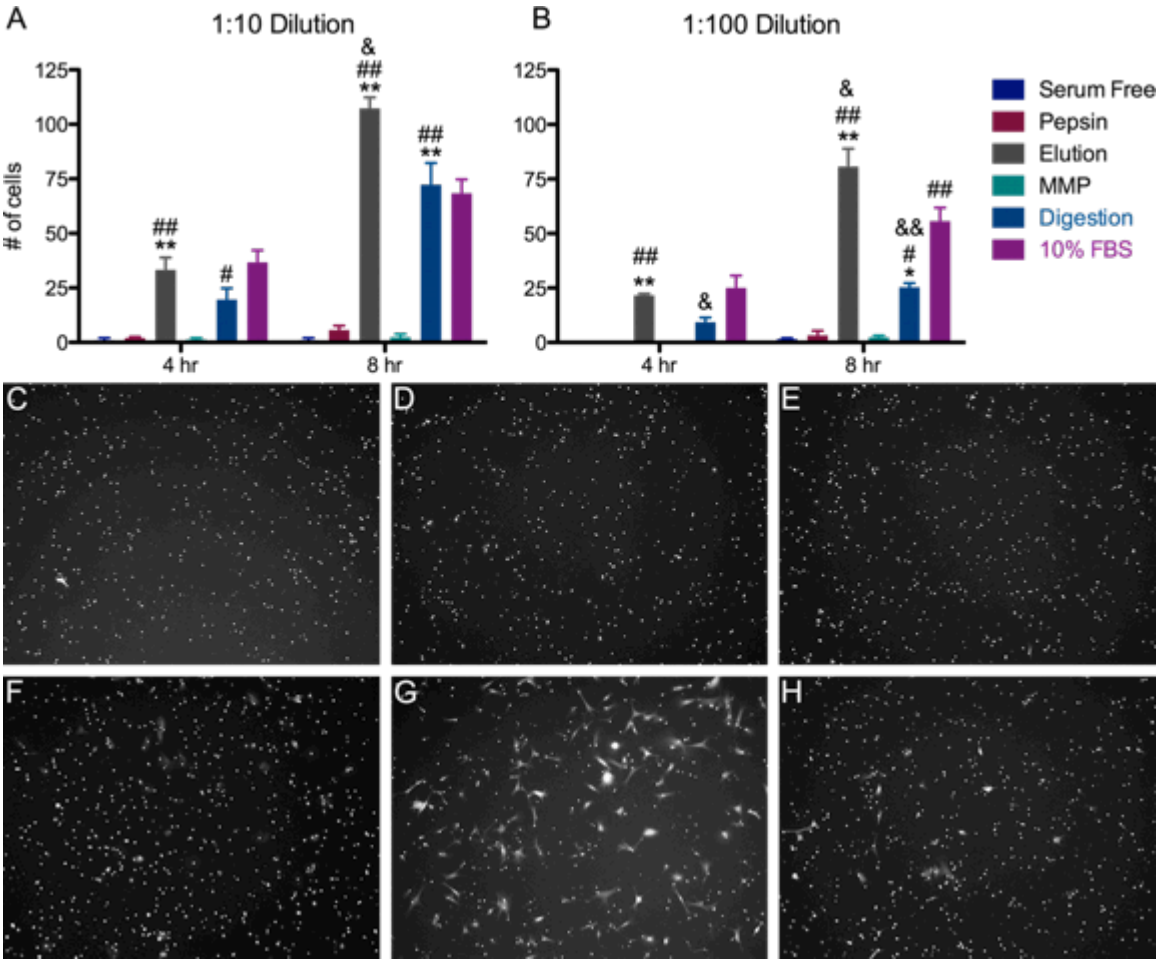

Figure 3.3 Human cardiomyocyte progenitor cell (hCMPC) migration. Migration of hCMPC towards myocardial matrix degradation products at 1:10 (A) and 1:100 (B) dilution. Representative images taken at 10x of cells at 8 hours after addition of the 1:200 dilution condition: C) serum free media, D) pepsin, E) matrix metalloproteinase (MMP), F) 10% FBS, G) elution fraction, and H) digestion fraction. * $p < 0.05$, ** $p < 0.01$; *: elution and digestion fraction compared to enzyme only controls pepsin and MMP, #: compared to serum free negative control, &: compared to 10% FBS positive control.

3.3.3. Culture of Cardiomyocytes on the Myocardial Matrix Improve Stress Response

Neonatal rat cardiomyocytes were isolated from 1-day-old rats using an enzymatic digestion protocol which yielded a cell population that was 75-85% cardiomyocytes, as determined by troponin I expression (Figure 3.4A). Cell viability of cardiomyocytes cultured on either myocardial matrix or collagen hydrogels under various stressed conditions were measured by the AlamarBlue assay. Cardiomyocytes cultured on myocardial matrix were able to better

withstand a switch to serum free media ($p < 0.001$). To simulate the reactive oxygen species (ROS) that are present in the myocardium post-ischemia reperfusion, increasing concentration of hydrogen peroxide were added to the serum free media (Figure 3.4B). At all the concentrations examined (200 μM to 5 mM), cardiomyocytes cultured on myocardial matrix had higher cell viability compared to collagen hydrogels ($p < 0.001$ at all concentrations). At 200 μM peroxide, cells cultured on the myocardial matrix have similar viability as the serum-free condition, while collagen groups still had significantly lower viability ($p < 0.01$).

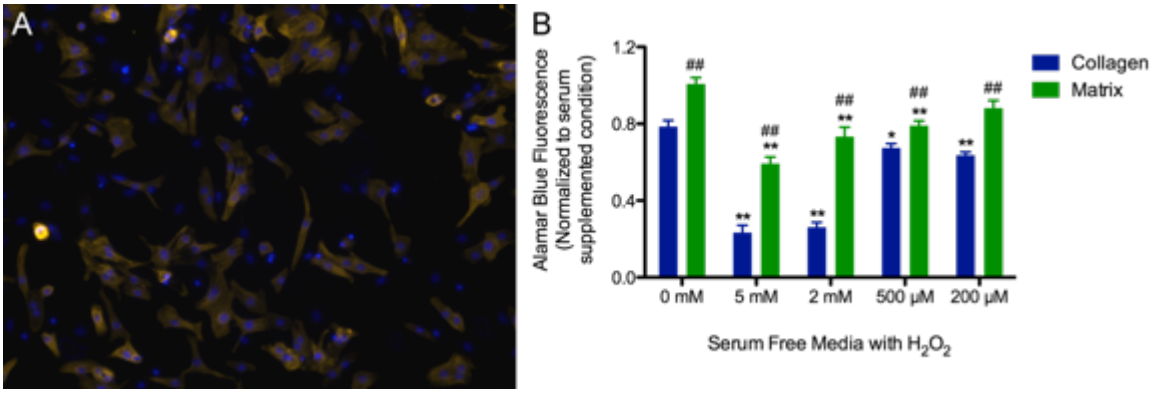

Figure 3.4 Neonatal rat cardiomyocyte response to stress. A) Purity of cardiomyocytes, measured by counting the percentage of Hoescht-stained nuclei (blue) within troponin I-positive (red) cells, was approximately 75-85%. B) Cell viability, determined by AlamarBlue fluorescence, of cardiomyocytes cultured on collagen versus myocardial matrix hydrogels under serum free conditions with various concentrations of hydrogen peroxide (H_2O_2). * $p < 0.05$, ** $p < 0.01$; *: one-way ANOVA for either hydrogel condition followed by Dunnett's multiple comparison correction compared to serum free media, #: student t-test comparing collagen and matrix culture within each H_2O_2 concentration.

3.3.4. Cardiac Fibroblasts Increase MMP Production in Response to the Myocardial Matrix

Tissue culture plastic-adherent cardiac fibroblasts were isolated as part of the protocol to isolated neonatal rat cardiomyocytes. To determine whether the myocardial matrix has any direct effects on cardiac fibroblast behavior, cells were cultured both on the hydrogel and exposed to the degradation products. Media from each culture condition were then analyzed by gel zymography using 10% gelatin gels, which allows for quantification of MMP2 and MMP9 (gelatinase A and B). Compared to fibroblasts cultured on collagen, myocardial matrix hydrogels

induced a dramatic increase in both MMP2 and MMP9 production (Figure 3.5A). Quantification of the band intensity showed significant increase in pro-MMP9 (92 kDA), pro-MMP-2 (72 kDA), and cleaved-MMP2 (67 kDA) (Figure 3.5B, $p < 0.001$ for all). For cells plated on tissue culture plastic and exposed to the degradation products and their enzyme only controls, differences in MMP production was less distinct (Figure 3.5C). However, quantification of band intensity showed that both MMP and digestion fraction significantly increased pro-MMP2 secretion compared to the serum free condition (Figure 3.5D). In addition, both the elution and digestion fraction significantly increased cleaved-MMP2 concentration compared to both their respective enzyme controls, pepsin and MMP, as well as serum free media.

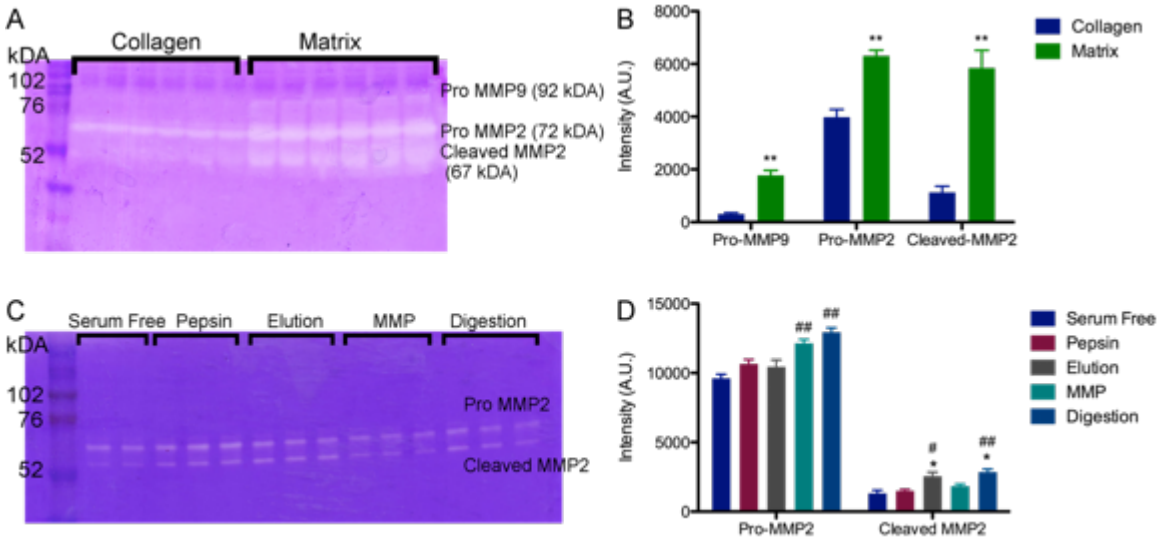

Figure 3.5 Cardiac fibroblast Production of MMPs. A) Zymogram of media collected from cardiac fibroblasts cultured on either collagen or myocardial matrix hydrogels. B) Analysis of band intensity (in A) show increased production of pro-MMP9, pro-MMP2, and cleaved MMP-2 in the matrix groups compared to collagen. C) Zymogram of media collected from cardiac fibroblasts cultured on tissue culture plastic, with serum free media and the degradation products or their enzyme controls at 1:10 dilution. D) Analysis of band intensity (in C). * $p < 0.05$, ** $p < 0.01$; *: compared to collagen or appropriate enzyme only control, #: compared to serum free media.

3.3.5. Myocardial Matrix Alters Macrophage Phenotype

Mouse bone marrow derived macrophages were used to examine how the myocardial matrix may affect macrophage phenotype by both encapsulation within the hydrogel and exposure to degradation products, representing macrophages that are actively infiltrating and at the periphery, respectively. Macrophage polarization was assessed by qPCR to quantify expression of iNOS and TNFα for the M1 phenotype, and Arg-1 and Ym-1 for the M2 phenotype. Calcein AM-labeled macrophages were encapsulated in myocardial matrix and collagen hydrogels. Macrophages remained fluorescently visible within both hydrogels after 48 hours of culture (Figure 3.6A). Furthermore, cell viability, measured by AlamarBlue fluorescence after 6 hour of culture, is similar between myocardial matrix and collagen groups (Figure 3.6B). Gene expression of encapsulated macrophages showed that myocardial matrix induces an increase in M1 genes iNOS and TNFα, as well as M2 marker Arg-1 (Figure 3.6C). In comparison, culture of macrophages with the degradation products of the myocardial matrices induces a much less definitive pattern (Figure 3.6D). Only the elution fraction significantly increased expression of TNFα in comparison to pepsin-only control. Neither fraction had significant effects on other gene expression independent of the enzyme only effects. While there were significant changes compared to media-only culture, these differences were negligible when compared to changes in gene expression elicited by polarization cytokines (IL-4 for M2 phenotype, LPS and IFNγ for M1 phenotype), which ranged for several hundred to tens of thousands fold change in the four transcripts that were measured (data not shown). The ability of myocardial matrix to blunt the changes induced by LPS was assessed by a 2-hour LPS challenge following culture with degradation products (Figure 3.6E). Both elution and digestion fraction diminished expression of iNOS and Ym-1 significantly compared to enzyme-only controls by approximately 2-fold.

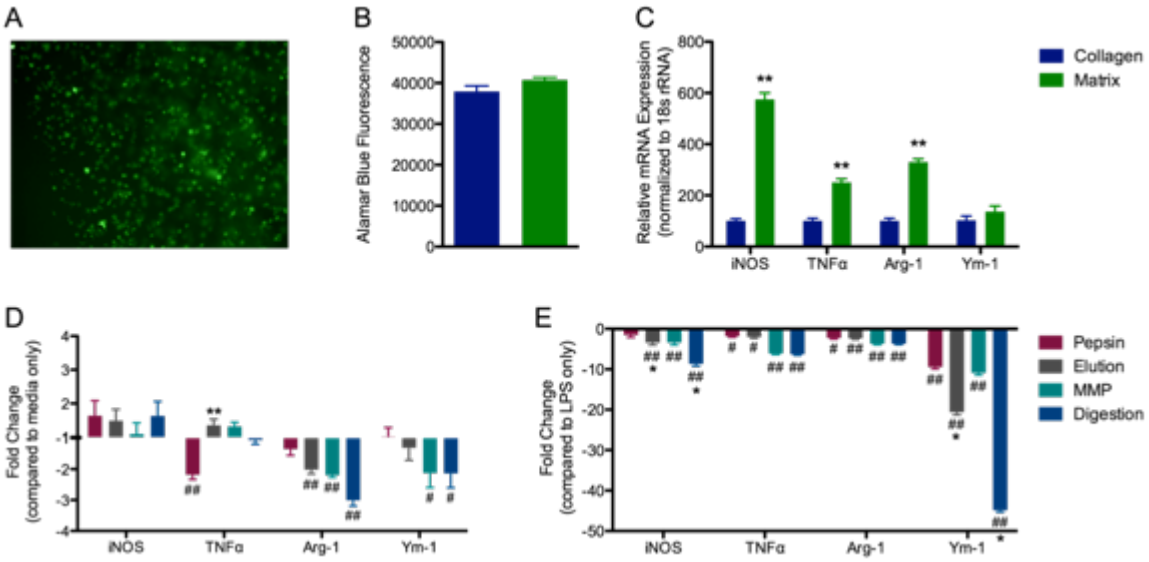

Figure 3.6 Macrophage polarization phenotype. A) Survival of encapsulated macrophages was confirmed with visualization of a high density of green fluorescent cells (Calcein AM-positive) after 48 hours of encapsulation. B) Difference in cell viability of myocardial matrix and collagen encapsulated macrophages were found to be non-significant when measured by AlamarBlue. C) Macrophages encapsulated in myocardial matrix hydrogels had significantly higher expression of iNOS, TNFα, and Arg-1 compared to collagen. D) Myocardial matrix degradation products had minimal intrinsic effect on macrophage phenotype at 1:10 dilution. E) Effects that degradation products have on macrophage gene expression in response to 100 ng/mL LPS challenge. * $p < 0.05$, ** $p < 0.01$; *: compared to collagen or appropriate enzyme only control, #: compared to macrophage culture media.

3.4. Discussion

While many studies have been performed on the bioactivity of the "degradation products" of ECM scaffolds, most of them have used pepsin as the protease or acid and heat treatment of up to 120 °C to break down material [191,193,201,202]. However, these are not representative of the types of peptides that cells are experiencing, since degradation *in vivo* of ECM scaffolds is likely mediated by MMPs secreted by infiltrating inflammatory cells and fibroblasts. Matricryptins, or matrikines, are enzymatic fragments of the ECM that contain biologically active cryptic sites and important mediators of the biologic effects of ECM molecules *in vivo* [156]. They have been known to affect a number of processes including angiogenesis, fibrosis, and inflammation [203]. Specifically post-MI, release of matricryptins due to increased expression of various MMPs and

resulting ECM turnover is known to regulate cardiac remodeling [204]. Given the importance of matricryptins in the tissue response to ECM biomaterials, a more accurate portrayal of the degradation products is essential. While use of pepsin as an *in vitro* mimic of implanted ECM scaffold degradation is not representative of *in vivo* processes, it does represent the first step of matricryptin generation when partial pepsin digestion is used to produce injectable ECM-derived hydrogels, such as the myocardial matrix. It is possible these ECM fragments are part of the peptides that do not participate in self-assembly and are able to diffuse away from the hydrogel, which we have defined as the elution fraction of the degradation products. In addition, the elution fraction may also contain cryptic peptide fragments that are generated by pepsin-mediated proteolysis of growth factors such as bFGF, TGFβ, and other heparin-sulfate bound growth factors that are known to be resident in ECM scaffolds [205]. The next step in the degradation of ECM-derived hydrogels *in vitro* is likely through endogenous MMPs as cell infiltrate the material. In the infarct myocardium, increase in both expression and activity of MMP2 and MMP9 is well documented in human patients as well as animal models [206]. Thus recombinant human MMP2 and MMP9 were used in this study to simulate active digestion of the myocardial matrix and further release of matricryptins *in vivo*.

To quantify the portion of protein that represent the elution and digestion fraction, a BCA protein assay was employed. Similar to Slivka *et al.* [207] who reported 58% of proteins to be measureable by BCA from a urinary bladder matrix, only 53% of the weight of the myocardial matrix was detectable. The unaccounted 47% of original mass is likely due to the heterogeneous nature of the myocardial matrix, since the BCA assay is best suited for quantification of homogeneous protein samples [208,209]. In addition, collagen rich samples, like the myocardial matrix, typically give low responses in commonly used protein assays [197]. Despite this limitation, results from the BCA assay can be used to relatively quantify the amount of protein in the degradation fractions. Notably, almost 40% of the protein in the myocardial matrix did not participate in self-assembly process of hydrogel formation and as able to diffuse out of the

hydrogel. These proteins likely represent the first peptide species that cells surrounding the injected hydrogel are exposed to post-injection. Using MMP2 and MMP9 mediated degradation, another 14% of proteins are released from the hydrogels and SDS Page indicates that these peptides have a different signature compared to non-MMP treated samples. However, solid hydrogel still remained after 24 hours of MMP2 and MMP9 incubation, indicating that other proteases may be involved in *in vivo* breakdown of the myocardial matrix hydrogel. Alternatively, recombinant MMPs may not fully represent *in vivo* activity. Since the effects of the myocardial matrix on post-MI repair at the tissue level has been previously characterized, as described in chapter 2, this study sought to investigate cell behaviors that would be relevant to the infarcted myocardium.

Microarray analysis of myocardial matrix injected infarcts showed an increase in cardiac development transcriptions factors including GATA4, Nkx2.5, and Tbx5. In addition, immunohistochemistry staining for cKit-positive/tryptase-negative cells indicated a potential increase of cardiac progenitors after matrix-injection. Result from this study indicate that one possible mechanism for this *in vivo* observation is recruitment of endogenous progenitor cells by the degradation products of the myocardial matrix. This was demonstrated through the use of transwell migration assays and human cardiomyocyte progenitor cells. The elution fraction of the myocardial matrix induced faster hCMPC migration compared to the digestion fraction. Notably, at both 1:10 and 1:100 dilutions, the elution fraction elicited significantly more cells to migrate than even the positive control of 10% FBS. Previous studies have demonstrated the ECM hydrogel products are able to stimulate recruitment of various progenitor cells [207,210,211]. However, differences in the ability of different fractions of these products to induce migration had not been shown.

In vivo gene expression changes consistently predicted a decrease in cell death in myocardial matrix injected infarcts while immunohistochemistry determined that this in part is due to reduced apoptosis specifically in cardiomyocytes. Culture of neonatal rat cardiomyocytes on

the hydrogels under stressed conditions of serum starvation and increasing concentrations of hydrogel peroxide simulate ROS showed that the myocardial matrix is able to better protect the cardiomyocytes compared to collagen controls. However, this result was determined using the AlamarBlue Cell Viability Assay, which is not a direct measure of apoptosis. The active compound in AlamarBlue is resazurin, a blue and nonfluorescent molecule that that is reduced by cells to a pink and fluorescent resorufin [212]. Thus the assay measures the reductive capacity of the cells, which reflects both the metabolic state as well as cell number. While this result is a promising indication of the protective effects of the myocardial matrix on cardiomyocytes, further studies are needed to ascertain whether this is due to an anti-apoptotic effect or alterations in myocardial metabolism.

Cardiac fibroblasts make up the majority of cells in the heart, and play an important role in regulating the mechanics and structure of the myocardium through production of ECM [213]. They are also critical to the pathogenesis of HF since they are particularly responsive to inflammatory cytokines post-MI and in turn produce a wide range of ECM proteins, MMPs, and other paracrine signaling. As a migratory cell type, fibroblasts may also be responding to the matrix injection by infiltrating the matrix and remodeling it in the process. Compared to collagen hydrogels, cardiac fibroblasts secrete significantly more MMP2 and MMP9 when cultured on myocardial matrix hydrogels. Similarly, concentration of cleaved MMP2 was significantly higher in media collected from fibroblasts exposed to both the elution and digestion fractions compared to their respective enzyme controls. While activation of MMPs have been associated with progression of LV remodeling and dysfunction due to degradation of native cardiac ECM and subsequent deposition of fibrotic proteins [214], results from previous studies show that this is not a long term effect of myocardial matrix injections [41,42]. At the same time, MMPs are known to be involved in several processes of infarct healing, including cell migration, angiogenesis, and regulation of growth factor activity [215]. Secretion of MMPs in cardiac fibroblasts can be induced by cytokines and growth factors [216], thus increased MMP activity in media collected from

fibroblasts culture with the myocardial matrix and its degradation products may be an indication that the matricryptins generated by proteolysis have similar activity.

Transcriptome differences at 3 days post-injection suggested that the inflammatory response is one of the first processes that differ between myocardial matrix and saline control injections. This initial response from infiltrating immune cells may be a determinant in altering the infarct milieu and triggering a pro-regenerative infarct resolution. In fact, implantation of ECM scaffolds *in vivo* is generally associated with a M2 macrophage phenotype, considered to be anti-inflammatory and pro-regenerative [133,135]. Similar to results with cardiac fibroblasts, culture of bone marrow derived macrophages encapsulated within the myocardial matrix hydrogel elicited a more dramatic response compared to exposure to the degradation products. This suggests that similarly, macrophages infiltrating the hydrogel *in vivo* may exert a different response than those in the perimeter of the hydrogel that experience only degradation products. However, the phenotype of the macrophage did not fit distinctly with the polarization scheme of M1 versus M2 macrophages, with increases in both M1 genes (iNOS and TNFα) as well as an M2 gene (Arg-1) when compared to encapsulation within collagen hydrogels. This result corroborates what was determined through microarray analysis, that myocardial matrix injections do not noticeably polarize macrophages to either phenotype. As discussed in chapter 2, there is growing appreciation for the need of both M1 and M2 macrophages in post-infarct repair [140,141]. Bone marrow derived macrophages were also cultured with the elution and digestion fractions of the myocardial matrix and their enzyme-only controls. While some significant differences were detected when compared to macrophage culture media alone, these fold changes were negligible when compared to the gene expression changes elicited by cytokine-induced changes in macrophage phenotype. Thus it is likely that the degradation products have an intrinsic effect on macrophage polarization. However, when cells are subjected to an LPS challenge, macrophages exposed to both degradation fractions had an approximate 2-fold decrease in iNOS and Ym-1 expression compared to enzyme controls. This result is similar to what was previous reported by

Slivka *et al.* [207], who showed that a similar 2-fold reduction in TNFα and IL-1β production by human THP-1 monocytes when cultured with the soluble component of urinary bladder matrix hydrogels after LPS challenge. This suggested that the degradation products of the myocardial matrix may also be able to modulate the behavior of surrounding inflammatory cells. However, further studies are needed to better characterize macrophage response beyond gene expression, such as functional assays examining phagocytic ability, cytokine secretion and production of other inflammatory mediators.

3.5. Conclusion

Through migration of cardiac progenitors, we showed that there is a distinct difference in the composition of the elution and digestion fractions of the hydrogel. Furthermore, behavior of macrophages and cardiac fibroblasts significantly differed when exposed to the matrix through the hydrogel form versus soluble peptides, suggesting that the form of ECM-derived materials presented to cells affect their response. Further experiments are needed to further elucidate these results and understand the molecular mechanisms behind these observed cell behaviors. However, this study represents the first step in understanding the bioactivity of the degradation products of the myocardial matrix which will aid in the design of novel ECM based materials for tissue engineering applications.

Chapter 4: Extracellular Matrix Protein Hydrogel Degradation in Post Infarct Repair

4.1. Introduction

As discussed in chapter 1, various hydrogels have been injected into the infarct myocardium and shown to have beneficial effects on post-infarct healing. Two mechanisms have been proposed to explain the above phenomenon: a) injected biomaterials act as passive structural reinforcement and increase wall thickness, thereby decreasing wall stress via Laplace's law, and 2) degraded biopolymer products act as stimuli for tissue repair and regeneration. The first mechanism is supported *in silico* by finite elements analysis, but only for immediately post-injection [63]. However, an *in vivo* study has shown that passive structural reinforcement alone, through a bio-inert, non-degradable poly(ethylene glycol) hydrogel was insufficient in preventing post-MI LV remodeling [56,217]. This suggests that bioactivity of the polymers and the degradation products as a possible mechanism in preserving cardiac function post-MI.

As discussed in chapter 3, ECM-derived hydrogels are known to be bioactive both as the hydrogel form and in its degradation products. Since cell migration, proliferation, and angiogenesis are all dependent on degradation of scaffold proteins, it follows that a decrease in degradation can prolong the release of chemoattractant peptides, thereby possibly increasing cell influx over time and further improving cardiac function. Currently, the most common technique for modifying naturally derived polymers is through crosslinking, however it also results in modifications in other material properties. Furthermore, implantation of some crosslinked ECM scaffolds is known to induce polarization of macrophages to a M1 phenotype, which is associated with a vigorous inflammatory response, while non-crosslinked ECM elicits a predominantly M2 response, indicative of a pro-regenerative environment [133,135]. An alternative method to prolonging degradation rate is through incorporation of degradation inhibitors within the scaffold. For protein-based scaffolds such as collagen, fibrin, Matrigel, and our myocardial matrix, the primary mechanism for scaffold breakdown is the MMP family of proteases. Thus, loading a MMP inhibitor could delay scaffold degradation without affecting other material properties such as matrix stiffness and pore size. Since we have already demonstrated the therapeutic benefits of

the myocardial matrix on post-infarct repair and established its bioactivity *in vitro*, we examined whether its cardioreparative effects could be enhanced by prolonging its degradation rate.

4.2. Materials and Methods

4.2.1. Myocardial Matrix Preparation and Modification

Porcine ventricular myocardium was decellularized with a solution of a 1% sodium dodecyl sulfate (SDS) as previously reported [40]. The resulting ECM was then processed into a liquid form through partial digestion with pepsin, adjusted to pH 7.4 and 8 mg/mL with sodium hydroxide and phosphate buffer saline (PBS). The liquid myocardial matrix was aliquoted and immediately frozen for lyophilization. Lyophilized matrix was rehydrated with water then mixed with the following to achieve a final concentration of 6 mg/mL: 1) 1x PBS for unmodified myocardial matrix, 2) 1% glutaraldehyde (Sigma-Aldrich) for 0.05% final concentration, 3) 4 mM genipin (Wako Chemicals) for 1 mM final concentration, 4) 480 mU/mL transglutaminase (from guinea pig liver, Sigma-Aldrich) for 120mU/mL and 5) 4 mg/mL doxycycline (Sigma-Aldrich) for 1 mg/mL final concentration. For *in vivo* degradation assessment, prepared liquid myocardial matrices were mixed with Alexa Fluor 568 Succinimidyl Ester (AF568, Life Technologies) dissolved in dimethyl sulfoxide (DMSO) at least 15 minutes prior to injection. Concentration of AF568 was 100 μg/mL, or approximately 21 nanomoles of the fluorophore per milligram of matrix. The final concentration of DMSO was 1%, which we had previously determined to be biocompatible and does not interfere with gelation of the myocardial matrix (unpublished data).

4.2.2. Cytotoxicity

The elution cytotoxicity assay was performed according to ISO 10993-5 standards for evaluating cytotoxicity of biomaterials [218]. After hydrogels were formed by overnight incubation at 37 °C, culture media were added and the resulting elution media collected after 24-hour extraction period. L929 mouse areolar fibroblasts were cultured in DMEM (Mediatech)

supplemented with 10% fetal bovine serum (FBS; Sigma-Aldrich) and 1% penicillin/streptomycin (P/S; Life Technologies). Cells were either split 1:3 using trypsin or plated at 20k/well in 24-well plates when 90% confluence was reached. After allowing cells to adhere overnight, culture media was replaced with elution media collected from various modified myocardial matrix hydrogels with media from unmodified hydrogels and 0.5% glutaraldehyde crosslinked hydrogels used as negative and positive controls, respectively (six conditions, n = 4 per condition, per assay). After a 48-hour culture period, the 3-(4,5-dimethylthiazol-2-yl)-2,5-diphenyltetrazolium bromide (MTT) Cell Proliferation Assay Kit (Life Technologies) and PicoGreen dsDNA Assay Kit (Life Technologies) were performed to assess cell viability and survival per manufacturer's directions.

4.2.3. Doxycycline Release

Unmodified and doxycycline loaded hydrogels (n = 3) were formed in glass scintillation vials after overnight incubation at 37 °C. Hydrogels were unmolded and placed in free floating in a known volume of PBS. The concentration of doxycycline diffused into solution was measured by a NanoDrop 2000c Spectrophotometer (Thermic Scientific) using the peak absorbance of 350 nm over 24 hours with periodic refreshment of PBS. To account for absorbance from components released by the myocardial matrix, readings taken the same time from an unmodified hydrogel were used as the blank.

4.2.4. *In vitro* Degradation Assessment

Bacterial collagenase (Worthington Biochemical Corporation) was used an as *in vitro* mimic to assess the degree to which crosslinking and doxycycline loading is able to affect degradation, measured by ninhydrin reactivity as previously described [16]. Briefly, after overnight gelation at 37 °C incubation, myocardial matrix hydrogels, unmodified and modified, were digested with an equal volume of collagenase at 125 U/mL in 0.1 M Tris-base, 0.25 M $CaCl_2$, pH 7.4 solution. After 4 and 24 hour incubation, samples were centrifuged for 10 minutes at 15000

rpm to pellet the undigested solid portion. The supernatant, containing degraded peptides, was reacted with 2% ninhydrin solution (Sigma-Aldrich) in a boiling water bath for 10 minutes. A standard curve made with acetyl-L-lysine (Tokyo Chemical Industry) was used to calculate the primary amine concentration from collagenase degradation. Samples were read on a BioTek Synergy 4 spectrophotometer (BioTek Instruments) at 570 nm. The same procedure was also used to determine whether the amount of doxycycline sequestered by the myocardial matrix hydrogel is sufficient to reduce degradation. Hydrogels, both unmodified and doxycycline loaded, after undergoing doxycycline release experiments described previously, were then digested with collagenase and assayed for ninhydrin reactivity.

4.2.5. Rheological Measurements

Liquid myocardial matrix (300 µL, n = 4), both unmodified and modified, was pipetted between two glass slides sandwiched by 1 mm spacers. Glass slides were hydrophobically treated with Rain-X to allow for easy removal of the hydrogels after overnight incubation at 37 °C. Rheological properties of the hydrogels was measured by a AR-2000 Rheometer (TA Instruments) using a 20 mm parallel plate geometry, set at 1 mm gap height and 37 °C. A frequency spread from 0.25 to 100 rad/s (0.5 to 10 is reported) was conducted at 2.5% strain, which was previously determined to be within the linear viscoelastic strain region [16]. Storage modulus (G') is reported for the different hydrogels at 0.4 rad/s.

4.2.6. Cellular Migration through Hydrogels

The effects of crosslinking and doxycycline loading on the ability of cells to migrate through the myocardial matrix hydrogel was assessed using Fluoroblok 24 Well Plate Inserts with 8.0 µm pores (Corning Incorporated) as previously described [16]. L929 fibroblasts were cultured as described above. Prior to passaging with trypsin, cells were serum starved DMEM with 1% P/S for 24 hours. Liquid myocardial matrices – unmodified, crosslinked or loaded with doxycycline

(100 µL, n = 3) – were pipetted onto the upper well of the transmembrane insert and incubated at 37 °C overnight for gelation. After trypsinization, serum starved cells were labeled with CFSE CellTrace (Life Technologies) diluted to 10 µM in PBS for 15 minutes at 37 °C. Cells were then washed and incubated with media alone for 37 °C for 30 minutes to remove excess CFSE and activate the fluorescent marker. Transwell inserts were placed into VisiPlate-24 Black Microplates (Perkin Elmer) with 1 mL of serum-supplemented media with FSB as the chemoattractant to induce migration. Fluorescently labeled L929s (150,000 cells/insert) were seeded on top of the hydrogels with 250 µL of serum-free media). Fluorescence was read on a Biotek Synergy 4 Spectrophotometer immediately after cell seeding and then periodically for 24 hours. Cells that have migrated through hydrogel and the opaque transmembrane would be detectable by fluorescence. Experiments were conducted in triplicate with results from one representative test shown.

4.2.7. Surgical Procedures

All procedures in this study were approved by the Committee on Animal Research at the University of California, San Diego and the American Association for Accreditation of Laboratory Animal Care. All *in vivo* experiments were performed on female adult Sprague-Dawley rats (225 to 250 g). MI was induced by 25-minute ischemia-reperfusion of the left coronary artery after left thoracotomy [41]. Injections of 75 µL of myocardial matrix were made directly into the myocardium by diaphragmatic access as previously described [20,40,41]. For the biocompatibility study, myocardial matrix crosslinked with 0.05% glutaraldehyde, 1 mM genipin, 120 mU/mL transglutaminase, or loaded with 1 mg/mL doxycycline was injected into healthy myocardium (n = 4). For the *in vivo* degradation study, myocardial matrices – unmodified, crosslinked with genipin or transglutaminase, or loaded with doxycycline – were fluorescently labeled with AF568 for visualization and injected into healthy myocardium (n = 3-4). To the study the long term effect on post-MI repair, 75 µL of the following (n = 8) were injected into infarcted myocardium one week

after ischemia-reperfusion surgery: 1) saline, 2) doxycycline 1 mg/mL in PBS, 3) unmodified myocardial matrix, or 4) myocardial matrix with 1 mg/mL doxycycline.

4.2.8. Magnetic Resonance Imaging

Cardiac Cine MR images were acquired using an 11.7T Bruker MRI System by Molecular Imaging Inc. at the Sanford Consortium for Regenerative Medicine. Rats were anesthetized using isoflurane in oxygen during imaging with continuous respiratory and ECG-monitoring. Following standard preparations (pulse power calibration, center frequency offset calculation, and shimming optimization), a scout image was acquired to ensure positioning and locate the heart. In the sagittal plane of the scout image, the long axis was defined and a second scout image obtained in the long axis plane perpendicular to the sagittal scout plane. In this second scout image, axial slices were defined, such that they were orthogonal to both long axes. Respiratory and ECG-gated, cine sequences were acquired over contiguous heart axial slices. The following parameters were used: repetition time = 20 ms, echo time = 1.18 ms, flip angle = 30°, field of view = 40 mm^2, data matrix size = 200 x 200. Eight or nine 1.5 mm, axial image slices were acquired with a total of 15 cine frames per image slice. ImageJ (NIH) was used to outline the endocardial surface at end diastole and end systole for each slice, defined as the minimum and maximum LV lumen area, respectively. Simpson's method was used to calculate the end diastolic volume (EDV) and end systolic volume (ESV), similar to previous reports [41,56]. Ejection fraction (EF) was calculated as [(EDV-ESV)/EDV] x 100. One day prior to injection surgery (6 days post-MI), rats underwent baseline magnetic resonance imaging (MRI). Healthy animals (n = 4) were also imaged, from which it was determined that EF was 73.8 ± 2.2%. Thus, animals that did have an EF one standard deviation below healthy values (< 71.6%) were excluded from the study. At 6 weeks post-MI (5 weeks post-injection), rats were imaged and their cardiac function assessed again for post-treatment evaluation.

4.2.9. Pressure Catheter Hemodynamics

After final MRI acquisition and prior to euthanasia, hemodynamic measurements were obtained in the contracting heart of a subset of animals using a pressure catheter. After induction of anesthesia using 5% isoflurane, rats were intubated and maintained at 2%. A 2 French SPR-407 Rat Pressure Catheter (Millar Instruments) was advanced through the ascending aorta and into the LV via the carotid-artery [219]. End diastolic pressure (EDP), peak systolic pressure (PSP), peak contractility (+dP/dt), and myocardial relaxation (-dP/dt) were measured from the pressure tracings.

4.2.10. Histology and Immunohistochemistry

Animals were euthanized according to the following experimental plan: 1) two weeks post-injection for the *in vivo* biocompatibility study, 2) one week post-injection for the *in vivo* degradation study, and 3) five weeks post-injection (six weeks after MI) for the long term post-infarct repair study. Rats that underwent the terminal catheter hemodynamics procedure were euthanized afterwards by thoracotomy and excision of the heart. All other rats were euthanized by an intraperitoneal injection of sodium pentobaribal (200 mg/kg) and the hearts immediately removed. For the long term post-infarct repair study, hearts were arrested in a solution of 20 mM $NaHCO_3$, 5 mM Dextrose, 2.7 mM $MgSO_4$, 22.8 mM KCl, 121.7 mM NaCl, and 20 mM 2,3 butanedione monoxime. All hearts were fresh frozen in Tissue Tek OCT freezing medium (Sakura Finetek) and cyrosectioned for histology and immunohistochemistry (IHC). Short axis sections of 10 μm spanned the ventricle at 16 locations, with approximately 350 μm between each location. All fluorescently labeled slides were mounted with Fluoromount (Sigma) and imaged on an Ariol Platform with the DM6000 B microscope (Leica Biosystems). All H&E and trichrome stained slides were mounted with Permount (Fisher Chemical) and scanned at 20x using the Aperio Scan Scope CS2 slide scanner (Leica Biosystems).

For the biocompatibility and degradation studies, one slide at each location was stained with H&E to identify the injection site and evaluate associated inflammatory response. To assess the amount of AF568-labeled hydrogel remaining at one week post-injection, neighboring slides at each location were stained with Hoescht 33342 (Life Technologies) to visualize nuclei and provide a counterstain for scanning. Slides from five locations with the largest area of red fluorescence were used for analysis. Number of red pixels within the entire heart section was quantified by ImageJ and summed for each heart.

For the long-term study on post-infarct repair, one slide per location was stained alternating for either H&E or Masson's Trichrome to visualize the infarct scar. Trichrome stained slides were also used to assess fibrosis, as previously described [220], using five slides from locations where the infarct was the largest. Non-nuclear blue staining was measured using the 'Positive Pixel Count V9' algorithm within ImageScope (Aperio) software. Interstitial and infarct fibrosis were determined in the non-infarct septal wall and infarct region, respectively. To access for infarct vascularization, three slides from the center of the infarct were stained with antibodies for alpha smooth muscle actin (αSMA, Dako 1A4; 1:75) and von Willebrand Factor (vWF, AbCam ab6994; 1:400), then visualized with Alexa Fluor 568 goat-anti-mouse (Life Technologies, 1:1000) and Alexa Fluor 488 goat-anti-rabbit (Life Technologies, 1:500). Nuclei were visualized with Hoescht 33342. Arteriole density was determined by counting from five 10x images randomly selected within the infarct using the following criteria: 1) co-localization of αSMA and vWF, 2) visible lumen, and 3) Feret diameter greater than 20 μm as determined by ImageJ. Cardiomyocyte cross-sectional area was assessed as previously reported [220]. Three sections from the center of the infarct were stained with antibodies for laminin (AbCam ab11575, 1:100) and α-actinin (Sigma A7811; 1:800), then visualized with Alexa Fluor 488 goat-anti-rabbit (Life Technologies, 1:500) and Alexa Fluor 568 goat-anti-mouse (Life Technologies, 1:500). Nuclei were stained with Hoescht 33342. Four images (20x) of the remote myocardium where myocardial fibers were running orthogonal to the plane of the section were selected for analysis.

Cross-sections of individual cardiomyocytes were outlined and the area measured by ImageJ. Each group had n > 300 cells.

4.2.11. Statistical Analysis

Data are presented as mean ± standard error of the mean (SEM). For analysis of *in vitro* characterization and *in vivo* degradation assessment, single-factor ANOVA with Dunnett's test comparing to unmodified hydrogels was used. For pre- and post-treatment MRI parameters within each group, paired t-test was used. For all other analysis from the long-term post-infarct repair study, single-factor ANOVAs with Tukey's post-hoc correction was used.

4.3. Results

4.3.1. *In vitro* Characterization of Crosslinked and Doxycycline Loaded Myocardial Matrix

The elution assay was performed in accordance to ISO 10993-5 standards for biomaterial testing to assess cytotoxicity of the modified myocardial matrices. L929 mouse fibroblasts were exposed to elution media extracted from unmodified, crosslinked, and doxycycline loaded hydrogels with 0.5% glutaraldehyde crosslinked hydrogels used as positive cytotoxic controls. After 48 hour incubation, DNA content was quantified by PicoGreen and cellular metabolism evaluated by MTT. Using both metrics, it was determined that the following concentrations were non-cytotoxic: 0.05% glutaraldehyde, 1 mM genipin, 120 mU/mL transglutaminase, and 1 mg/mL doxycycline (Figure 4.1A). All results described in subsequent experiments were based on these concentrations. To evaluate whether the concentrations of crosslinkers and doxycycline were sufficient to modulate degradation kinetics, an *in vitro* assay was performed using bacterial collagenase. Ninhydrin reactivity of the supernatant collected from hydrogels after 4 and 24 hours of collagenase incubation were used to assess the amount of peptides released, which showed that degradation was inhibited at both time points in glutaraldehyde, genipin, and doxycycline modified groups (Figure 4.1B).

Since doxycycline was not covalently linked to the myocardial matrix, the release profile was determined by submerging doxycycline-loaded hydrogels in PBS and measuring the concentration of doxycycline diffusing into solution by absorbance using a spectrophotometer. The results indicated that doxycycline had a burst release profile from the myocardial matrix with most of the loaded amount diffusing out over the first few hours, as expected for a small molecule in a hydrogel (Figure 4.1C). However, by 8 hours, the release plateaued and an undetectable amount of doxycycline was released by the hydrogel, indicating that approximately 30% of doxycycline was sequestered by the myocardial matrix hydrogel. No further release occurred out to day 7 (data not shown). Since this likely represents the amount of doxycycline retained by the myocardial matrix once injected into the myocardium and the burst release of doxycycline likely inhibited collagenase in the previous degradation assay, the ability of this sequestered doxycycline to inhibit degradation was similarly evaluated using bacterial collagenase. After both unmodified and doxycycline loaded hydrogels underwent 24 hours of PBS submersion for release experiments, the same hydrogels were subjected to collagenase digestion. Ninhydrin reactivity showed that the reduced amount of doxycycline sequestered by the myocardial matrix hydrogel is still sufficient in reducing the degradation of the hydrogel (Figure 4.1D).

Changes in the rheological properties of crosslinked and doxycycline loaded hydrogels were measured using a parallel plate rheometer at a constant strain of 2.5%. Figure 4.1E shows the frequency sweep from 0.25 to 10 rad/s from one experimental replicate (n = 4 per group). Since collagen fibrils show minimal shear thinning at frequencies below 0.6 rad/s [221], the storage modulus (G') is reported at 0.4 rad/s (Figure 4.1E). At this frequency, unmodified myocardial matrix had a storage modulus of 11.3 ± 2.0 Pa, similar to previously reported values [16]. Both 0.05% glutaraldehyde and 1 mM genipin crosslinked hydrogels increased the stiffness of the hydrogel by a similar magnitude, at 59.5 ± 9.8 Pa and 62.4 ± 17.4 Pa respectively, while transglutaminase crosslinking had no effect (G' = 7.9 ± 0.8 Pa). Doxycycline loaded also did not affect the mechanical properties of the hydrogel (G' = 8.1 ± 0.6 Pa), which was expected since it

does not chemically altering the myocardial matrix.

The effect that crosslinking and doxycycline loading has on cell migration through the myocardial matrix hydrogel was assessed using the FluoroBlok transwell migration inserts. Fluorescently labeled L929 mouse fibroblasts, the same cells used in the cytotoxicity experiments, were plated atop hydrogels formed in the upper chamber of the transwell insert. Cells that have migrated through the hydrogel and the opaque membrane are fluorescently detectable. One-way ANOVA analysis showed that while migration rates were significantly different initially, fibroblast were still able to migrate through crosslinked and doxycycline loaded hydrogels, as indicated by the non-significant levels of fluorescence by later time points (Figure 4.1G). Post-hoc analysis using Tukey's correction revealed that there was significantly faster migration of fibroblasts through transglutaminase crosslinked hydrogels, while other crosslinking methods and doxycycline loading had no significant effect (Figure 4.1H).

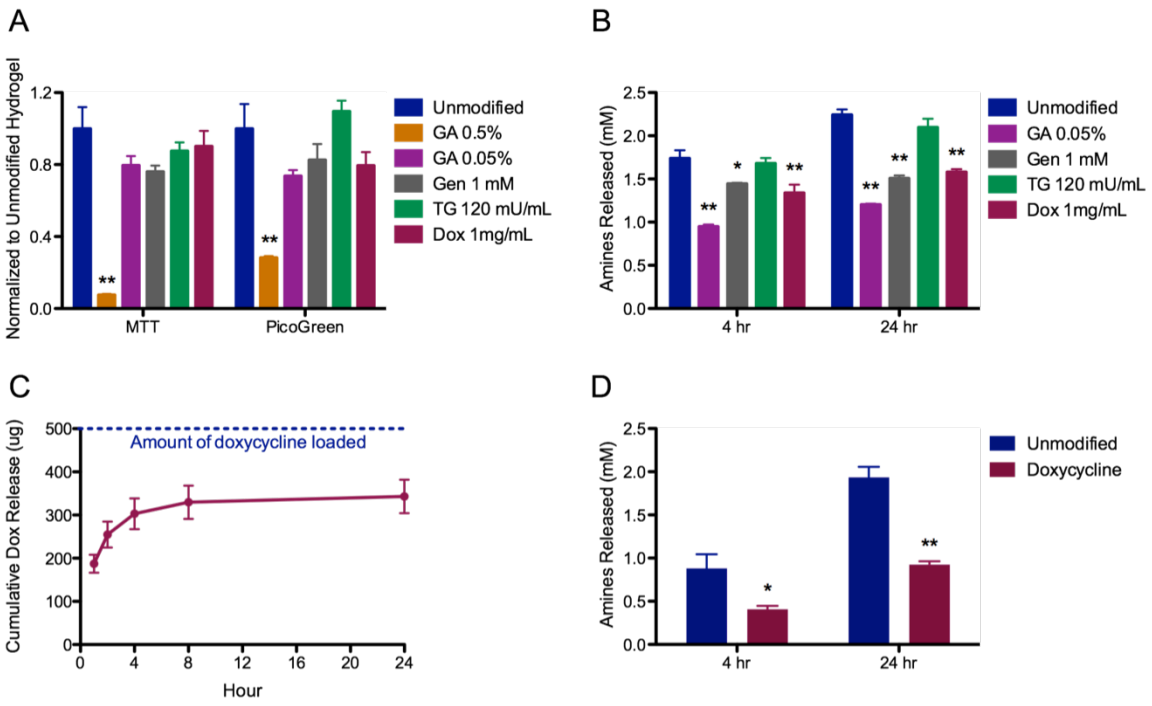

Figure 4.1 In vitro characterization of crosslinked and doxycycline loaded myocardial matrix hydrogels. A) Effect on L929 fibroblasts cytotoxicity measured by the MTT and PicoGreen assays. B) Degradation of hydrogels by bacterial collagenase as measured by amount of amines released through ninhydrin reactivity. C) Release profile of doxycycline from myocardial matrix hydrogels follows the typical burst release profile, but approximately 30% of loaded doxycycline is sequestered by hydrogel; D) degradation of the same hydrogels show that this retained amount of doxycycline is sufficient to inhibit collagense collagenase (student t-test). E) Storage modulus of hydrogels measured by a parallel plate rheometer from a frequency sweep of 0.5 to 10 rad/s. F) Both 0.05% glutaraldehyde and 1 mM genipin crosslinking significantly increases storage modulus of the hydrogels by approximately 6-7 fold, transglutaminase and doxycycline had no effect. G) Fluorescently labeled L929 migration through hydrogels within transwell migration inserts over 24 hours. H) Migration through transglutaminase crosslinked hydrogels is significantly faster at earlier time points compared to unmodified matrices. GA: glutaraldehyde, Gen: genipin, TG: transglutaminase, Dox: doxycycline. * $p < 0.05$, ** $p < 0.01$ using one way ANOVA followed by Dunnett's multiple comparison correction compared to unmodified hydrogel controls.

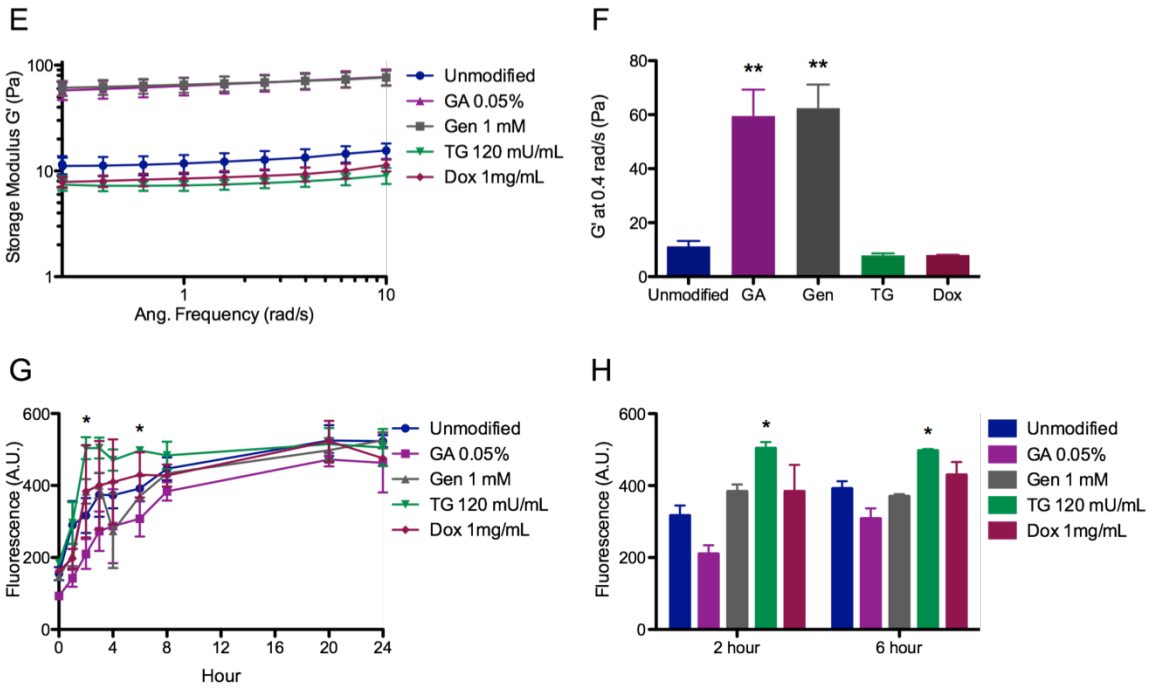

Figure 4.1 In vitro characterization of crosslinked and doxycycline loaded myocardial matrix hydrogels. Continued.

4.3.2. *In vivo* Biocompatibility Assessment

To assess the biocompatibility of crosslinked and doxycycline loaded myocardial matrix hydrogels, modified matrices were injected into healthy myocardium. The inflammatory response at two weeks post-injection was evaluated by a pathologist blinded to the treatment groups, who identified the injection sites as morphologically similar among the groups, with areas of spindle cells and/or interconnecting (branching) elongate cells – suggestive of degenerative/regenerative myocardial fibers, plus usually minimal inflammatory infiltrate consisting of lymphocyte-type small mononuclear cells. The doxycycline group did not exhibit a notable difference in injection site morphology suggesting that the amount of doxycycline that is released had minimal effect on the overall inflammatory response to the hydrogel. Across all the groups, only within the glutaraldehyde crosslinked group did the pathologist note moderate to marked focal non-suppurative inflammation with lymphocytic infiltrate and foreign-body giant cells (Figure 4.2), which led glutaraldehyde crosslinking to be excluded from subsequent *in vivo* studies.

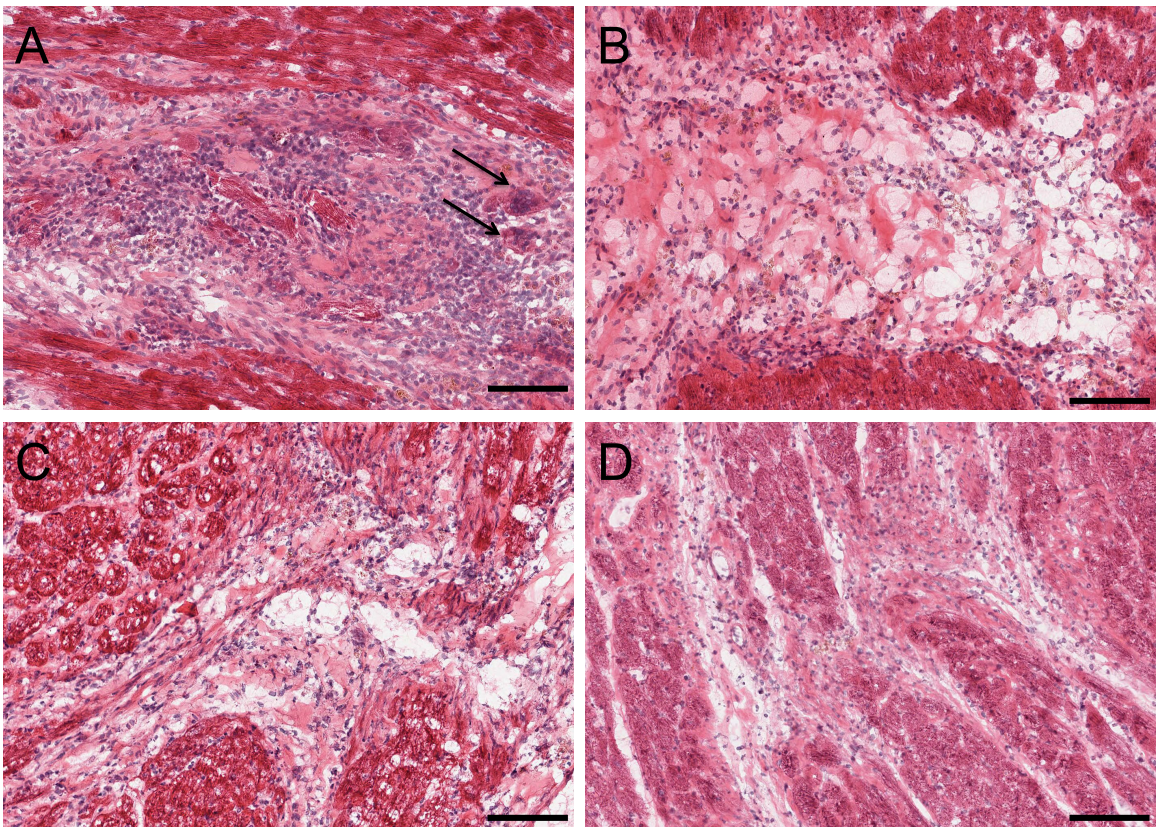

Figure 4.2 Biocompatibility of crosslinked and doxycycline loaded myocardial matrix in vivo. Representative H&E images of the myocardial matrix with 0.05% glutaraldehyde (A), 1 mM genipin (B), 120 mU/mL transglutaminase (C), or 1 mg/mL doxycycline (D) injected into healthy myocardium. Injection sites were made up of elongate spindle to branching cells suggestive of degenerative/regenerative myocardial fibeers, plus usually minimally inflammatory infiltrate consisting of lymphocyte-type small mononuclear cells. Only the glutaraldehyde crosslinked hydrogel injection site showed marked lymphocytic infiltrate and foreign body giant cells (arrows). Scale bars = 100 μm.

4.3.3. Doxycycline Reduces Myocardial Matrix Degradation *In Vivo*

To more clearly identify presence of the hydrogel from histological sections, liquid matrices were fluorescently labeled with AF568. Labeled myocardial matrices – unmodified, crosslinked with genipin or transglutaminase, or loaded with doxycycline – were injected into healthy myocardium to evaluate effects on *in vivo* degradation. Comparisons of H&E stained sections (Figure 4.3A) with fluorescently scanned neighboring sections (Figure 4.3B) show good correlation between the morphology of the injection sites. Changes in the degradation rate of the modified myocardial matrix were approximated by the amount of hydrogel remaining at one-week

post-injection, which was chosen based on previous studies showing that unmodified hydrogels degraded by approximately three weeks [42]. Quantification of the degree of red fluorescence through the tissues sections by ImageJ revealed that only doxycycline loading significantly increased the amount of myocardial matrix remaining (Figure 4.3C), suggesting that it is able to reduce *in vivo* degradation through MMP inhibition. Neither genipin or transglutaminase crosslinking had an effect in altering the degradation rate.

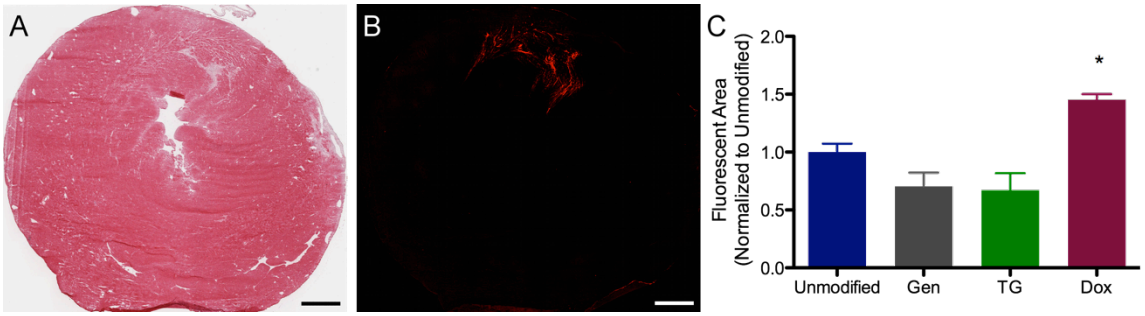

Figure 4.3 Doxycycline reduces myocardial matrix degradation in vivo. A) H&E image of an entire heart section showing the injection site. B) Alexa Fluor 568 (red) labeled myocardial matrix is visible fluorescently. C) Quantification of the amount of fluorescence remaining at one-week after injection. Gen: genipin, TG: transglutaminase, Dox: doxycycline; * $p < 0.05$ using Dunnett's multiple comparison correction comparing against unmodified hydrogel controls; scale bar = 1 mm.

4.3.4. Effects on Cardiac Function Post-MI

Effect of prolonged myocardial matrix degradation on cardiac function post-MI was evaluated by both MRI and pressure catheter hemodynamics. LV EF, ESV, and EDV were measured by MRI at 6 days post-MI (1 day before injection) and 6 weeks post-MI (5 weeks post injection). As expected, EF significantly declined ($p = 0.01$) in the saline-injected group, while ESV ($p < 0.001$) and EDV ($p = 0.004$) both significantly expanded (Figures 4.4A-C). A similar trend for changes in EF ($p = 0.007$), ESV ($p = 0.007$), and EDV ($p = 0.001$) also occurred in the doxycycline-injected group. Both matrix- ($p = 0.94$) and matrix with doxycycline- ($p = 0.24$) injected infarcts did not demonstrate a decline in EF (Figure 4.4A). For the LV volumes, neither matrix alone ($p = 0.004$) nor matrix with doxycycline ($p < 0.001$) was able to prevent EDV dilatation (Figure 4.4B). However, matrix with doxycycline was able to prevent ESV expansion (p

= 0.22) while matrix alone (p = 0.028) did not (Figure 4.4C). Analysis was also made in the percent change in EF, ESV, and EDV across treatment groups. Matrix with doxycycline significantly increased percent change in EF compared to both saline- and doxycycline- injected groups (Figure 4.4D). Both matrix- and matrix with doxycycline- groups had significantly lower percent change in ESV compared to both saline- and doxycycline- injected infarcts (Figure 4.4E), however there were no significant difference across groups for percent change in EDV (Figure 4.4F).

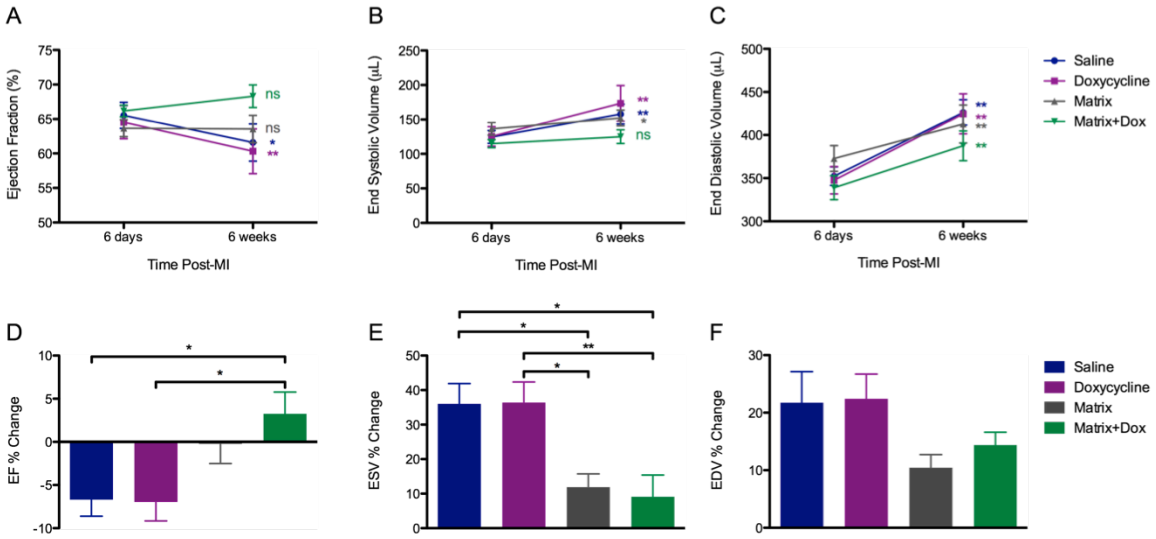

Figure 4.4 Magnetic Resonance Imaging (MRI) analysis of cardiac function. Changes between baseline imaging performed at 6 days post-myocardial infarction (MI), 1 day prior to injection and 6 weeks post-MI at study termination. Paired t-test were performed within each treatment group for A) ejection fraction (EF), B) end systolic volume (ESV), and C) end diastolic volume (EDV). Percent change between pre- and post-injection EF (D), ESV (E), and EDV (F) were compared across all groups using one-way ANOVA followed by Tukey's multiple comparison correction. * $p < 0.05$, ** $p < 0.01$.

LV hemodynamics were measured invasively using a pressure catheter via carotid artery access prior to euthanization at 6 weeks post-MI (5 weeks post-injection). No differences were detected in LV EDP across groups (Figure 4.5A). However, both matrix- and matrix with doxycycline-groups had higher LV PSP compared to saline-injected controls (Figure 4.5B). Myocardial relaxation, as measured by $-dP/dt_{max}$, was significantly higher in the matrix-injected

group compared to saline-injected control (Figure 4.5C). Lastly, myocardial contractility, as measured by $+dP/dt_{max}$, was significantly higher in both the matrix- and matrix with doxycycline-groups compared to saline groups (Figure 4.5D). Doxycycline injection did not have significant differences from saline injection in any of the parameters measured.

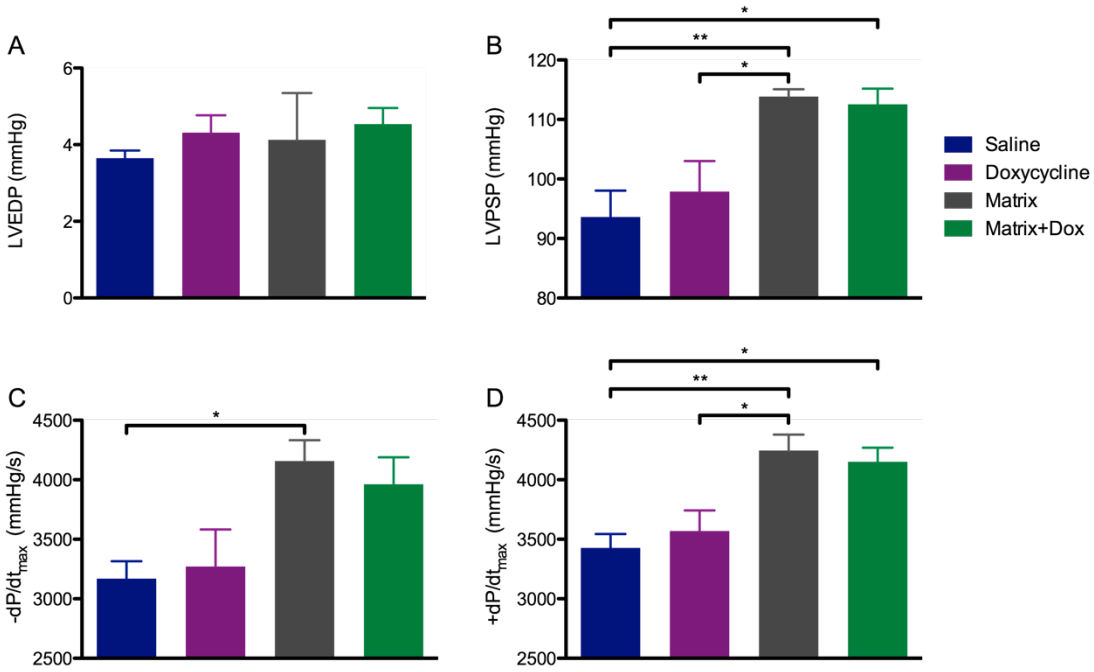

Figure 4.5 Pressure hemodynamics analysis of cardiac function. Differences in A) left ventricular end diastolic pressure (LVEDP), B) left ventricular peak systolic pressure (LVPSP), C) myocardial contractility as indicated by maximum change in pressure over time ($+dP/dt_{max}$), and D) myocardial relaxation as indicated by minimum change in pressure over time ($-dP/dt_{max}$) were assessed by one-way ANOVA followed by Tukey's multiple comparison correction. * $p < 0.05$, ** $p < 0.01$.

4.3.5. Effects on Infarct Fibrosis, Vascularization, and Myocardial Hypertrophy

Masson's trichome staining was used to determine the degree of fibrosis in both the infarct and remote interstitium (Figure 4.6A). Quantification of the collagen content (blue pixels) in the two regions showed no significant decrease in infarct fibrosis in either matrix alone or matrix with doxycycline compared to the saline controls. However, there was a significant decrease in interstitial fibrosis after matrix injection compared to both saline and doxycycline-only injections.

Visualization of infarct vasculature was performed using antibodies for αSMA and vWF (Figure 4.6C). One-way ANOVA determined that there were no significant differences across groups for the density of blood vessels within the infarct (Figure 4.6D). To evaluate changes in cardiac hypertrophy, laminin staining was performed to visualize the outlines of cardiomyocytes (Figure 4.6E). Cross-sectional area of cardiomyocytes from remote healthy myocardium where myocardial fibers are running orthogonal to the tissue section were quantified and showed that only the matrix with doxycycline group had significantly smaller cell size compared to saline controls.

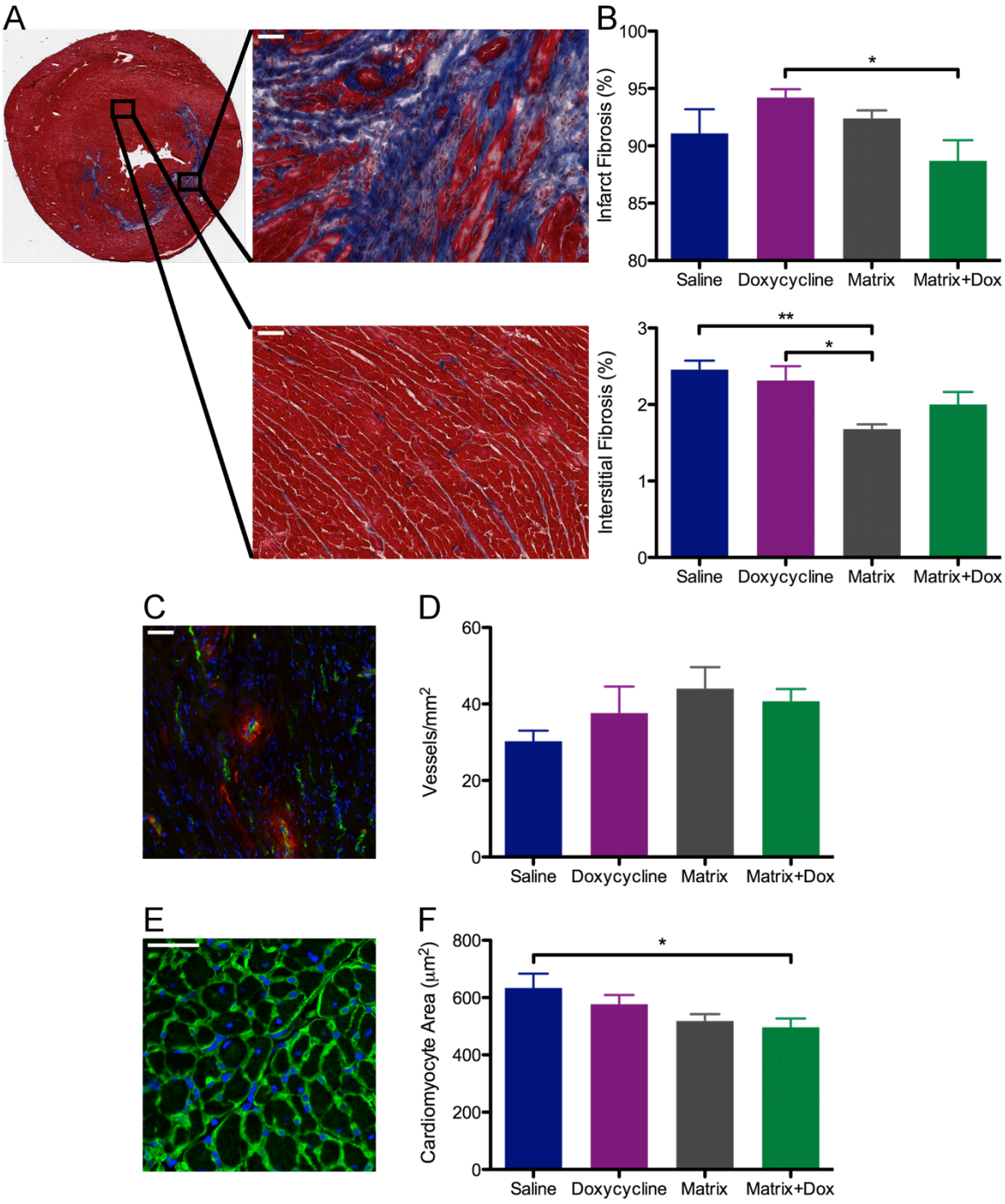

Figure 4.6 Histological changes in infarcted hearts. A) Representative Masson's trichrome staining for fibrosis in the infarct (top) and remote interstitium (bottom). B) Quantification of percent collagen content (blue pixels). C) Representative image of the infarct stained with antibodies for α-smooth muscle actin (red) and von Willebrand Factor (green) to identify vessels, D) Quantification of vessel density in the infarct. E) Representative image of the remote myocardium stained with laminin antibody (green) to outline cardiomyocytes. E) Quantification of cardiomyocyte cross-sectional area. * p <

0.05, ** $p < 0.01$ for one-way ANOVA followed by Tukey's multiple-comparison correction; nuclei were visualized with Hoescht (blue); scale bar = 50 μm.

4.4. Discussion

For the many naturally derived hydrogels that have been injected intramyocardially for post-infarct repair, modulation of degradation rate has not been investigated. Most studies, including those previously published from our lab on the myocardial matrix [41], have simply relied on the natural tempo of the myocardium's protease system. Results from two studies on crosslinked hydrogels and materials with varying residence times suggest that prolonged degradation of a biomaterial could have a beneficial effect on tissue regeneration. In a study that compared alginate and fibrin injections in a rat MI model, it was shown that while both materials initially improved LV geometry and function at 2 days post-injection as compared to saline controls, only the alginate treated groups showed significant persistent improvement at 5 weeks [67]. The authors observed that at 5 weeks, presence of alginate could still be identified by histology while fibrin was completed reabsorbed, leading them to propose that long-term benefits on cardiac function could be affected by persistence of the inject material. However, this study was performed on two different biopolymers, each with its unique bioactive properties. In a more recent study, degradable hyaluronic acid (HA) hydrogels were synthesized and their effect on post-infarct LV remodeling examined [39]. The authors reported that non-degradable HA hydrogels were better able to preserve wall thickness in comparison to their degradable counterparts, likely due to presence of the material acting as a wall-bulking agent. Unfortunately, there were no difference in LV volumes or EF in any of the hydrogel treated groups. We hypothesized that prolonged degradation of the decellularized myocardial matrix hydrogel can further benefit post-MI repair and regeneration through extended cell recruitment.

Two methods were used to modulate the degradation rate of the myocardial matrix in this study – crosslinking and use of MMP inhibitors. We chose to examine the effects on three types of crosslinkers on myocardial matrix hydrogel properties both *in vitro* and *in vivo*. Glutaraldehyde

was chosen because it is commonly used chemical crosslinker for modifying collagen-based materials. In addition, our lab had previously demonstrated that various concentrations of glutaraldehyde could be used to tailor the material properties of the myocardial matrix hydrogel [16]. Genipin, a small molecule crosslinker derived from gardenia fruit, and tissue transglutaminase, a mammalian enzyme that catalyzes the formation of γ-glutamyl-ε-lysine bonds between two peptide chains, were also investigated based on previous reports of their use in crosslinking collagen gels [222-225]. Transglutaminase, in particular, provides an additional advantage because it is an enzymatic crosslinker, so no chemical residues or by-products are generated from the reaction, reducing the risk of cytotoxicity [226]. For MMP inhibition, doxycycline was selected because it is a widely used tetracycline antibiotic with independent, broad spectrum MMP inhibition activity at sub-antimicrobial dosages [227]. In addition, MMP inhibition by doxycycline has already been explored in both experimental and clinical settings as a therapy for coronary artery diseases [227], thus making it unlikely to exacerbate post-MI progression to HF when injected in conjunction with the myocardial matrix.

As expected, crosslinking with glutaraldehyde and genipin was effective in modifying several aspects of the material properties evaluated *in vitro*, including inhibiting collagenase degradation and increasing the storage modulus of the myocardial matrix hydrogel. However, crosslinking with transglutaminase did not have an effect an either properties despite usage at a relatively high concentration of 120 mU/mL [228]. While 1 mg/mL of doxycycline was chosen for these studies based on cytotoxicity results, it was estimated that approximately 30% is bound by the myocardial matrix, possibly through secondary interactions, while the rest diffuses away. Both concentrations, 1 mg/mL and the lower retained concentration, were sufficient to reduce degradation by collagenase. Importantly, doxycycline did not affect other properties such as storage modulus, which may be preferable over crosslinkers when changes in degradation rate of hydrogels need to be studied in isolation from other effects. The effects on how crosslinking and doxycycline loading on cellular interactions with the myocardial matrix hydrogel *in vitro* was

examined through both cytotoxicity and migration assays. At the concentrations chosen, none of the modification agents appear to affect L929 fibroblast viability and survival. Importantly for tissue engineering applications, the ability of cells to migrate through the modified hydrogels was also not significantly affected. Interestingly, L929s were able to migrate more quickly through transglutaminase crosslinked compared to unmodified hydrogels. A previous study using transglutaminase to crosslink an adipose tissue-derived ECM hydrogels showed that while, similar to our results, 100 mU/mL of the enzyme had no effect on hydrogel rheology, it did change the fiber diameter of the hydrogel under scanning electron microscopy [229]. A similar change in the microstructure of the myocardial matrix may explain why fibroblasts were able to transverse the hydrogels more quickly in the transwell inserts. Further evidence that transglutaminase may affect the bioactivity of ECM hydrogel *in vivo* came from the same study, where crosslinked matrices induces higher vascularization than hydrogel alone [229]. Thus, transglutaminase was included in further *in vivo* characterization along with glutaraldehyde, genipin, and doxycycline.

While cytotoxicity of the compounds at the chosen concentrations were determined to be negligible *in vitro* using established ISO 10993-5 standards for biomaterial testing, biocompatibility of the modified hydrogels *in vivo* was also examined. Evaluation from a trained pathologist suggested that 0.05% glutaraldehyde crosslinked hydrogels elicited an aggressive inflammatory response with presence of foreign body giant cells. This results contradicted many previous *in vitro* and *in vivo* studies, which had shown that up to 0.25% glutaraldehyde to be considered biocompatible [230-232]. However, many studies evaluate the biocompatibility of the biomaterial by implantation in the subcutaneous space. In comparison, the myocardium is much more vascularized and therefore may be under increased surveillance by the immune system, resulting in heightened sensitivity to potentially toxic compounds. This result had been previously reported in a study where thiolated-hyaluronic acid hydrogels showed minimal immune response when injected subcutaneously, but induced granuloma formation when intramyocardially injected [233]. Due to the associated inflammatory response, glutaraldehyde was not evaluated further in

subsequent *in vivo* experiments.

To better identify the hydrogels post-injection, liquid myocardial matrices were fluorescently labeled with AF568. The fluorophore was conjugated to an NHS ester, allowing it to react with the primary amines on the protein component of the myocardial matrix. The reaction is rapid at neutral pH and forms a stable amide bond [234]. Analysis of the amount of fluorescent material remaining at one-week post-injection indicated that only doxycycline-loaded hydrogels had a slower degradation rate compared to unmodified controls. Despite showing promise *in vitro* in reducing degradation by bacterial collagenase, genipin crosslinking did not affect *in vivo* degradation of the myocardial matrix. This may be due to the slower reaction rate of genipin crosslinking, which occurs over the span of hours after it is combined with the polymer [235]. As a result, injected genipin likely diffuse away from the myocardial matrix before it is able to react. Alternatively, the crosslinker may react non-specifically to primary amines on the proteins and peptides in the surrounding myocardium. This result highlights the importance of evaluating degradation *in vivo*; while degradation *in vitro* can be simulated with use of various proteases, allowing relative comparisons of multiple materials and concentrations, the results often do not correlate with *in vivo* degradation rates [236]. A careful survey of literature on reagents used for collagen-based materials show that an ideal crosslinker for modifying injectable ECM-derived hydrogels may not currently exist. Like genipin crosslinking, glycation crosslinking occurs too slow to have an effect [237]. Faster reacting reagents such as di-isocyanates, carbodiimides, and azides occur at conditions that are not physiological – higher temperatures, acidic or basic pH, or use of solvents and surfactants – making them unsuitable to be injected for *in situ* crosslinking [238-243]. In addition, these reagents were typically developed for crosslinking scaffolds, intended for implantation, rather than hydrogels that are injected into host tissue. This makes cytotoxicity an even higher priority since unreacted crosslinkers can diffuse away from the injected bolus, which may have contributed to the adverse inflammatory reaction seen with glutaraldehyde-injected groups.

For functional evaluation of the effects of prolonged myocardial matrix degradation time on post-infarct repair, only doxycycline was evaluated. In addition, saline, doxycycline alone, and myocardial matrix alone were also injected as controls. Similar to previous studies, myocardial matrix injection attenuated the decrease in cardiac function and LV remodeling post-MI compared to saline injection [41,42]. However, addition of doxycycline to the hydrogel did not drastically improve either ejection fraction or LV volumes beyond the effects of the myocardial matrix. Pressure hemodynamic measurements also corroborated these results where myocardial contractility, relaxation, and peak systolic pressure were higher in matrix injected groups, with or without doxycycline, compared to saline injections. Doxycycline-only injections also did not produce significant differences compared to saline in any of the parameters assessed by MRI or pressure hemodynamics. Previous studies in rats have shown that oral doxycycline therapy post-MI is able to improve LV morphology and function [244]. However, others have reported that subcutaneous injections of doxycycline do not have any affect on LV remodeling or dysfunction [245]. Similarly, MMP inhibition in clinical trials for patients with acute MIs has also shown conflicting results [246,247]. Differences in these studies from our result is likely due to timing of the treatment, dosage, and delivery route. Oral administration of doxycycline at 30 mg/kg used by Garcia *et al.* [244] achieves a serum level of approximately 2 μg/mL [248]. In addition, treatment was initiated earlier, beginning either immediately or two days post-MI. In comparison, 75 μg of doxycycline at 1 mg/mL was intramyocardially injected in a single dose at one week post-infarct for this study, which is unlikely to provide a sustained level of MMP inhibition to alter infarct healing or too late to have an effect.

Histological analysis of the infarcted hearts also showed a similar trend in the effects doxycycline, myocardial matrix, or myocardial matrix with doxycycline. Namely, addition of doxycycline inhibition of MMPs to the myocardial matrix did not significantly reduce myocardial fibrosis, enhance angiogenesis, or reduce cardiac hypertrophy compared to hydrogel alone. Similarly, doxycycline alone did not significantly alter infarct histology compared to saline-injected

control animals. Taken together with the results on cardiac function, this suggested that prolonging the degradation of the myocardial matrix does not further enhance nor reduce the effects of the myocardial matrix on post-infarct repair. It is possible that the amount of doxycycline loaded was insufficient to slow down myocardial matrix degradation in the context of the post-infarct myocardium, where MMP levels are known to be elevated [206]. Alternatively, altering the release profile of the myocardial matrix degradation products may not result in increased overall bioactivity of the hydrogel. In this regard, increasing the concentration, or in effect increasing the dosage, from the concentration of 6 mg/mL used in this and previous studies to a higher concentration that is still suitable for catheter delivery, may be another option for enhance the beneficial effects of the myocardial matrix.

4.5. Conclusion

We have demonstrated through *in vitro* characterization that properties of the myocardial matrix hydrogel could be easily modified by various crosslinking methods commonly used for collagen-based materials. In addition, loading the hydrogel with doxycycline is a novel method to alter the degradation rate without affecting other properties of the material. However, *in vivo* experiments on biocompatibility and degradation kinetics showed that there are currently no crosslinkers that are able to modulate injectable ECM-derived hydrogels *in situ*. Thus there is a need for the development of new crosslinkers with the following criteria: 1) Rapid reaction kinetics, 2) ability to react at physiological conditions including 37 °C, neutral pH, and without surfactants or solvents, and 3) minimal cytotoxicity. Prolonged degradation by doxycycline did not significantly enhance the effects of the myocardial matrix on cardiac function, LV remodeling, or histology post-MI. However, as a thoroughly studied antibiotic and potent MMP inhibitor, doxycycline was able to prolong ECM-derived hydrogel degradation *in vivo* and may represent an effective and non-cytotoxic way of tailoring hydrogel degradation in other tissue engineering applications.

Chapter 4, in part, is a reprint of the material as it is published in: Jean W. Wassenaar, Robert G. Gaetani, Julian J. Garcia, Rebecca L. Braden, Colin G. Luo, Diane Huang, Anthony N. DeMaria, Jeffrey H. Omens and Karen L. Christman. “Evidence for the Mechanisms Underlying the Functional Benefits of a Myocardial Matrix Hydrogel for Post-MI treatment”. (2016) *J Am Coll Cardiol*, 67(9):1074-86; and also in part, a reprint of material as it is published in: Jean W. Wassenaar, Rebecca L. Braden, Colin G. Luo, and Karen L. Christman. “Modulating *in vivo* degradation rate of injectable extracellular matrix hydrogels”. (2016) *J Mater Chem B*, 4: 2794-802. The dissertation author was the primary author of both manuscripts.

Chapter 5: Conclusions and Future Directions

5.1 Summary of Work

This dissertation represented the first steps in a comprehensive understanding of the mechanisms of action of the myocardial matrix hydrogel in post-infarct repair. We showed through transcriptome and histological analysis that the myocardial matrix can directly or indirectly affect many tissue-level changes in the infarcted myocardium. These changes included reducing apoptosis of existing cardiomyocytes, limiting cardiac hypertrophy, stimulating blood vessel formation, altering myocardial metabolism towards more efficient modalities, and increasing cardiac development. This study was the first to utilize whole transcriptome analysis to evaluate the effect of a biomaterial injection as a post-MI treatment. To our knowledge, it is also the first to show that a biologic (non-pharmaceutical) therapy for MI can induce such dramatic changes in the infarct transcriptome such that it is distinctly different from that of the control.

To better study the tissue level changes described in chapter 2, we began to explore the response of cells to culture with the myocardial matrix *in vitro*. Post-injection, cells may interact with the myocardial matrix through different ways, including being surrounded by the 3D hydrogel or in response to the degradation products that are released. Thus we chose to recapitulate these two modalities through both cell culture on and encapsulation within the hydrogel, as well as exposure of cells to the degradation products. Previous studies on the bioactivity of the degradation products of ECM scaffolds have used pepsin or heat and acid treatment to breakdown the material. However, we believed that this does not accurately represent the cryptic peptide fragments that are generated through degradation and presented to the cells. Thus, MMP proteolysis was used to produce digestion products that better mimic degradation *in vivo*, which had not been examined previously with ECM-derived materials. In addition, we hypothesized that the first peptide species that cells experience immediately post-injection are those that are not able to self assemble during the gelation process and diffuse out rapidly once injected. Based on the tissue-level processes that were affected by myocardial matrix injection identified in chapter 2, *in vitro* experiments designed to recapitulate these behaviors were carried out. Preliminary data

demonstrated that these two fractions have differing bioactivity when added to cell culture media but this cellular response is dramatically different when cells are cultured on or encapsulated within the 3D hydrogel. Additional experiments are necessary to better elucidate these mechanisms and identify other relevant cell behaviors, some of which will be discussed in the subsequent section.

Since results from chapter 3 showed the wide range of bioactivity of the myocardial matrix degradation products *in vitro*, this led to the hypothesis that bioactivity of the degradation products of the myocardial matrix may be integral to its beneficial effects on post-infarct repair. Thus, we wanted determine whether prolonging the degradation of the hydrogel would enhance the effects. We chose to accomplish this through use the antibiotic doxycycline for its MMP inhibition properties and looked at how this affected post-MI healing through several methods, including MRI, pressure hemodynamics, and histology. Unfortunately, all these modalities were relatively consistent in demonstrating that addition of doxycycline did not enhance the effects of the myocardial matrix. However, through these experiments, we were able to show that doxycycline is an effective and non-toxic modifier of ECM-derived hydrogel degradation *in vivo*; this represents a novel use of doxycycline for tissue engineering applications.. In addition, results from the study along with an exhaustive search through the literature of reagents used to crosslink collagen-based materials to the conclusion that there are no current crosslinkers that can be used for modifying injectable ECM-derived hydrogels *in situ*.

5.2 Future Directions

As novel non-traditional therapies are being prepared to enter the clinic, it is essential to understand their underlying mechanisms of action. In the field of post-MI therapies, the past decade has shown many promising results such as cellular cardiomyoplasty. While many cell types and delivery preparations have been explored, with several showing very promising results in animal studies, none so far have translated into definitive and clinically significant benefit for

patients. Part of the understanding of how cell transplantation is able to induce benefit in animal MI models has evolved from hypothesizing that the implanted cells are able to differentiate into functional contractile cardiomyocytes to discovering that the effects that are likely due to paracrine effects from the cells. Due to this understanding, more recent efforts have expanded into delivery of biologics derived from the products of cell types previously used for cardiomyoplasty, such as secretomes and exosomes. This represents perhaps an even more promising treatment for patients since issues such as immunogenicity and accessibility of cytotherapy are less of a concern.

If we can improve the understanding of the mechanisms of action of the myocardial matrix, perhaps similar progress can be made to improve its design. Ideally, delivery of just the important components of the myocardial matrix, at concentrations or timing that is fine-tuned to cardiac repair post-MI, may enhance healing. But to do this, several advancements need to be made. As discussed in chapter 2, we now have a good comprehension of the tissue level changes, with both transcriptional and histological evidence, that occur post-injection. The easiest way to study these mechanisms is to recapitulate these observations with relevant cell types *in vitro*. This was begun in chapter 3, but further experiments are needed to pinpoint the exact molecular mechanisms responsible and demonstrate that they are indeed involved in the *in vivo* observations. For example, while we were able to show that the elution and digestion fraction of the myocardial matrix degradation products elicited distinctly different chemotaxis from cardiac progenitor cells, the next step would be to distinguish whether different receptors and signaling pathways are activated. Conversely, use of cell culture assays can be employed to identify the fractions of the myocardial matrix that are eliciting these specific cell responses. A simple way of dividing the fractions of the degradation products was used in chapter 3, but an improved understanding of the bioactivity within even smaller fractions, such as via chromatography and mass-spectrometry, may allow us to fine-tune the dosage and timing of administration to maximize therapeutic effects.

Furthermore, we showed that the form of the myocardial matrix that is presented to the cells can an important factor in determining the cellular response, comparing the differences between 3D hydrogel and soluble peptides. Previous studies from our lab on the bioactivity of various ECM-derived hydrogels have primarily utilized adsorption of the myocardial matrix onto tissue culture plastic and thus presenting it to the cultured cells as a 2D coating. One interesting result from these studies was the ability of the myocardial matrix to enhance maturation of cardiac progenitors. However, this result was not replicated when human induced pluripotent stem cells were exposed to the degradation products of the myocardial matrix at various stages of a standard cardiac differentiation protocol. Thus, the form of ECM-derived hydrogels that are presented to the cells – as soluble peptides, 2D coating, or 3D hydrogel – can greatly alter the bioactivity and warrants future experiments which will further its development as a scaffold for tissue engineering applications.

While it is clear that the myocardial matrix offers a protective effect to the post infarct myocardium, it is also evident that our understanding of its mechanism of action is still incomplete. Improving this understanding will aid in improving the design of the myocardial matrix and other ECM-derived hydrogels for post-MI repair.

References

1. Mann, D.L. *Mechanisms and models in heart failure: A combinatorial approach.* Circulation, **1999**. 100(9): p. 999-1008.

2. Yang, F., Y.-H. Liu, X.-P. Yang, J. Xu, A. Kapke, and O.A. Carretero. *Myocardial infarction and cardiac remodelling in mice.* Exp Physiol, **2002**. 87(5): p. 547-555.

3. Christman, K.L. and R.J. Lee. *Biomaterials for the treatment of myocardial infarction.* J Am Coll Cardiol, **2006**. 48(5): p. 907-913.

4. Rane, A.A. and K.L. Christman. *Biomaterials for the treatment of myocardial infarction a 5-year update.* J Am Coll Cardiol, **2011**. 58(25): p. 2615-2629.

5. Sarig, U. and M. Machluf. *Engineering cell platforms for myocardial regeneration.* Expert Opin Drug Deliv, **2011**. 11(8): p. 1055-1077.

6. Lakshmanan, R., U.M. Krishnan, and S. Sethuraman. *Living cardiac patch: the elixir for cardiac regeneration.* Expert Opin Drug Deliv, **2012**. 12(12): p. 1623-1640.

7. Yu, L. and J. Ding. *Injectable hydrogels as unique biomedical materials.* Chem Soc Rev, **2008**. 37(8): p. 1473.

8. Guvendiren, M., H.D. Lu, and J.A. Burdick. *Shear-thinning hydrogels for biomedical applications.* Soft Matter, **2012**. 8(2): p. 260-272.

9. Lee, K.Y. and D.J. Mooney. *Hydrogels for Tissue Engineering.* Chem Rev, **2001**. 101(7): p. 1869-1880.

10. Huang-Lee, L.L., D.T. Cheung, and M.E. Nimni. *Biochemical changes and cytotoxicity associated with the degradation of polymeric glutaraldehyde derived crosslinks.* J Biomed Mater Res, **1990**. 24(9): p. 1185-1201.

11. Augst, A.D., H.J. Kong, and D.J. Mooney. *Alginate Hydrogels as Biomaterials.* Macromol Biosci, **2006**. 6(8): p. 623-633.

12. Cooper, S.L., S.A. Visser, R.W. Hergenrother, and N.M.K. Lambda, *Polymers*, in *Biomater Sci*, B.D. Ratner, et al., Editors. 2004, Elsevier Academic Press: San Diego.

13. Schmaljohann, D. *Thermo- and pH-responsive polymers in drug delivery.* Adv Drug Delivery Rev, **2006**. 58(15): p. 1655-1670.

14. Ulubayram, K., E. Aksu, S.I.D. Gurhan, K. Serbetci, and N. Hasirci. *Cytotoxicity evaluation of gelatin sponges prepared with different cross-linking agents.* Journal of Biomaterials Science, Polymer Edition, **2002**. 13(11): p. 1203-1219.

15. Grover, C.N., J.H. Gwynne, N. Pugh, S. Hamaia, R.W. Farndale, S.M. Best, and R.E. Cameron. *Crosslinking and composition influence the surface properties, mechanical stiffness and cell reactivity of collagen-based films.* Acta Biomater, **2012**. 8(8): p. 3080-3090.

16. Singelyn, J.M. and K.L. Christman. *Modulation of material properties of a decellularized myocardial matrix scaffold.* Macromol Biosci, **2011**. 11(6): p. 731-738.

17. Yannas, I.V., *Natural Materials*, in *Biomater Sci*, B.D. Ratner, et al., Editors. 2004, Elsevier Academic Press: San Diego.

18. Hoshiba, T., H. Lu, N. Kawazoe, and G. Chen. *Decellularized matrices for tissue engineering.* Expert Opin Biol Ther, **2010**. 10(12): p. 1717-1728.

19. Badylak, S.F., D.O. Freytes, and T.W. Gilbert. *Extracellular matrix as a biological scaffold material: Structure and function.* Acta Biomater, **2009**. 5(1): p. 1-13.

20. Christman, K.L., H.H. Fok, R.E. Sievers, Q. Fang, and R.J. Lee. *Fibrin glue alone and skeletal myoblasts in a fibrin scaffold preserve cardiac function after myocardial infarction.* Tissue Eng, **2004**. 10(3/4): p. 403-409.

21. Christman, K.L., A.J. Vardanian, Q. Fang, R.E. Sievers, H.H. Fok, and R.J. Lee. *Injectable Fibrin Scaffold Improves Cell Transplant Survival, Reduces Infarct Expansion, and Induces Neovasculature Formation in Ischemic Myocardium.* J Am Coll Cardiol, **2004**. 44(3): p. 654-660.

22. Janmey, P.A., J.P. Winer, and J.W. Weisel. *Fibrin gels and their clinical and bioengineering applications.* J R Soc Interface, **2009**. 6(30): p. 1-10.

23. Thompson, W.D., E.B. Smith, C.M. Stirk, F.I. Marshall, A.J. Stout, and A. Kocchar. *Angiogenic activity of fibrin degradation products is located in fibrin fragment E.* J Pathol, **1992**. 168(1): p. 47-53.

24. Bootle-Wilbraham, C.A., S. Tazzyman, W.D. Thompson, C.M. Stirk, and C.E. Lewis. *Fibrin fragment E stimulates the proliferation, migration and differentiation of human microvascular endothelial cells in vitro.* Angiogenesis, **2001**. 4(4): p. 269-275.

25. Naito, M., C.M. Stirk, E.B. Smith, and W.D. Thompson. *Smooth Muscle Cell Outgrowth Stimulated by Fibrin Degradation Products: The Potential Role of Fibrin Fragment E in Restenosis and Atherogenesis.* Thromb Res, **2000**. 98(2): p. 165-174.

26. Nelson, D.M., Z. Ma, K.L. Fujimoto, R. Hashizume, and W.R. Wagner. *Intra-myocardial biomaterial injection therapy in the treatment of heart failure: Materials, outcomes and challenges.* Acta Biomater, **2011**. 7(1): p. 1-15.

27. Tous, E., B. Purcell, J.L. Ifkovits, and J.A. Burdick. *Injectable Acellular Hydrogels for Cardiac Repair.* J Cardiovasc Trans Res, **2011**. 4(5): p. 528-542.

28. Johnson, T.D. and K.L. Christman. *Injectable hydrogel therapies and their delivery strategies for treating myocardial infarction.* Expert Opin Drug Deliv, **2012**. 10(1): p. 59-72.

29. Leor, J., S. Miller, M.S. Feinberg, M. Shachar, N. Landa, R. Holbova, and S. Cohen. *A novel injectable alginate scaffold promotes angiogenesis and preserves left ventricular geometry and function after extensive myocardial infarction in rat.* Circulation, **2004**. 110(17): p. 279.

30. Leor, J., S. Tuvia, V. Guetta, F. Manczur, D. Castel, U. Willenz, O. Petneházy, N. Landa, M.S. Feinberg, E. Konen, O. Goitein, O. Tsur-Gang, M. Shaul, L. Klapper, and S. Cohen. *Intracoronary Injection of In Situ Forming Alginate Hydrogel Reverses Left Ventricular Remodeling After Myocardial Infarction in Swine.* J Am Coll Cardiol, **2009**. 54(11): p. 1014-1023.

31. Cabrales, P., A.G. Tsai, and M. Intaglietta. *Alginate plasma expander maintains perfusion and plasma viscosity during extreme hemodilution.* Am J Physiol Heart Circ Physiol, **2005**. 288(4): p. H1708-H1716.

32. Keuren, J.F.W., S.J.H. Wielders, G.M. Willems, M. Morra, L. Cahalan, P. Cahalan, and T. Lindhout. *Thrombogenicity of polysaccharide-coated surfaces.* Biomaterials, **2003**. 24(11): p. 1917-1924.

33. Bella, J.N., V. Palmieri, M.J. Roman, J.E. Liu, T.K. Welty, E.T. Lee, R.R. Fabsitz, B.V. Howard, and R.B. Devereux. *Mitral Ratio of Peak Early to Late Diastolic Filling Velocity as a Predictor of Mortality in Middle-Aged and Elderly Adults: The Strong Heart Study.* Circulation, **2002**. 105(16): p. 1928-1933.

34. Yu, J., Y. Gu, K.T. Du, S. Mihardja, R.E. Sievers, and R.J. Lee. *The effect of injected RGD modified alginate on angiogenesis and left ventricular function in a chronic rat infarct model.* Biomaterials, **2009**. 30(5): p. 751-756.

35. Tsur-Gang, O., E. Ruvinov, N. Landa, R. Holbova, M.S. Feinberg, J. Leor, and S. Cohen. *The effects of peptide-based modification of alginate on left ventricular remodeling and function after myocardial infarction.* Biomaterials, **2009**. 30(2): p. 189-195.

36. Mukherjee, R., J.A. Zavadzkas, S.M. Saunders, J.E. McLean, L.B. Jeffords, C. Beck, R.E. Stroud, A.M. Leone, C.N. Koval, W.T. Rivers, S. Basu, A. Sheehy, G. Michal, and F.G. Spinale. *Targeted Myocardial Microinjections of a Biocomposite Material Reduces Infarct Expansion in Pigs.* Ann Thorac Surg, **2008**. 86(4): p. 1268-1276.

37. Anderson, J.M., A. Rodriguez, and D.T. Chang. *Foreign body reaction to biomaterials.* Semin Immunol, **2008**. 20(2): p. 86-100.

38. Ifkovits, J.L., E. Tous, M. Minakawa, M. Morita, J.D. Robb, K.J. Koomalsingh, J.H.I. Gorman, R.C. Gorman, and J.A. Burdick. *Injectable hydrogel properties influence infarct expansion and extent of postinfarction left ventricular remodeling in an ovine model.* Proc Natl Acad Sci, **2010**. 107(25): p. 11507-11512.

39. Tous, E., J.L. Ifkovits, K.J. Koomalsingh, T. Shuto, T. Soeda, N. Kondo, J.H. Gorman, R.C. Gorman, and J.A. Burdick. *Influence of injectable hyaluronic acid hydrogel degradation behavior on infarction-induced ventricular remodeling.* Biomacromolecules, **2011**. 12(11): p. 4127-4135.

40. Singelyn, J.M., J.A. Dequach, S.B. Seif-Naraghi, R.B. Littlefield, P.J. Schup-Magoffin, and K.L. Christman. *Naturally derived myocardial matrix as an injectable scaffold for cardiac tissue engineering.* Biomaterials, **2009**. 30(29): p. 5409-5416.

41. Singelyn, J.M., P. Sundaramurthy, T.D. Johnson, P.J. Schup-Magoffin, D.P. Hu, D.M. Faulk, J. Wang, K.M. Mayle, K. Bartels, M. Salvatore, A.M. Kinsey, A.N. Demaria, N. Dib, and K.L. Christman. *Catheter-deliverable hydrogel derived from decellularized ventricular extracellular matrix increases endogenous cardiomyocytes and preserves cardiac function post-myocardial infarction.* J Am Coll Cardiol, **2012**. 59(8): p. 751-763.

42. Seif-Naraghi, S.B., J.M. Singelyn, M.A. Salvatore, K. Osborn, J.J. Wang, J.A. Dequach, U. Sampat, O.L. Kwan, M. Strachan, J. Wong, K. Bartels, A.M. Kinsey, M. Preul, A.N. DeMaria, N. Dib, and K.L. Christman. *Safety and efficacy of an injectable extracellular matrix hydrogel for treating myocardial infarction in pre-clinical animal studies.* Sci Transl Med, **2013**. 5: p. 173ra125.

43. Holmes, T.C. *Novel peptide-based biomaterial scaffolds for tissue engineering.* Trends Biotechnol, **2002**. 20(1): p. 16-21.

44. Chen, Q.-Z., S.E. Harding, N.N. Ali, A.R. Lyon, and A.R. Boccaccini. *Biomaterials in cardiac tissue engineering: Ten years of research survey.* Mater Sci Eng R Rep, **2008**. 59(1–6): p. 1-37.

45. Griffith, L.G. *Polymeric biomaterials.* Acta Mater, **2000**. 48(1): p. 263-277.

46. Zhang, S., T. Holmes, C. Lockshin, and A. Rich. *Spontaneous assembly of a self-complementary oligopeptide to form a stable macroscopic membrane.* Proc Natl Acad Sci, **1992**. 90: p. 3334-3338.

47. Zhang, S., T.C. Holmes, C.M. DiPersio, R.O. Hynes, X. Su, and A. Rich. *Self-complementary oligopeptide matrices support mammalian cell attachment.* Biomaterials, **1995**. 16(18): p. 1385-1393.

48. Prieto, A.L., G.M. Edelman, and K.L. Crossin. *Multiple integrins mediate cell attachment to cytotactin/tenascin.* Proc Natl Acad Sci, **1993**. 90(21): p. 10154-10158.

49. Zhang, S. *Fabrication of novel biomaterials through molecular self-assembly.* Nat Biotechnol, **2003**. 21(10): p. 1171-1178.

50. Holmes, T.C., S. de Lacalle, X. Su, G. Liu, A. Rich, and S. Zhang. *Extensive neurite outgrowth and active synapse formation on self-assembling peptide scaffolds.* Proc Natl Acad Sci, **2000**. 97(12): p. 6728-6733.

51. Semino, C.E., J.R. Merok, G.G. Crane, G. Panagiotakos, and S. Zhang. *Functional differentiation of hepatocyte-like spheroid structures from putative liver progenitor cells in three-dimensional peptide scaffolds.* Differentiation, **2003**. 71(4–5): p. 262-270.

52. Davis, M.E., J.P.M. Motion, D.A. Narmoneva, T. Takahashi, D. Hakuno, R.D. Kamm, S. Zhang, and R.T. Lee. *Injectable Self-Assembling Peptide Nanofibers Create Intramyocardial Microenvironments for Endothelial Cells.* Circulation, **2005**. 111: p. 442-450.

53. Lin, Y.-D., M.-L. Yeh, Y.-J. Yang, D.-C. Tsai, T.-Y. Chu, Y.-Y. Shih, M.-Y. Chang, Y.-W. Liu, A.C.L. Tang, T.-Y. Chen, C.-Y. Luo, K.-C. Chang, J.-H. Chen, H.-L. Wu, T.-K. Hung, and P.C.H. Hsieh. *Intramyocardial Peptide Nanofiber Injection Improves Postinfarction Ventricular Remodeling and Efficacy of Bone Marrow Cell Therapy in Pigs.* Circulation, **2010**: p. S132-S141.

54. Dobner, S., D. Bezuidenhout, P. Govender, P. Zilla, and N. Davies. *A Synthetic Non-degradable Polyethylene Glycol Hydrogel Retards Adverse Post-infarct Left Ventricular Remodeling.* J Card Fail, **2009**. 15(7): p. 629-636.

55. Jiang, X.-J., T. Wang, X.-Y. Li, D.-Q. Wu, Z.-B. Zheng, J.-F. Zhang, J.-L. Chen, B. Peng, H. Jiang, C. Huang, and X.-Z. Zhang. *Injection of a novel synthetic hydrogel preserves left ventricle function after myocardial infarction.* J Biomed Mater Res A, **2009**. 90A(2): p. 472-477.

56. Rane, A.A., J.S. Chuang, A. Shah, D.P. Hu, N.D. Dalton, Y. Gu, K.L. Peterson, J.H. Omens, and K.L. Christman. *Increased infarct wall thickness by a bio-inert material is insufficient to prevent negative left ventricular remodeling after myocardial infarction.* PLoS ONE, **2011**. 6(6): p. e21571.

57. Wu, J., F. Zeng, X.-P. Huang, J.C.-Y. Chung, F. Konecny, R.D. Weisel, and R.-K. Li. *Infarct stabilization and cardiac repair with a VEGF-conjugated, injectable hydrogel.* Biomaterials, **2011**. 32(2): p. 579-586.

58. Fujimoto, K.L., Z. Ma, D.M. Nelson, R. Hashizume, J. Guan, K. Tobita, and W.R. Wagner. *Synthesis, characterization and therapeutic efficacy of a biodegradable, thermoresponsive hydrogel designed for application in chronic infarcted myocardium.* Biomaterials, **2009**. 30(26): p. 4357-4368.

59. Garbern, J.C., E. Minami, P.S. Stayton, and C.E. Murry. *Delivery of basic fibroblast growth factor with a pH-responsive, injectable hydrogel to improve angiogenesis in infarcted myocardium.* Biomaterials, **2011**. 32(9): p. 2407-2416.

60. Wall, S.T., C.-C. Yeh, R.Y.K. Tu, M.J. Mann, and K.E. Healy. *Biomimetic matrices for myocardial stabilization and stem cell transplantation.* J Biomed Mater Res A, **2010**. 95A(4): p. 1055-1066.

61. Wang, T., D.Q. Wu, X.J. Jiang, X.Z. Zhang, X.Y. Li, J.F. Zhang, Z.B. Zheng, R. Zhuo, H. Jiang, and C. Huang. *Novel thermosensitive hydrogel injection inhibits post-infarct ventricle remodelling.* Eur J Heart Fail, **2009**. 11(1): p. 14-19.

62. Hoffman, A.S., *Applications of "Smart Polymers" as Biomaterials*, in *Biomater Sci*, B.D. Ratner, et al., Editors. 2004, Elsevier Academic Press: San Diego.

63. Wall, S.T., J.C. Walker, K.E. Healy, M.B. Ratcliffe, and J.M. Guccione. *Theoretical impact of the injection of material Into the myocardium.* Circulation, **2006**. 114(24): p. 2647-2635.

64. Huang, N.F., J. Yu, R. Sievers, S. Li, and R.J. Lee. *Injectable biopolymers enhance angiogenesis after myocardial infarction.* Tissue Eng, **2005**. 11(11-12): p. 1860-1866.

65. Trial, J., R.D. Rossen, J. Rubio, and A.A. Knowlton. *Inflammation and ischemia: macrophages activated by fibronectin fragments enhance the survival of injured cardiac myocytes.* Exp Biol Med, **2004**. 229(6): p. 538-545.

66. Mihardja, S.S., D. Gao, R.E. Sievers, Q. Fang, J. Feng, J. Wang, H.F. Vanbrocklin, J.W. Larrick, M. Huang, M. Dae, and R.J. Lee. *Targeted In Vivo Extracellular Matrix Formation Promotes Neovascularization in a Rodent Model of Myocardial Infarction.* PLoS ONE, **2010**. 5(4): p. e10384.

67. Yu, J., K.L. Christman, E. Chin, R.E. Sievers, M. Saeed, and R.J. Lee. *Restoration of left ventricular geometry and improvement of left ventricular function in a rodent model of chronic ischemic cardiomyopathy.* J Thorac Cardiov Sur, **2009**. 137(1): p. 180-187.

68. Mohsin, S., S. Siddiqi, B. Collins, and M.A. Sussman. *Empowering Adult Stem Cells for Myocardial Regeneration.* Circ Res, **2011**. 109(12): p. 1415-1428.

69. Huu, A.L., S. Prakash, and D. Shum-Tim. *Cellular cardiomyoplasty: current state of the field.* Regen Med, **2012**. 7(4): p. 571-582.

70. Passier, R., L.W. van Laake, and C.L. Mummery. *Stem-cell-based therapy and lessons from the heart.* Nature, **2008**. 453(7193): p. 322-329.

71. Wollert, K.C., *Bone Marrow Cell Therapy After Myocardial Infarction: What have we Learned from the Clinical Trials and Where Are We Going?*, in *Regenerating the Heart*, I.S. Cohen and G.R. Gaudette, Editors. 2011, Humana Press. p. 111-129.

72. Reinecke, H. and C.E. Murry. *Taking the Death Toll After Cardiomyocyte Grafting: A Reminder of the Importance of Quantitative Biology.* J Mol Cell Cardiol, **2002**. 34(3): p. 251-253.

73. Haider, H.K. and M. Ashraf. *Strategies to promote donor cell survival: Combining preconditioning approach with stem cell transplantation.* J Mol Cell Cardiol, **2008**. 45(4): p. 554-566.

74. Robey, T.E., M.K. Saiget, H. Reinecke, and C.E. Murry. *Systems approaches to preventing transplanted cell death in cardiac repair.* J Mol Cell Cardiol, **2008**. 45(4): p. 567-581.

75. Nakamuta, J.S., M.E. Danoviz, F.L.N. Marques, L. dos Santos, C. Becker, G.A. Gonçalves, P.F. Vassallo, I.T. Schettert, P.J.F. Tucci, and J.E. Krieger. *Cell Therapy Attenuates Cardiac Dysfunction Post Myocardial Infarction: Effect of Timing, Routes of Injection and a Fibrin Scaffold.* PLoS ONE, **2009**. 4(6): p. e6005.

76. Guo, H.D., H.J. Wang, Y.Z. Tan, and J.H. Wu. *Transplantation of marrow-derived cardiac stem cells carried in fibrin improves cardiac function after myocardial infarction.* Tissue Eng Pt A, **2011**. 17(1-2): p. 45-58.

77. Danoviz, M.E., J.S. Nakamuta, F.L.N. Marques, L. dos Santos, E.C. Alvarenga, A.A. dos Santos, E.L. Antonio, I.T. Schettert, P.J. Tucci, and J.E. Krieger. *Rat Adipose Tissue-Derived Stem Cells Transplantation Attenuates Cardiac Dysfunction Post Infarction and Biopolymers Enhance Cell Retention.* PLoS ONE, **2010**. 5(8): p. e12077.

78. Zhang, G., Q. Hu, E.A. Braunlin, L.J. Suggs, and J. Zhang. *Enhancing Efficacy of Stem Cell Transplantation to the Heart with a PEGylated Fibrin Biomatrix.* Tissue Eng Pt A, **2008**. 14(6): p. 1025-1036.

79. Lu, W.-N., S.-H. Lü, H.-B. Wang, D.-X. Li, C.-M. Duan, Z.-Q. Liu, T. Hao, W.-J. He, B. Xu, Q. Fu, Y.C. Song, X.-H. Xie, and C.-Y. Wang. *Functional Improvement of Infarcted Heart by Co-Injection of Embryonic Stem Cells with Temperature-Responsive Chitosan Hydrogel.* Tissue Eng Pt A, **2009**. 15(6): p. 1437-1447.

80. Lü, S., H. Wang, W. Lu, S. Liu, Q. Lin, D. Li, C. Duan, T. Hao, J. Zhou, Y. Wang, S. Gao, and C. Wang. *Both the Transplantation of Somatic Cell Nuclear Transfer- and Fertilization-Derived Mouse Embryonic Stem Cells with Temperature-Responsive Chitosan Hydrogel Improve Myocardial Performance in Infarcted Rat Hearts.* Tissue Eng Pt A, **2010**. 16(4): p. 1303-1315.

81. Laflamme, M.A., K.Y. Chen, A.V. Naumova, V. Muskheli, J.A. Fugate, S.K. Dupras, H. Reinecke, C. Xu, M. Hassanipour, S. Police, C. O'Sullivan, L. Collins, Y. Chen, E. Minami, E.A. Gill, S. Ueno, C. Yuan, J. Gold, and C.E. Murry. *Cardiomyocytes derived from human embryonic stem cells in pro-survival factors enhance function of infarcted rat hearts.* Nat Biotechnol, **2007**. 25(9): p. 1015-1024.

82. Yu, J., K.T. Du, Q. Fang, Y. Gu, S.S. Mihardja, R.E. Sievers, J.C. Wu, and R.J. Lee. *The use of human mesenchymal stem cells encapsulated in RGD modified alginate microspheres in the repair of myocardial infarction in the rat.* Biomaterials, **2010**. 31(27): p. 7012-7020.

83. Kraehenbuehl, T.P., L.S. Ferreira, A.M. Hayward, M. Nahrendorf, A.J. van der Vlies, E. Vasile, R. Weissleder, R. Langer, and J.A. Hubbell. *Human embryonic stem cell-derived microvascular grafts for cardiac tissue preservation after myocardial infarction.* Biomaterials, **2011**. 32(4): p. 1102-1109.

84. Wang, T., X.-J. Jiang, Q.-Z. Tang, X.-Y. Li, T. Lin, D.-Q. Wu, X.-Z. Zhang, and E. Okello. *Bone marrow stem cells implantation with α-cyclodextrin/MPEG–PCL–MPEG hydrogel improves cardiac function after myocardial infarction.* Acta Biomater, **2009**. 5(8): p. 2939-2944.

85. Li, X.Y., T. Wang, X.J. Jiang, T. Lin, D.Q. Wu, X.Z. Zhang, E. Okello, H.X. Xu, and M.J. Yuan. *Injectable Hydrogel Helps Bone Marrow-Derived Mononuclear Cells Restore Infarcted Myocardium.* Cardiology, **2010**. 115(3): p. 194-199.

86. Dubois, G., V.F.M. Segers, V. Bellamy, L. Sabbah, S. Peyrard, P. Bruneval, A.A. Hagège, R.T. Lee, and P. Menasché. *Self-assembling peptide nanofibers and skeletal myoblast transplantation in infarcted myocardium.* J Biomed Mater Res B, **2008**. 87B(1): p. 222-228.

87. Mathieu, E., G. Lamirault, C. Toquet, P. Lhommet, E. Rederstorff, S. Sourice, K. Biteau, P. Hulin, V. Forest, P. Weiss, J. Guicheux, and P. Lemarchand. *Intramyocardial Delivery of Mesenchymal Stem Cell-Seeded Hydrogel Preserves Cardiac Function and Attenuates Ventricular Remodeling after Myocardial Infarction.* PLoS ONE, **2012**. 7(12): p. e51991.

88. Yanagisawa-Miwa, A., Y. Uchida, F. Nakamura, T. Tomaru, H. Kido, T. Kamijo, T. Sugimoto, K. Kaji, M. Utsuyama, and C. Kurashima. *Salvage of infarcted myocardium by angiogenic action of basic fibroblast growth factor.* Science, **1992**. 257(5075): p. 1401-1403.

89. Battler, A., M. Scheinowitz, A. Bor, D. Hasdai, Z. Vered, E. Di Segni, N. Varda-Bloom, D. Nass, S. Engelberg, M. Eldar, M. Belkin, and N. Savion. *Intracoronary injection of basic fibroblast growth factor enhances angiogenesis in infarcted swine myocardium.* J Am Coll Cardiol, **1993**. 22(7): p. 2001-2006.

90. Landau, C., A.K. Jacobs, and C.C. Haudenschild. *Intrapericardial basic fibroblast growth factor induces myocardial angiogenesis in a rabbit model of chronic ischemia.* Am Heart J, **1995**. 129(5): p. 924-931.

91. Yamamoto, T., N. Suto, T. Okubo, A. Mikuniya, H. Hanada, S. Yagihashi, M. Fujita, and K. Okumura. *Intramyocardial Delivery of Basic Fibroblast Growth Factor-Impregnated Gelatin Hydrogel Microspheres Enhances Collateral Circulation to Infarcted Canine Myocardium.* Jpn Circ J, **2001**. 65(5): p. 439-444.

92. Sakakibara, Y., K. Nishimura, K. Tambara, M. Yamamoto, F. Lu, Y. Tabata, and M. Komeda. *Prevascularization with gelatin microspheres containing basic fibroblast growth factor enhances the benefits of cardiomyocyte transplantation.* J Thorac Cardiovasc Surg, **2002**. 124(1): p. 50-56.

93. Iwakura, A., M. Fujita, K. Kataoka, K. Tambara, Y. Sakakibara, M. Komeda, and Y. Tabata. *Intramyocardial sustained delivery of basic fibroblast growth factor improves angiogenesis and ventricular function in a rat infarct model.* Heart Vessels, **2003**. 18(2): p. 93-99.

94. Liu, Y., L. Sun, Y. Huan, H. Zhao, and J. Deng. *Effects of basic fibroblast growth factor microspheres on angiogenesis in ischemic myocardium and cardiac function: analysis with dobutamine cardiovascular magnetic resonance tagging.* Eur J Cardio-Thorac, **2006**. 30(1): p. 103-107.

95. Shao, Z.-Q., K. Takaji, Y. Katayama, R. Kunitomo, H. Sakaguchi, Z.-F. Lai, and M. Kawasuji. *Effects of intramyocardial administration of slow-release basic fibroblast growth factor on angiogenesis and ventricular remodeling in a rat infarct model.* Circ J, **2006**. 70(4): p. 471-477.

96. Young, S., M. Wong, Y. Tabata, and A.G. Mikos. *Gelatin as a delivery vehicle for the controlled release of bioactive molecules.* J Control Release, **2005**. 109(1–3): p. 256-274.

97. Wang, H., X. Zhang, Y. Li, Y. Ma, Y. Zhang, Z. Liu, J. Zhou, Q. Lin, Y. Wang, C. Duan, and C. Wang. *Improved myocardial performance in infarcted rat heart by co-injection of basic fibroblast growth factor with temperature-responsive Chitosan hydrogel.* J Heart Lung Transpl, **2010**. 29(8): p. 881-887.

98. Nie, S.-p., X. Wang, S.-b. Qiao, Q.-t. Zeng, J.-q. Jiang, X.-q. Liu, X.-m. Zhu, G.-x. Cao, and C.-s. Ma. *Improved myocardial perfusion and cardiac function by controlled-release basic fibroblast growth factor using fibrin glue in a canine infarct model.* J ZheJiang Univ Sci B, **2010**. 11(12): p. 895-904.

99. Lin, Y.-D., C.-Y. Luo, Y.-N. Hu, M.-L. Yeh, Y.-C. Hsueh, M.-Y. Chang, D.-C. Tsai, J.-N. Wang, M.-J. Tang, E.I.H. Wei, M.L. Springer, and P.C.H. Hsieh. *Instructive Nanofiber Scaffolds with VEGF Create a Microenvironment for Arteriogenesis and Cardiac Repair.* Sci Transl Med, **2012**. 4(146): p. 146ra109-146ra109.

100. Hsieh, P.C.H., M.E. Davis, J. Gannon, C. MacGillivray, and R.T. Lee. *Controlled delivery of PDGF-BB for myocardial protection using injectable self-assembling peptide nanofibers.* J Clin Invest, **2006**. 116(1): p. 237-248.

101. Hsieh, P.C.H., C. MacGillivray, J. Gannon, F.U. Cruz, and R.T. Lee. *Local Controlled Intramyocardial Delivery of Platelet-Derived Growth Factor Improves Postinfarction Ventricular Function Without Pulmonary Toxicity.* Circulation, **2006**. 114: p. 637-644.

102. Davis, M.E., P.C.H. Hsieh, T. Takahashi, Q. Song, S. Zhang, R.D. Kamm, A.J. Grodzinky, P. Anversa, and R.T. Lee. *Local myocardial insulin-like growth factor 1 (IGF-1) delivery*

with biotinylated peptide nanofibers improves cell therapy for myocardial infarction. Proc Natl Acad Sci, **2006**. 103(21): p. 8155-8160.

103. Segers, V.F.M., T. Tokunou, L.J. Higgins, C. MacGillivray, J. Gannon, and R.T. Lee. *Local Delivery of Protease-Resistant Stromal Cell Derived Factor-1 for Stem Cell Recruitment After Myocardial Infarction.* Circulation, **2007**. 116(15): p. 1683-1692.

104. Wang, T., X.-J. Jiang, T. Lin, S. Ren, X.-Y. Li, X.-Z. Zhang, and Q.-z. Tang. *The inhibition of postinfarct ventricle remodeling without polycythaemia following local sustained intramyocardial delivery of erythropoietin within a supramolecular hydrogel.* Biomaterials, **2009**. 30(25): p. 4161-4167.

105. Hao, X., E.A. Silva, A. Mansson-Broberg, K.-H. Grinnemo, A.J. Siddiqui, G. Dellgren, E. Wardell, L.A. Brodin, D.J. Mooney, and C. Sylven. *Angiogenic effects of sequential release of VEGF-A165 and PDGF-BB with alginate hydrogels after myocardial infarction.* Cardiovasc Res, **2007**. 75(1): p. 178-185.

106. Kim, J.H., Y. Jung, S.-H. Kim, K. Sun, J. Choi, H.C. Kim, Y. Park, and S.H. Kim. *The enhancement of mature vessel formation and cardiac function in infarcted hearts using dual growth factor delivery with self-assembling peptides.* Biomaterials, **2011**. 32: p. 6080-6088.

107. Ruvinov, E., J. Leor, and S. Cohen. *The promotion of myocardial repair by the sequential delivery of IGF-1 and HGF from an injectable alginate biomaterial in a model of acute myocardial infarction.* Biomaterials, **2011**. 32(2): p. 565-578.

108. Salimath, A.S., E.A. Phelps, A.V. Boopathy, P.-l. Che, M. Brown, A.J. García, and M.E. Davis. *Dual Delivery of Hepatocyte and Vascular Endothelial Growth Factors via a Protease-Degradable Hydrogel Improves Cardiac Function in Rats.* PLoS ONE, **2012**. 7(11): p. e50980.

109. Kwon, J.S., I.K. Park, A.S. Cho, S.M. Shin, M.H. Hong, S.Y. Jeong, Y.S. Kim, J.-J. Min, M.H. Jeong, W.J. Kim, S. Jo, S.H. Pun, J.G. Cho, J.C. Park, J.C. Kang, and Y. Ahn. *Enhanced angiogenesis mediated by vascular endothelial growth factor plasmid-loaded thermo-responsive amphiphilic polymer in a rat myocardial infarction model.* J Control Release, **2009**. 138(2): p. 168-176.

110. Christman, K.L., Q. Fang, M.S. Yee, K.R. Johnson, R.E. Sievers, and R.J. Lee. *Enhanced neovasculature formation in ischemic myocardium following delivery of pleiotrophin plasmid in a biopolymer.* Biomaterials, **2005**. 26(10): p. 1139-1144.

111. Stamm, C., B. Nasseri, Y.-H. Choi, and R. Hetzer. *Cell Therapy for Heart Disease: Great Expectations, As Yet Unmet.* Heart Lung Circ, **2009**. 18(4): p. 245-256.

112. Dib, N., A. Campbell, D.B. Jacoby, A. Zawadzka, J. Ratliff, B.M. Miedzybrocki, A. Gahremanpour, E.B. Diethrich, and S.R. Opie. *Safety and feasibility of percutaneous autologous skeletal myoblast transplantation in the coil-infarcted swine myocardium.* J Pharmacol Toxicol Methods, **2006**. 54(1): p. 71-77.

113. Grover, G.N., R.L. Braden, and K.L. Christman. *Oxime cross-linked injectable hydrogels for catheter delivery.* Adv Mater, **2013**. In Press.

114. Frey, N., A. Linke, T. Süselbeck, J. Müller-Ehmsen, P. Vermeersch, D. Schoors, M. Rosenberg, F. Bea, S. Tuvia, and J. Leor. *Intracoronary Delivery of Injectable Bioabsorbable Scaffold (IK-5001) to Treat Left Ventricular Remodeling After ST-Elevation Myocardial Infarction: A First-in-Man Study.* Circ Cardiovasc Interv, **2014**. 7(6): p. 806-812.

115. Leri, A., J. Kajstura, and P. Anversa. *Role of Cardiac Stem Cells in Cardiac Pathophysiology: A Paradigm Shift in Human Myocardial Biology.* Circ Res, **2011**. 109(8): p. 941-961.

116. Xin, M., E.N. Olson, and R. Bassel-Duby. *Mending broken hearts: cardiac development as a basis for adult heart regeneration and repair.* Nat Rev Mol Cell Biol, **2013**. 14(8): p. 529-541.

117. Ventura-Clapier, R., A. Garnier, V. Veksler, and F. Joubert. *Bioenergetics of the failing heart.* BBA - Mol Cel Res, **2011**. 1813(7): p. 1360-1372.

118. Siddiqi, N., S. Singh, R. Beadle, D. Dawson, and M. Frenneaux. *Cardiac metabolism in hypertrophy and heart failure: implications for therapy.* Heart Fail Rev, **2013**. 18(5): p. 595-606.

119. Wang, Z.V., D.L. Li, and J.A. Hill. *Heart Failure and Loss of Metabolic Control.* J Cardiovasc Pharm, **2014**. 63(4): p. 302-313.

120. Go, A.S., D. Mozaffarian, V.L. Roger, E.J. Benjamin, J.D. Berry, W.B. Borden, D.M. Bravata, S. Dai, E.S. Ford, C.S. Fox, S. Franco, H.J. Fullerton, C. Gillespie, S.M. Hailpern, J.A. Heit, V.J. Howard, M.D. Huffman, B.M. Kissela, S.J. Kittner, D.T. Lackland, J.H. Lichtman, L.D. Lisabeth, D. Magid, G.M. Marcus, A. Marelli, D.B. Matchar, D.K. McGuire, E.R. Mohler, C.S. Moy, M.E. Mussolino, G. Nichol, N.P. Paynter, P.J. Schreiner, P.D. Sorlie, J. Stein, T.N. Turan, S.S. Virani, N.D. Wong, D. Woo, and M.B. Turner. *Heart disease and stroke statistics—2013 Update: A report from the American Heart Association.* Circulation, **2013**. 127(1): p. e6-e245.

121. Hastings, C.L., E.T. Roche, E. Ruiz-Hernandez, K. Schenke-Layland, C.J. Walsh, and G.P. Duffy. *Drug and cell delivery for cardiac regeneration.* Adv Drug Delivery Rev, (0).

122. Clifford, D.M., S.A. Fisher, S.J. Brunskill, C. Doree, A. Mathur, S. Watt, and E. Martin‐Rendon. *Stem cell treatment for acute myocardial infarction.* The Cochrane Library, **2012**.

123. Hsiao, A., T. Ideker, J.M. Olefsky, and S. Subramaniam. *VAMPIRE microarray suite: a web-based platform for the interpretation of gene expression data.* Nucleic Acids Res, **2005**. 33(suppl 2): p. W627-W632.

124. Gottfried, E., L.A. Kunz-Schughart, A. Weber, M. Rehli, A. Peuker, A. Müller, M. Kastenberger, G. Brockhoff, R. Andreesen, and M. Kreutz. *Expression of CD68 in Non-Myeloid Cell Types.* Scand J Immunol, **2008**. 67(5): p. 453-463.

125. Dean, R.A., J.H. Cox, C.L. Bellac, A. Doucet, A.E. Starr, and C.M. Overall. *Macrophage-specific metalloelastase (MMP-12) truncates and inactivates ELR+ CXC chemokines and generates CCL2, -7, -8, and -13 antagonists: potential role of the macrophage in terminating polymorphonuclear leukocyte influx.* Blood, **2008**. 112(8): p. 3455-3464.

126. Laflamme, M.A. and C.E. Murry. *Heart regeneration.* Nature, **2011**. 473(7347): p. 326-335.

127. Zhou, Y., P. Pan, L. Yao, M. Su, P. He, N. Niu, M.A. McNutt, and J. Gu. *CD117-positive Cells of the Heart: Progenitor Cells or Mast Cells?* J Histochem Cytochem, **2010**. 58(4): p. 309-316.

128. Jameel, M.N., Q. Li, A. Mansoor, X. Qiang, A. Sarver, X. Wang, C. Swingen, and J. Zhang. *Long-term functional improvement and gene expression changes after bone marrow-derived multipotent progenitor cell transplantation in myocardial infarction.* Am J Physiol Heart Circ Physiol, **2010**. 298(5): p. H1348-H1356.

129. Burt, R.K., Y.-h. Chen, L. Verda, C. Lucena, S. Navale, J. Johnson, X. Han, J. Lomasney, J.M. Baker, K.-L. Ngai, A. Kino, J. Carr, J. Kajstura, and P. Anversa. *Mitotically Inactivated Embryonic Stem Cells can be Utilized as an In Vivo Feeder Layer to Nurse Damaged Myocardium Following Acute Myocardial Infarction: A Pre-Clinical Study.* Circ Res, **2012**. 111: p. 1286-1296.

130. Lachtermacher, S., B.B. Esporcatte, F. da Silva de Azevedo Fortes, N. Rocha, F. Montalvão, P. Costa, L. Belem, A. Rabischoffisky, H.C. Faria Neto, R. Vasconcellos, D. Iacobas, S. Iacobas, D. Spray, N. Thomas, R.S. Goldenberg, and A. Campos de Carvalho. *Functional and Transcriptomic Recovery of Infarcted Mouse Myocardium Treated with Bone Marrow Mononuclear Cells.* Stem Cell Rev and Rep, **2012**. 8(1): p. 251-261.

131. Pavo, N., M. Zimmermann, D. Pils, M. Mildner, Z. Petrási, Ö. Petneházy, J. Fuzik, A. Jakab, C. Gabriel, W. Sipos, G. Maurer, M. Gyöngyösi, and H.J. Ankersmit. *Long-acting*

beneficial effect of percutaneously intramyocardially delivered secretome of apoptotic peripheral blood cells on porcine chronic ischemic left ventricular dysfunction. Biomaterials, **2014**. 35(11): p. 3541-3550.

132. Martinez, F.O., A. Sica, A. Mantovani, and M. Locati. *Macrophage activation and polarization.* Front Biosci, **2008**. 13: p. 453-461.

133. Badylak, S.F., J.E. Valentin, A.K. Ravindra, G.P. McCabe, and A.M. Stewart-Akers. *Macrophage phenotype as a determinant of biologic scaffold remodeling.* Tissue Eng Pt A, **2008**. 14(11): p. 1835-1842.

134. Brown, B.N., J.E. Valentin, A.M. Stewart-Akers, G.P. McCabe, and S.F. Badylak. *Macrophage phenotype and remodeling outcomes in response to biologic scaffolds with and without a cellular component.* Biomaterials, **2009**. 30(8): p. 1482-1491.

135. Valentin, J.E., A.M. Stewart-Akers, T.W. Gilbert, and S.F. Badylak. *Macrophage Participation in the Degradation and Remodeling of Extracellular Matrix Scaffolds.* Tissue Eng Pt A, **2009**. 15(7): p. 1687.

136. Nahrendorf, M., M.J. Pittet, and F.K. Swirski. *Monocytes: Protagonists of Infarct Inflammation and Repair After Myocardial Infarction.* Circulation, **2010**. 121(22): p. 2437-2445.

137. Troidl, C., H. Möllmann, H. Nef, F. Masseli, S. Voss, S. Szardien, M. Willmer, A. Rolf, J. Rixe, and K. Troidl. *Classically and alternatively activated macrophages contribute to tissue remodelling after myocardial infarction.* J Cell Mol Med, **2009**. 13(9b): p. 3485-3496.

138. Novak, M.L. and T.J. Koh. *Phenotypic Transitions of Macrophages Orchestrate Tissue Repair.* Am J Pathol, **2013**. 183(5): p. 1352-1363.

139. Wermuth, P. and S. Jimenez. *The significance of macrophage polarization subtypes for animal models of tissue fibrosis and human fibrotic diseases.* Clin Transl Med, **2015**. 4(1): p. 2.

140. Nahrendorf, M., F.K. Swirski, E. Aikawa, L. Stangenberg, T. Wurdinger, J.-L. Figueiredo, P. Libby, R. Weissleder, and M.J. Pittet. *The healing myocardium sequentially mobilizes two monocyte subsets with divergent and complementary functions.* J Exp Med, **2007**. 204(12): p. 3037-3047.

141. Aurora, A.B., E.R. Porrello, W. Tan, A.I. Mahmoud, J.A. Hill, R. Bassel-Duby, H.A. Sadek, and E.N. Olson. *Macrophages are required for neonatal heart regeneration.* J Clin Invest, **2014**. 124(3): p. 1382-1392.

142. Bischoff, S.C. *Role of mast cells in allergic and non-allergic immune responses: comparison of human and murine data.* Nat Rev Immunol, **2007**. 7(2): p. 93-104.

143. Frangogiannis, N.G., C.W. Smith, and M.L. Entman. *The inflammatory response in myocardial infarction.* **2002**. 53(1): p. 31-47.

144. Frangogiannis, N. and M. Entman, *Identification of Mast Cells in the Cellular Response to Myocardial Infarction*, in *Mast Cells*, G. Krishnaswamy and D. Chi, Editors. 2005, Humana Press. p. 91-101.

145. Levick, S.P., G.C. Meléndez, E. Plante, J.L. McLarty, G.L. Brower, and J.S. Janicki. *Cardiac mast cells: the centrepiece in adverse myocardial remodelling.* Cardiovasc Res, **2010**. 89(1): p. 12-19.

146. Somasundaram, P., G. Ren, H. Nagar, D. Kraemer, L. Mendoza, L.H. Michael, G.H. Caughey, M.L. Entman, and N.G. Frangogiannis. *Mast cell tryptase may modulate endothelial cell phenotype in healing myocardial infarcts.* J Pathol, **2005**. 205(1): p. 102-111.

147. Kwon, J.S., Y.S. Kim, A.S. Cho, H.H. Cho, J.S. Kim, M.H. Hong, S.Y. Jeong, M.H. Jeong, J.G. Cho, J.C. Park, J.C. Kang, and Y. Ahn. *The novel role of mast cells in the microenvironment of acute myocardial infarction.* J Mol Cell Cardiol, **2011**. 50(5): p. 814-825.

148. Tang, L., T. Jennings, and J.W. Eaton. *Mast Cells Mediate Acute Inflammatory Responses to Implanted Blomaterials.* Pediatr Res, **1997**. 41(S4): p. 116-116.

149. Palojoki, E., A. Saraste, A. Eriksson, K. Pulkki, M. Kallajoki, L.-M. Voipio-Pulkki, and I. Tikkanen. *Cardiomyocyte apoptosis and ventricular remodeling after myocardial infarction in rats.* Am J Physiol Heart Circ Physiol, **2001**. 280(6): p. H2726-H2731.

150. Pendergrass, K.D., S.T. Varghese, K. Maiellaro-Rafferty, M.E. Brown, W.R. Taylor, and M.E. Davis. *Temporal Effects of Catalase Overexpression on Healing After Myocardial Infarction.* Circ Heart Fail, **2011**. 4(1): p. 98-106.

151. Wu, M.-L., Y.-C. Ho, and S.-F. Yet. *A Central Role of Heme Oxygenase-1 in Cardiovascular Protection.* Antioxid Redox Signaling, **2010**. 15(7): p. 1835-1846.

152. Lee, S.H., P.L. Wolf, R. Escudero, R. Deutsch, S.W. Jamieson, and P.A. Thistlethwaite. *Early Expression of Angiogenesis Factors in Acute Myocardial Ischemia and Infarction.* New Engl J Med, **2000**. 342(9): p. 626-633.

153. Virag, J.I. and C.E. Murry. *Myofibroblast and Endothelial Cell Proliferation during Murine Myocardial Infarct Repair.* Am J Pathol, **2003**. 163(6): p. 2433-2440.

154. Conway, E.M., D. Collen, and P. Carmeliet. *Molecular mechanisms of blood vessel growth.* Cardiovasc Res, **2001**. 49(3): p. 507-521.

155. Carmeliet, P. *Angiogenesis in health and disease.* Nat Med, **2003**. 9(6): p. 653-660.

156. Davis, G.E., K.J. Bayless, M.J. Davis, and G.A. Meininger. *Regulation of Tissue Injury Responses by the Exposure of Matricryptic Sites within Extracellular Matrix Molecules.* Am J Pathol, **2000**. 156(5): p. 1489-1498.

157. Neely, J.R. and H.E. Morgan. *Relationship Between Carbohydrate and Lipid Metabolism and the Energy Balance of Heart Muscle.* Annu Rev Physiol, **1974**. 36(1): p. 413-459.

158. Alaynick, W.A., R.P. Kondo, W. Xie, W. He, C.R. Dufour, M. Downes, Johan W. Jonker, W. Giles, R.K. Naviaux, V. Giguère, and R.M. Evans. *ERRγ Directs and Maintains the Transition to Oxidative Metabolism in the Postnatal Heart.* Cell Metab, **2007**. 6(1): p. 13-24.

159. Duncan, J. and B. Finck, *PPAR/PGC-1 Regulation of Metabolism in Cardiac Disease*, in *Translational Cardiology*, C. Patterson and M.S. Willis, Editors. 2012, Humana Press. p. 83-111.

160. Rowe, G.C., A. Jiang, and Z. Arany. *PGC-1 Coactivators in Cardiac Development and Disease.* Circ Res, **2010**. 107(7): p. 825-838.

161. Cherry, A.D. and C.A. Piantadosi. *Regulation of Mitochondrial Biogenesis and Its Intersection with Inflammatory Responses.* Antioxid Redox Signaling, **2015**.

162. Piantadosi, C.A., M.S. Carraway, A. Babiker, and H.B. Suliman. *Heme Oxygenase-1 Regulates Cardiac Mitochondrial Biogenesis via Nrf2-Mediated Transcriptional Control of Nuclear Respiratory Factor-1.* Circ Res, **2008**. 103(11): p. 1232-1240.

163. Piantadosi, C.A., C.M. Withers, R.R. Bartz, N.C. MacGarvey, P. Fu, T.E. Sweeney, K.E. Welty-Wolf, and H.B. Suliman. *Heme Oxygenase-1 Couples Activation of Mitochondrial*

Biogenesis to Anti-inflammatory Cytokine Expression. J Biol Chem, **2011**. 286(18): p. 16374-16385.

164. Gallardo-Soler, A., C. Gómez-Nieto, M.L. Campo, C. Marathe, P. Tontonoz, A. Castrillo, and I. Corraliza. *Arginase I Induction by Modified Lipoproteins in Macrophages: A Peroxisome Proliferator-Activated Receptor-γ/δ-Mediated Effect that Links Lipid Metabolism and Immunity.* Mol Endocrinol, **2008**. 22(6): p. 1394-1402.

165. Marín-García, J., *Signaling Pathways in Cardiovascular Development*, in *Signaling in the Heart*. 2011, Springer US. p. 155-196.

166. Kim, Y., D. Phan, E. van Rooij, D.-Z. Wang, J. McAnally, X. Qi, J.A. Richardson, J.A. Hill, R. Bassel-Duby, and E.N. Olson. *The MEF2D transcription factor mediates stress-dependent cardiac remodeling in mice.* J Clin Invest, **2008**. 118(1): p. 124-132.

167. Akhmedov, A.T. and J. Marín-García. *Myocardial regeneration of the failing heart.* Heart Fail Rev, **2012**. 18(6): p. 815-833

168. Loffredo, Francesco S., Matthew L. Steinhauser, J. Gannon, and Richard T. Lee. *Bone Marrow-Derived Cell Therapy Stimulates Endogenous Cardiomyocyte Progenitors and Promotes Cardiac Repair.* Cell Stem Cell, **2011**. 8(4): p. 389-398.

169. Amado, L.C., A.P. Saliaris, K.H. Schuleri, M. St. John, J.-S. Xie, S. Cattaneo, D.J. Durand, T. Fitton, J.Q. Kuang, G. Stewart, S. Lehrke, W.W. Baumgartner, B.J. Martin, A.W. Heldman, and J.M. Hare. *Cardiac repair with intramyocardial injection of allogeneic mesenchymal stem cells after myocardial infarction.* P Natl Acad Sci USA, **2005**. 102(32): p. 11474-11479.

170. Hatzistergos, K.E., H. Quevedo, B.N. Oskouei, Q. Hu, G.S. Feigenbaum, I.S. Margitich, R. Mazhari, A.J. Boyle, J.P. Zambrano, J.E. Rodriguez, R. Dulce, P.M. Pattany, D. Valdes, C. Revilla, A.W. Heldman, I. McNiece, and J.M. Hare. *Bone Marrow Mesenchymal Stem Cells Stimulate Cardiac Stem Cell Proliferation and Differentiation.* Circ Res, **2010**. 107(7): p. 913-922.

171. Malliaras, K., Y. Zhang, J. Seinfeld, G. Galang, E. Tseliou, K. Cheng, B. Sun, M. Aminzadeh, and E. Marbán. *Cardiomyocyte proliferation and progenitor cell recruitment underlie therapeutic regeneration after myocardial infarction in the adult mouse heart.* EMBO Mol Med, **2013**. 5(2): p. 191-209.

172. Ellison, Georgina M., C. Vicinanza, Andrew J. Smith, I. Aquila, A. Leone, Cheryl D. Waring, Beverley J. Henning, Giuliano G. Stirparo, R. Papait, M. Scarfò, V. Agosti, G. Viglietto, G. Condorelli, C. Indolfi, S. Ottolenghi, D. Torella, and B. Nadal-Ginard. *Adult c-*

kitpos Cardiac Stem Cells Are Necessary and Sufficient for Functional Cardiac Regeneration and Repair. Cell, **2013**. 154(4): p. 827-842.

173. van Berlo, J.H., O. Kanisicak, M. Maillet, R.J. Vagnozzi, J. Karch, S.-C.J. Lin, R.C. Middleton, E. Marban, and J.D. Molkentin. *c-kit+ cells minimally contribute cardiomyocytes to the heart.* Nature, **2014**. 509(7500): p. 337-341.

174. Fazel, S., M. Cimini, L. Chen, S. Li, D. Angoulvant, P. Fedak, S. Verma, R.D. Weisel, A. Keating, and R.-K. Li. *Cardioprotective c-kit+ cells are from the bone marrow and regulate the myocardial balance of angiogenic cytokines.* J Clin Invest, **2006**. 116(7): p. 1865-1877.

175. Oka, T., M. Maillet, A.J. Watt, R.J. Schwartz, B.J. Aronow, S.A. Duncan, and J.D. Molkentin. *Cardiac-Specific Deletion of Gata4 Reveals Its Requirement for Hypertrophy, Compensation, and Myocyte Viability.* Circ Res, **2006**. 98(6): p. 837-845.

176. Shen, T., I. Aneas, N. Sakabe, R.J. Dirschinger, G. Wang, S. Smemo, J.M. Westlund, H. Cheng, N. Dalton, Y. Gu, C.J. Boogerd, C.-I. Cai, K. Peterson, J. Chen, M.A. Nobrega, and S.M. Evans. *Tbx20 regulates a genetic program essential to adult mouse cardiomyocyte function.* J Clin Invest, **2011**. 121(12): p. 4640-4654.

177. Toko, H., W. Zhu, E. Takimoto, I. Shiojima, Y. Hiroi, Y. Zou, T. Oka, H. Akazawa, M. Mizukami, M. Sakamoto, F. Terasaki, Y. Kitaura, H. Takano, T. Nagai, R. Nagai, and I. Komuro. *Csx/Nkx2-5 Is Required for Homeostasis and Survival of Cardiac Myocytes in the Adult Heart.* J Biol Chem, **2002**. 277(27): p. 24735-24743.

178. Huang, J., M. Min Lu, L. Cheng, L.-J. Yuan, X. Zhu, A.L. Stout, M. Chen, J. Li, and M.S. Parmacek. *Myocardin is required for cardiomyocyte survival and maintenance of heart function.* Proc Natl Acad Sci, **2009**. 106(44): p. 18734-18739.

179. Perrino, C. and H.A. Rockman. *GATA4 and the Two Sides of Gene Expression Reprogramming.* Circ Res, **2006**. 98(6): p. 715-716.

180. Azakie, A., J.R. Fineman, and Y. He. *Myocardial transcription factors are modulated during pathologic cardiac hypertrophy in vivo.* J Thorac Cardiov Sur, **2006**. 132(6): p. 1262-1271.e1264.

181. Furtado, M.B., M.W. Costa, E.M. Adi Pranoto, E. Salimova, A.R. Pinto, N.T. Lam, A. Park, P. Snider, A. Chandran, R.P. Harvey, R. Boyd, S.J. Conway, J.T. Pearson, D.M. Kaye, and N. Rosenthal. *Cardiogenic Genes Expressed in Cardiac Fibroblasts Contribute to Heart Development and Repair.* Circ Res, **2014**. 114: p. 1422-1434.

182. Dequach, J.A., V. Mezzano, A. Miglani, S. Lange, G.M. Keller, F. Sheikh, and K.L. Christman. *Simple and high yielding method for preparing tissue specific extracellular matrix coatings for cell culture.* PLoS ONE, **2010**. 5(9): p. e13039.

183. Seif-Naraghi, S.B., M.A. Salvatore, P.J. Schup-Magoffin, D.P. Hu, and K.L. Christman. *Design and characterization of an injectable pericardial matrix gel: a potentially autologous scaffold for cardiac tissue engineering.* **2010**. 16(6): p. 2017-2027.

184. DeQuach, J.A., J.E. Lin, C. Cam, D. Hu, M.A. Salvatore, F. Sheikh, and K.L. Christman. *Injectable skeletal muscle matrix hydrogel promotes neovascularization and muscle cell infiltration in a hindlimb ischemia model.* Eur Cells Mater, **2012**. 23: p. 400.

185. Dequach, J.A., S.H. Yuan, L.S.B. Goldstein, and K.L. Christman. *Decellularized Porcine Brain Matrix for Cell Culture and Tissue Engineering Scaffolds.* Tissue Eng Pt A, **2011**. 17(21-22): p. 2583-2592.

186. Young, D.A., D.O. Ibrahim, D. Hu, and K.L. Christman. *Injectable hydrogel scaffold from decellularized human lipoaspirate.* **2011**. 7(3): p. 1040-1049.

187. Freytes, D.O., J. Martin, S.S. Velankar, A.S. Lee, and S.F. Badylak. *Preparation and rheological characterization of a gel form of the porcine urinary bladder matrix.* Biomaterials, **2008**. 29(11): p. 1630-1637.

188. Okada, M., T.R. Payne, H. Oshima, N. Momoi, K. Tobita, and J. Huard. *Differential efficacy of gels derived from small intestinal submucosa as an injectable biomaterial for myocardial infarct repair.* Biomaterials, **2010**. 31(30): p. 7678-7683.

189. Wolf, M.T., K.A. Daly, E.P. Brennan-Pierce, S.A. Johnson, C.A. Carruthers, A. D'Amore, S.P. Nagarkar, S.S. Velankar, and S.F. Badylak. *A hydrogel derived from decellularized dermal extracellular matrix.* Biomaterials, **2012**. 33(29): p. 7028-7038.

190. Sawkins, M.J., W. Bowen, P. Dhadda, H. Markides, L.E. Sidney, A.J. Taylor, F.R.A.J. Rose, S.F. Badylak, K.M. Shakesheff, and L.J. White. *Hydrogels derived from demineralized and decellularized bone extracellular matrix.* Acta Biomater, **2013**. 9(8): p. 7865-7873.

191. Reing, J.E., L. Zhang, J. Myers-Irvin, K.E. Cordero, D.O. Freytes, E. Heber-Katz, K. Bedelbaeva, D. McIntosh, A. Dewilde, S.J. Braunhut, and S.F. Badylak. *Degradation products of extracellular matrix affect cell migration and proliferation.* Tissue Eng Pt A, **2009**. 15(3): p. 605-614.

192. Li, F., W. Li, S. Johnson, D. Ingram, M. Yoder, and S. Badylak. *Low-molecular-weight peptides derived from extracellular matrix as chemoattractants for primary endothelial cells.* Endothelium - J Endoth, **2004**. 11(3-4): p. 199-206.

193. Brennan, E.P., J. Reing, D. Chew, J.M. Myers-Irvin, E.J. Young, and S.F. Badylak. *Antibacterial activity within degradation products of biological scaffolds composed of extracellular matrix.* Tissue Eng, **2006**. 12(10): p. 2949-2955.

194. Badylak, S.F. *The extracellular matrix as a biologic scaffold material.* Biomaterials, **2007**. 28(25): p. 3587-3593.

195. Vanhoutte, D., M. Schellings, Y. Pinto, and S. Heymans. *Relevance of matrix metalloproteinases and their inhibitors after myocardial infarction: A temporal and spatial window.* Cardiovasc Res, **2006**. 69(3): p. 604-613.

196. Seif-Naraghi, S.B., D. Horn, P.J. Schup-Magoffin, and K.L. Christman. *Injectable extracellular matrix derived hydrogel provides a platform for enhanced retention and delivery of a heparin-binding growth factor.* Acta Biomater, **2012**. 8(10): p. 3695-3703.

197. López, J., S. Imperial, R. Valderrama, and S. Navarro. *An improved bradford protein assay for collagen proteins.* Clin Chim Acta, **1993**. 220(1): p. 91-100.

198. Smits, A.M., P. van Vliet, C.H. Metz, T. Korfage, J.P.G. Sluijter, P.A. Doevendans, and M.-J. Goumans. *Human cardiomyocyte progenitor cells differentiate into functional mature cardiomyocytes: an in vitro model for studying human cardiac physiology and pathophysiology.* Nat. Protocols, **2009**. 4(2): p. 232-243.

199. Zhang, X., R. Goncalves, and D.M. Mosser, *The Isolation and Characterization of Murine Macrophages*, in *Current Protocols in Immunology*. 2001, John Wiley & Sons, Inc.

200. Weischenfeldt, J. and B. Porse. *Bone Marrow-Derived Macrophages (BMM): Isolation and Applications.* Cold Spring Harb Protoc, **2008**. 2008(12): p. pdb.prot5080.

201. Tottey, S., M. Corselli, E.M. Jeffries, R. Londono, B. Peault, and S.F. Badylak. *Extracellular Matrix Degradation Products and Low-Oxygen Conditions Enhance the Regenerative Potential of Perivascular Stem Cells.* Tissue Eng Pt A, **2010**. 17(1-2): p. 37-44.

202. Vorotnikova, E., D. McIntosh, A. Dewilde, J. Zhang, J.E. Reing, L. Zhang, K. Cordero, K. Bedelbaeva, D. Gourevitch, E. Heber-Katz, S.F. Badylak, and S.J. Braunhut. *Extracellular matrix-derived products modulate endothelial and progenitor cell migration and*

proliferation in vitro and stimulate regenerative healing in vivo. Matrix Biol, **2010**. 29(8): p. 690-700.

203. Ricard-Blum, S. and R. Salza. *Matricryptins and matrikines: biologically active fragments of the extracellular matrix.* Exp Dermatol, **2014**. 23(7): p. 457-463.

204. Zamilpa, R. and M.L. Lindsey. *Extracellular matrix turnover and signaling during cardiac remodeling following MI: Causes and consequences.* J Mol Cell Cardiol, **2010**. 48(3): p. 558-563.

205. Vlodavsky, I., R. Bar-Shavit, G. Korner, and Z. Fuks, *Extracellular matrix bound growth factors, enzymes and plasma proteins*, in *Molecular and Cellular Aspects of Basement Membrane*, D.H. Rohrbach and R. Timpl, Editors. 1993, Academic Press: San Diego, CA. p. 327-343.

206. Spinale, F.G. *Myocardial Matrix Remodeling and the Matrix Metalloproteinases: Influence on Cardiac Form and Function.* Physiol Rev, **2007**. 87(4): p. 1285-1342.

207. Slivka, P.F., C.L. Dearth, T.J. Keane, F.W. Meng, C.J. Medberry, R.T. Riggio, J.E. Reing, and S.F. Badylak. *Fractionation of an ECM hydrogel into structural and soluble components reveals distinctive roles in regulating macrophage behavior.* Biomater Sci, **2014**.

208. Lundblad, R.L., *Techniques in Protein Modification*. 1994, Boca Raton, FL: CRC Press.

209. Sapan, C.V., R.L. Lundblad, and N.C. Price. *Colorimetric protein assay techniques.* Biotechnol Appl Biochem, **1999**. 29(2): p. 99-108.

210. Beattie, A.J., T.W. Gilbert, J.P. Guyot, A.J. Yates, and S.F. Badylak. *Chemoattraction of Progenitor Cells by Remodeling Extracellular Matrix Scaffolds.* Tissue Eng Pt A, **2008**. 15(5): p. 1119-1125.

211. Crapo, P.M., S. Tottey, P.F. Slivka, and S.F. Badylak. *Effects of Biologic Scaffolds on Human Stem Cells and Implications for CNS Tissue Engineering.* Tissue Eng Pt A, **2013**. 20(1-2): p. 313-323.

212. O'Brien, J., I. Wilson, T. Orton, and F. Pognan. *Investigation of the Alamar Blue (resazurin) fluorescent dye for the assessment of mammalian cell cytotoxicity.* Eur J Biochem, **2000**. 267(17): p. 5421-5426.

213. Porter, K.E. and N.A. Turner. *Cardiac fibroblasts: At the heart of myocardial remodeling.* Pharmacol Ther, **2009**. 123(2): p. 255-278.

214. Spinale, F.G. *Matrix Metalloproteinases: Regulation and Dysregulation in the Failing Heart.* Circ Res, **2002**. 90(5): p. 520-530.

215. Creemers, E.E.J.M., J.P.M. Cleutjens, J.F.M. Smits, and M.J.A.P. Daemen. *Matrix Metalloproteinase Inhibition After Myocardial Infarction: A New Approach to Prevent Heart Failure?* Circ Res, **2001**. 89(3): p. 201-210.

216. Turner, N.A. and K.E. Porter. *Regulation of myocardial matrix metalloproteinase expression and activity by cardiac fibroblasts.* IUBMB Life, **2012**. 64(2): p. 143-150.

217. McGarvey, J.R., S. Pettaway, J.A. Shuman, C.P. Novack, K.N. Zellars, P.D. Freels, R.L. Echols, J.A. Burdick, J.H. Gorman, R.C. Gorman, and F.G. Spinale. *Targeted Injection of a Biocomposite Material Alters Macrophage and Fibroblast Phenotype and Function following Myocardial Infarction: Relation to Left Ventricular Remodeling.* J Pharmacol Exp Ther, **2014**. 350(3): p. 701-709.

218. International standard ISO 10993-5, Biological evaluation of medical devices. 2002. Part 5: Cytotoxicity Testing.

219. Costandi, P.N., L.R. Frank, A.D. McCulloch, and J.H. Omens. *Role of diastolic properties in the transition to failure in a mouse model of the cardiac dilatation.* Am J Physiol Heart Circ Physiol, **2006**. 291(6): p. H2971-H2979.

220. Sonnenberg, S.B., A.A. Rane, C.J. Liu, N. Rao, G. Agmon, S. Suarez, R. Wang, A. Munoz, V. Bajaj, S. Zhang, R. Braden, P.J. Schup-Magoffin, O.L. Kwan, A.N. DeMaria, J.R. Cochran, and K.L. Christman. *Delivery of an engineered HGF fragment in an extracellular matrix-derived hydrogel prevents negative LV remodeling post-myocardial infarction.* Biomaterials, **2015**. 45(0): p. 56-63.

221. Rosenblatt, J., B. Devereux, and D.G. Wallace. *Dynamic rheological studies of hydrophobic interactions in injectable collagen biomaterials.* J Appl Polym Sci, **1993**. 50(6): p. 953-963.

222. Orban, J.M., L.B. Wilson, J.A. Kofroth, M.S. El-Kurdi, T.M. Maul, and D.A. Vorp. *Crosslinking of collagen gels by transglutaminase.* J Biomed Mater Res A, **2004**. 68(4): p. 756-762.

223. Chen, R.-N., H.-O. Ho, and M.-T. Sheu. *Characterization of collagen matrices crosslinked using microbial transglutaminase.* Biomaterials, **2005**. 26(20): p. 4229-4235.

224. Sundararaghavan, H.G., G.A. Monteiro, N.A. Lapin, Y.J. Chabal, J.R. Miksan, and D.I. Shreiber. *Genipin-induced changes in collagen gels: Correlation of mechanical properties to fluorescence.* J Biomed Mater Res A, **2008**. 87A(2): p. 308-320.

225. de Castro Brás, L.E., J.L. Proffitt, S. Bloor, and P.D. Sibbons. *Effect of crosslinking on the performance of a collagen-derived biomaterial as an implant for soft tissue repair: A rodent model.* J Biomed Mater Res B, **2010**. 95B(2): p. 239-249.

226. Yung, C.W., L.Q. Wu, J.A. Tullman, G.F. Payne, W.E. Bentley, and T.A. Barbari. *Transglutaminase crosslinked gelatin as a tissue engineering scaffold.* J Biomed Mater Res A, **2007**. 83A(4): p. 1039-1046.

227. Castro, M.M., A.D. Kandasamy, N. Youssef, and R. Schulz. *Matrix metalloproteinase inhibitor properties of tetracyclines: Therapeutic potential in cardiovascular diseases.* Pharmaco Res, **2011**. 64(6): p. 551-560.

228. Chau, D.Y.S., R.J. Collighan, E.A.M. Verderio, V.L. Addy, and M. Griffin. *The cellular response to transglutaminase-cross-linked collagen.* **2005**. 26(33): p. 6518-6529.

229. Adam Young, D., V. Bajaj, and K.L. Christman. *Decellularized adipose matrix hydrogels stimulate in vivo neovascularization and adipose formation.* J Biomed Mater Res A, **2014**. 102(6): p. 1641-1651.

230. DeLustro, F., R.A. Condell, M.A. Nguyen, and J.M. McPherson. *A comparative study of the biologic and immunologic response to medical devices derived from dermal collagen.* J Biomed Mater Res, **1986**. 20(1): p. 109-120.

231. Sheu, M.-T., J.-C. Huang, G.-C. Yeh, and H.-O. Ho. *Characterization of collagen gel solutions and collagen matrices for cell culture.* Biomaterials, **2001**. 22(13): p. 1713-1719.

232. Ma, L., C. Gao, Z. Mao, J. Zhou, J. Shen, X. Hu, and C. Han. *Collagen/chitosan porous scaffolds with improved biostability for skin tissue engineering.* Biomaterials, **2003**. 24(26): p. 4833-4841.

233. Young, J.L., J. Tuler, R. Braden, P. Schüp-Magoffin, J. Schaefer, K. Kretchmer, K.L. Christman, and A.J. Engler. *In vivo response to dynamic hyaluronic acid hydrogels.* Acta Biomater, **2013**. 9(7): p. 7151-7157.

234. Nanda, J.S. and J.R. Lorsch, *Chapter Eight - Labeling a Protein with Fluorophores Using NHS Ester Derivitization*, in *Methods in Enzymology*, L. Jon, Editor. 2014, Academic Press. p. 87-94.

235. Butler, M.F., Y.-F. Ng, and P.D.A. Pudney. *Mechanism and kinetics of the crosslinking reaction between biopolymers containing primary amine groups and genipin.* J Polym Sci A Polym Chem, **2003**. 41(24): p. 3941-3953.

236. Friess, W. *Collagen – biomaterial for drug delivery1.* Eur J Pharm Biopharm, **1998**. 45(2): p. 113-136.

237. Girton, T.S., T.R. Oegema, and R.T. Tranquillo. *Exploiting glycation to stiffen and strengthen tissue equivalents for tissue engineering.* J Biomed Mater Res, **1999**. 46(1): p. 87-92.

238. Olde Damink, L.H.H., P.J. Dijkstra, M.J.A. Van Luyn, P.B. Van Wachem, P. Nieuwenhuis, and J. Feijen. *Crosslinking of dermal sheep collagen using hexamethylene diisocyanate.* J Mater Sci: Mater Med, **1995**. 6(7): p. 429-434.

239. Huang, R.-H., G.-H. Chen, M.-K. Sun, and C.-J. Gao. *Hexamethylene diisocyanate crosslinking 2-hydroxypropyltrimethyl ammonium chloride chitosan/poly(acrylonitrile) composite nanofiltration membrane.* J Appl Polym Sci, **2007**. 105(2): p. 673-679.

240. Yang, C. *Enhanced physicochemical properties of collagen by using EDC/NHS-crosslinking.* Bull Mater Sci, **2012**. 35(5): p. 913-918.

241. Pieper, J.S., T. Hafmans, J.H. Veerkamp, and T.H. van Kuppevelt. *Development of tailor-made collagen–glycosaminoglycan matrices: EDC/NHS crosslinking, and ultrastructural aspects.* Biomaterials, **2000**. 21(6): p. 581-593.

242. Anselme, K., H. Petite, and D. Herbage. *Inhibition of Calcification In Vivo by Acyl Azide Cross-Linking of a Collagen-Glycosarninoglycan Sponge.* Matrix, **1992**. 12(4): p. 264-273.

243. Petite, H., I. Rault, A. Huc, P. Menasche, and D. Herbage. *Use of the acyl azide method for cross-linking collagen-rich tissues such as pericardium.* J Biomed Mater Res, **1990**. 24(2): p. 179-187.

244. Garcia, R.A., K.V. Go, and F.J. Villarreal. *Effects of timed administration of doxycycline or methylprednisolone on post-myocardial infarction inflammation and left ventricular remodeling in the rat heart.* Mol Cell Biochem, **2006**. 300(1-2): p. 159-169.

245. Tessone, A., M.S. Feinberg, I.M. Barbash, R. Reich, R. Holbova, M. Richmann, Y. Mardor, and J. Leor. *Effect of Matrix Metalloproteinase Inhibition by Doxycycline on Myocardial Healing and Remodeling after Myocardial Infarction.* Cardiovasc Drugs Ther, **2006**. 19(6): p. 383-390.

246. Hudson, M.P., P.W. Armstrong, W. Ruzyllo, J. Brum, L. Cusmano, P. Krzeski, R. Lyon, M. Quinones, P. Theroux, D. Sydlowski, H.E. Kim, M.J. Garcia, W.A. Jaber, and W.D. Weaver. *Effects of Selective Matrix Metalloproteinase Inhibitor (PG-116800) to Prevent Ventricular Remodeling After Myocardial InfarctionResults of the PREMIER (Prevention of Myocardial Infarction Early Remodeling) Trial.* J Am Coll Cardiol, **2006**. 48(1): p. 15-20.

247. Cerisano, G., P. Buonamici, R. Valenti, R. Sciagrà, S. Raspanti, A. Santini, N. Carrabba, E.V. Dovellini, R. Romito, A. Pupi, P. Colonna, and D. Antoniucci. *Early short-term doxycycline therapy in patients with acute myocardial infarction and left ventricular dysfunction to prevent the ominous progression to adverse remodelling: the TIPTOP trial.* Eur Heart J, **2014**. 35(3): p. 184-191.

248. Prall, A.K., G.M. Longo, W.G. Mayhan, E.A. Waltke, B. Fleckten, R.W. Thompson, and B.T. Baxter. *Doxycycline in patients with abdominal aortic aneurysms and in mice: Comparison of serum levels and effect on aneurysm growth in mice.* J Vasc Surg, **2002**. 35(5): p. 923-929.